EUROPEAN COOPERATION

ECSS

FOR SPACE STANDARDIZATION

Space engineering

Thermal design handbook - Part 10: Phase-Change Capacitors

Foreword

This Handbook is one document of the series of ECSS Documents intended to be used as supporting material for ECSS Standards in space projects and applications. ECSS is a cooperative effort of the European Space Agency, national space agencies and European industry associations for the purpose of developing and maintaining common standards.

The material in this Handbook is a collection of data gathered from many projects and technical journals which provides the reader with description and recommendation on subjects to be considered when performing the work of Themal design.

The material for the subjects has been collated from research spanning many years, therefore a subject may have been revisited or updated by science and industry.

The material is provided as good background on the subjects of thermal design, the reader is recommended to research whether a subject has been updated further, since the publication of the material contained herein.

This handbook has been prepared by TEC MT/QR, reviewed by the ECSS Executive Secretariat and approved by the ECSS Technical Authority.

Disclaimer

ECSS does not provide any warranty whatsoever, whether expressed, implied, or statutory, including, but not limited to, any warranty of merchantability or fitness for a particular purpose or any warranty that the contents of the item are error-free. In no respect shall ECSS incur any liability for any damages, including, but not limited to, direct, indirect, special, or consequential damages arising out of, resulting from, or in any way connected to the use of this document, whether or not based upon warranty, business agreement, tort, or otherwise; whether or not injury was sustained by persons or property or otherwise; and whether or not loss was sustained from, or arose out of, the results of, the item, or any services that may be provided by ECSS.

Table of contents

Figures

Tables

1
Scope

Solid-liquid phase-change materials (PCM) are a favoured approach to spacecraft passive thermal control for incident orbital heat fluxes or when there are wide fluctuations in onboard equipment.

The PCM thermal control system consists of a container which is filled with a substance capable of undergoing a phase-change. When there is an the increase in surface temperature of spacecraft the PCM absorbs the excess heat by melting. If there is a temperature decrease, then the PCM can provide heat by solidifying.

Many types of PCM systems are used in spacecrafts for different types of thermal transfer control.

Characteristics and performance of phase control materials are described in this Part. Existing PCM systems are also described.

The Thermal design handbook is published in 16 Parts

ECSS-E-HB-31-01 Part 1	Thermal design handbook – Part 1: View factors
ECSS-E-HB-31-01 Part 2	Thermal design handbook – Part 2: Holes, Grooves and Cavities
ECSS-E-HB-31-01 Part 3	Thermal design handbook – Part 3: Spacecraft Surface Temperature
ECSS-E-HB-31-01 Part 4	Thermal design handbook – Part 4: Conductive Heat Transfer
ECSS-E-HB-31-01 Part 5	Thermal design handbook – Part 5: Structural Materials: Metallic and Composite
ECSS-E-HB-31-01 Part 6	Thermal design handbook – Part 6: Thermal Control Surfaces
ECSS-E-HB-31-01 Part 7	Thermal design handbook – Part 7: Insulations
ECSS-E-HB-31-01 Part 8	Thermal design handbook – Part 8: Heat Pipes
ECSS-E-HB-31-01 Part 9	Thermal design handbook – Part 9: Radiators
ECSS-E-HB-31-01 Part 10	Thermal design handbook – Part 10: Phase – Change Capacitors
ECSS-E-HB-31-01 Part 11	Thermal design handbook – Part 11: Electrical Heating
ECSS-E-HB-31-01 Part 12	Thermal design handbook – Part 12: Louvers
ECSS-E-HB-31-01 Part 13	Thermal design handbook – Part 13: Fluid Loops
ECSS-E-HB-31-01 Part 14	Thermal design handbook – Part 14: Cryogenic Cooling
ECSS-E-HB-31-01 Part 15	Thermal design handbook – Part 15: Existing Satellites
ECSS-E-HB-31-01 Part 16	Thermal design handbook – Part 16: Thermal Protection System

2
References

ECSS-S-ST-00-01	ECSS System - Glossary of terms
ECSS-E-HB-30-09 Part 6	Thermal design handbook – Part 6: Thermal Control Surfaces
ECSS-E-HB-30-09 Part 11	Thermal design handbook – Part 11: Electrical Heating

All other references made to publications in this Part are listed, alphabetically, in the **Bibliography**.

3
Terms, definitions and symbols

3.1   Terms and definitions

For the purpose of this Standard, the terms and definitions given in ECSS-S-ST-00-01 apply.

3.2   Abbreviated terms

The following abbreviated terms are defined and used within this Standard.

ATC	air traffic control (aerosat)
B & K	Brennan & Kroliczek
GfW	Gessellschaft für Weltraumforschung
HEPP	heat pipe experiment package
HLS	
IHPE	international heat pipe experiment
IKE	institut für kernenenergetik (university of Stuttgart)
LDEF	long duration exposure facility
MEK	methyl-ethyl ketone
MLI	multilayer insulation
PCM	phase-change material
SINDA	systems improved numerical differencing analyzer
SS	stainless steel
SSM	second surface mirror
S day	stoichiometric day, see clause 8.5
TIG	tungsten-inert gas
TIROS	television and infra-red observation satellite

TOC	tag open cup	
TCC	tag closed cup	
TPHP	transporter heat pipe	

Other Symbols, mainly used to define the geometry of the configuration, are introduced when required.

3.3 Symbols

A	cross-sectional area, [m²]	
E	modulus of elasticity, [Pa]	
E_{max}	maximum energy stored in the PCM device, [J]	
L	thickness of the PCM device, one-dimensional model, [m]	
M	mass, [kg]	
Q	heat transfer rate, [W]	
T	temperature, [K]	
T_M	melting (or freezing) temperature, [K]	
T_0	temperature of the components being controlled, [K]	
T_R	reference temperature, [K]	
ΔT	excursion temperature, [K], $\Delta T = T_0 - T_M$	
c	specific heat, [J.kg⁻¹.K⁻¹]	
h_f	heat of fusion, [J.kg⁻¹]	
h_t	heat of transition, [J.kg⁻¹]	
k	thermal conductivity, [W.m⁻¹.K⁻¹]	
p_v	vapor pressure, [Pa]	
q_0	heat flux to the PCM device, one-dimensional model, [W.m⁻²]	
q_R	heat flux from the PCM device to the heat sink, one-dimensional model, [W.m⁻²]	
s(t)	interface position, measured from $x = 0$, one-	

dimensional model, [m]

t	time, [d], [h], [min], [s]
t_{max}	time for complete melting, [h]
t_{90}	time for melting 90% of the volume of the PCM, [h]
x	geometrical coordinate, one-dimensional model, [m]
α	thermal diffusivity, [m^2.s^{-1}], $\alpha = k/\rho c$
β	thermal expansion coefficient, volumetric (unless otherwise stated), [K^{-1}]
μ	dynamic viscosity, [Pa.s]
ρ	density, [kg.m^{-3}]
σ	surface tension, [N.m^{-1}]
σ_{ult}	ultimate tensile strength, [pa]
χ	isothermal compressibility, [Pa^{-1}]

Subscripts

C	Container
F	Filler
PCM	Phase-Change Material
T	Total
l	Liquid
s	Solid

4
Introduction

Solid-liquid phase-change materials (PCM) present an attractive approach to spacecraft passive thermal control when the incident orbital heat fluxes or the onboard equipment heat dissipation fluctuate widely.

Basically the PCM thermal control system consists of a container which is filled with a substance capable of undergoing a phase-change. When the temperature of the spacecraft surface increases, either because external radiation or inner heat dissipation, the PCM will absorb the excess heat through melting, and will restore it through solidification when the temperature decreases again. Because of the obvious electrical analogy this thermal control system is also called PCM capacitor.

To control the temperature of a cyclically operating equipment, the PCM cell is normally sandwiched between the equipment and the heat sink.

When the PCM system aims at absorbing the abnormal heat dissipation peaks of an equipment which somehow the excess heat to a sink, the cell is placed in contact with the equipment, without interfering in the normal heat patch between equipment and heat sink.

For achieving the thermal control of solitary equipment, the PCM capacitor may be used as the sole heat sink, provided that the heat transferred during the heating period does not exceed that required to completely melt the material.

5
PC working materials

5.1 General

The ideal PCM would have the following characteristics:

1. Melting point within the allowed temperature range of the thermally controlled component. In general between 260 K and 315 K.

2. High heat of fusion. This property defines the available energy storage and may be important either on a mass basis or on a volume basis.

3. Reversible solid-to-liquid transition. The chemical composition of the solid and liquid phases should be the same.

4. High thermal conductivity. This property is necessary to reduce thermal gradients. Unfortunately most PCM are very poor thermal conductors, so that fillers are used to increase the conductivity of the system.

5. High specific heat and high density.

6. Long term reliability during repeated cycling.

7. Low volume change during phase transition.

8. Low vapor pressure.

9. Non-toxic.

10. Non-corrosive. Compatible with structural materials.

11. No tendency to supercooling.

12. Availability and reasonable cost.

Relevant physical characteristics of phase-changing system are discussed, from a general point of view, in the following pages.

5.1.1 Supercooling

Supercooling is the process of cooling a liquid below the solid-liquid equilibrium temperature without formation of the solid phase. Supercooling when only one phase is present is called one-phase supercooling. Supercooling in the presence of both solid and liquid, or two-phase supercooling, depends upon the particular material and the environment surrounding it. The best way to reduce supercooling is to ensure that the original crystalline material has not been completely molten In such a case the seeds which are present in the melt tend to nucleate the solid phase when heat is removed. Nucleating catalysts are available for many materials.

Several PCMs have been tested under repeated heating and freezing cycles by DONIER SYSTEM. The main purpose of these tests has been the detection of eventual supercooling phenomena. Among the tested materials, the normal paraffins did not show any supercooling tendency. This result is also confirmed by the available literature. However, according to investigations carried out by Bentilla, Sterrett & Karre (1966) [5], contamination of the paraffins with water leads to supercooling of the molten substance down to 283 K. Care should therefore be taken to prevent this contamination.

5.1.1.1 Experimental investigations

An experimental investigation has been performed by DORNIER SYSTEM with the aim of finding out the variables having any influence on the supercooling behavior of the PCM; namely: total number of cycles, cooling rate, and type of container.

In these experiments, the temperature of the test chamber was alternatively increased and decreased at constant steps within a range of 240 to 320 K. The results are summarized in Table 5-1, and Figure 5-1 and Figure 5-2.

The temperature history of both the PCM inside the containers and the honey comb packages was measured by means of copper-constant thermocouples, and continuously recorded. The test points were located in the center of the container.

5.1.1.2 Results

Water and paraffins did not show any tendency to supercooling during freezing, not even at the maximum realizable cooling rate of 2×10^{-2} K.s^{-1}.

Acetic acid showed supercooling of different orders of magnitude. It could not be determined whether or not supercooling is a function of cooling rate. Supercooling was also independent, at least not noticeably dependent, on the number of cells constituting the container. If however, Al-chips were added to facilitate heterogeneous nucleation, supercooling was reduced during the first cycles, although it augmented when the test time increased.

Supercooling of disodium hydroxide heptahydrate amounted to 3-3,5 K regardless of cooling rate and number of temperature cycles.

Table 5-1: Supercooling Tests

PCM	Container	Number of Cycles	FIRST CYCLE		Maximum Supercooling	Comments
			Plateau Temperature [K]	Supercooling		
DODECANE	Aluminium Cell. Honeycomb adhesive-bonded to end plate.	146	265	NO	NO	
TETRADECANE	Aluminium Cell. Honeycomb adhesive-bonded to end plate.	50	280	NO	NO	Slightly ascending temperature.
HEXADECANE	Test tube without honeycomb.	50	293	NO	NO	
	Aluminium Cell. Honeycomb adhesive-bonded to end plate.	70	300	ΔT =9,5 K	ΔT = 10 K	
ACETIC ACID	Neck flash with splinters.	70	301	NO	ΔT = 6,5 K	Normal supercooling: ΔT= 5 K
	Aluminium Cell. Honeycomb inserted (not adhered).	23	299	ΔT = 1,5 K	ΔT = 5 K	
DISODIUM HYDROXIDE HEPTAHYDRATE	Neck flash with splinters.	36 22	286,5 287	ΔT = 3,5 K ΔT = 2,5 K	ΔT = 3,5 K ΔT = 3 K	No plateau temperature during heating-up.
DISTILLED WATER	Aluminium Cell. Honeycomb adhesive-bonded to end plate.	85	274	NO	NO	

NOTE   From DORNIER SYSTEM (1971) [9].
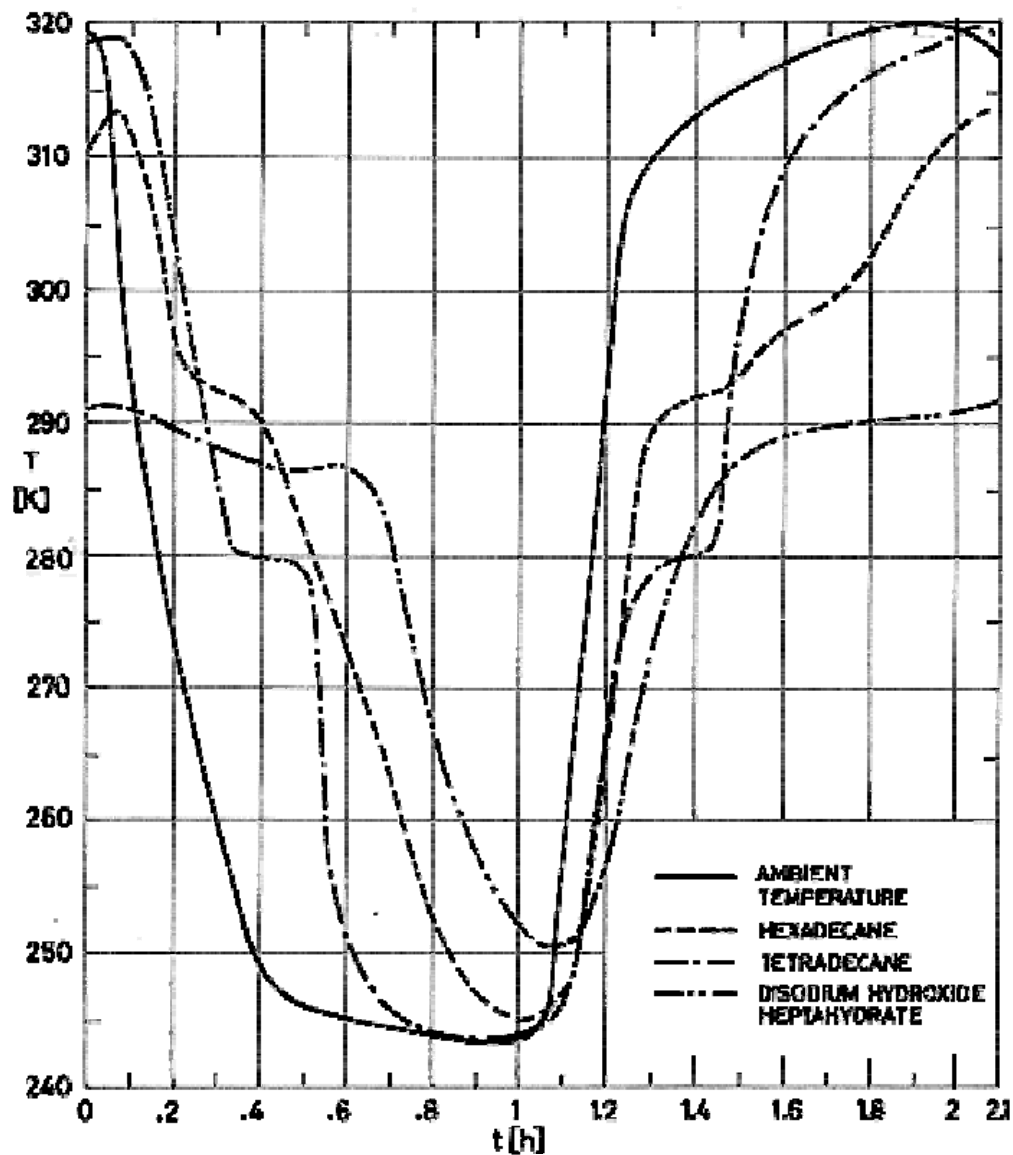
Note: non-si units are used in this figure

Figure 5-1: Temperature, *T*, vs. time, *t*, curves for heating and cooling of several PCMs. From DORNIER SYSTEM (1971) [9].
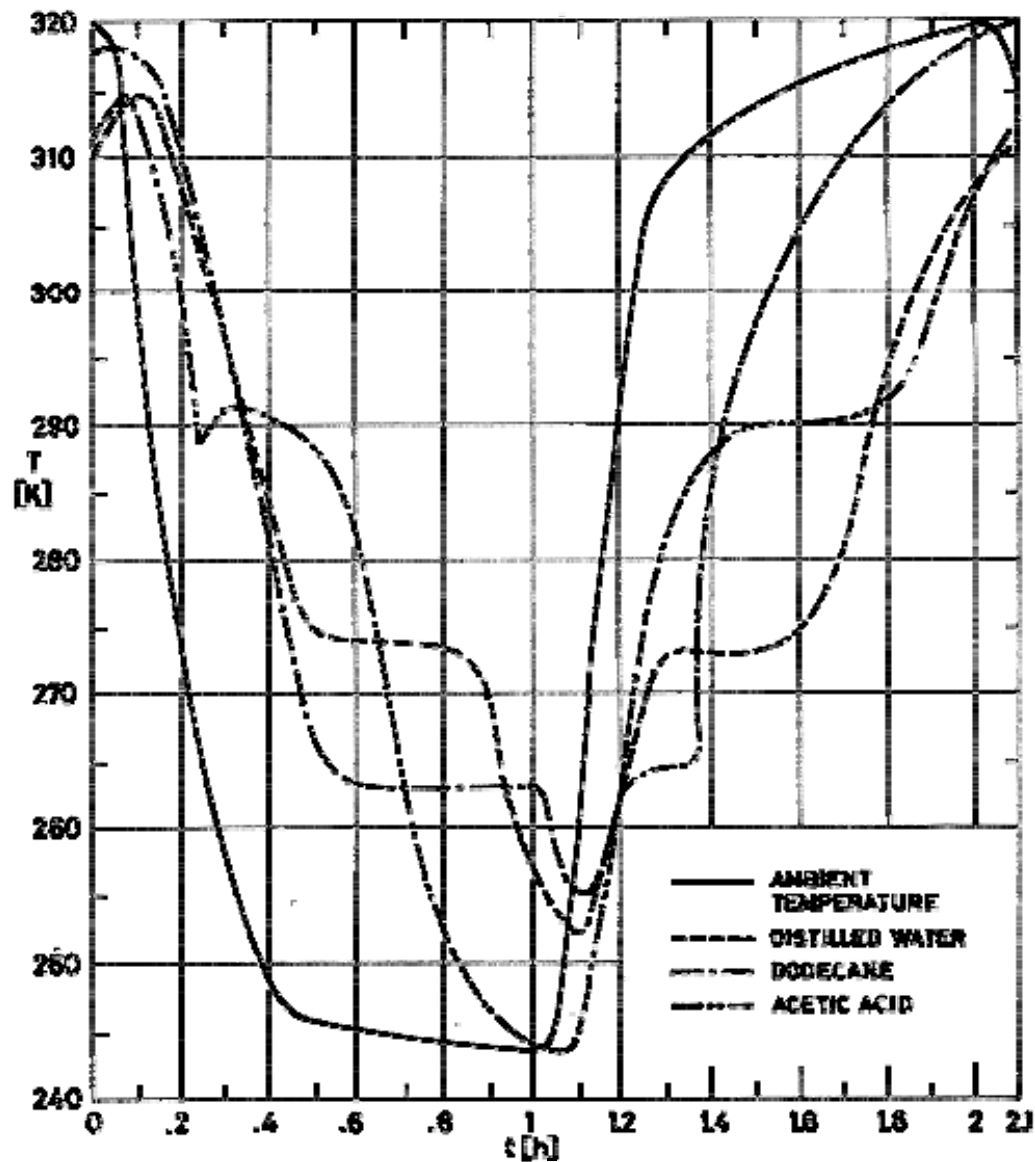
Note: non-si units are used in this figure

Figure 5-2: Temperature, *T*, vs. time, *t*, curves for heating and cooling of several PCMs. From DORNIER SYSTEM (1971) [9].

5.1.2   Nucleation

Nucleation is the formation of the first crystals capable of spontaneous growth into large crystals in an unstable liquid phase. These first crystals are called nuclei.

Homogeneous nucleation occurs when the nuclei may be generated spontaneously from the liquid itself at the onset of freezing. The rates of formation and dissociation do not depend on the presence or absence of surfaces, such as container walls or foreign particles.

Heterogeneous nucleation occurs when the nuclei are formed on solid particles already in the system or at the container walls. Supercooling (see clause 5.1.1) can be considerably reduced or even eliminated when heterogeneous nucleation is present.

5.1.3   The effect of gravity on melting and freezing of the pcm

Gravitational forces between molecules are comparatively small relative to intermolecular or interatomic forces; for example, the ratio between gravitational and intermolecular forces between two molecules of carbon dioxide is of the order of 10^{-30}.

Since phase-change is controlled by intermolecular forces, the rate of melting or freezing should be the same under microgravity as it is under normal gravity conditions, provided that thermal and solutal fields are the same.

However, phase change happens to be indirectly influenced by gravity through the following effects:

1.   Convection in the liquid phase which propagates nuclei and enhances heat transfer, and

2.   thermal contact conductance between the heated (or cooled) wall and the PCM.

1.   Convection can be induced by volume forces and/or by surface forces.

When the density gradient (due to thermal, solutal, or other effects) is not aligned with the body force (gravitational) vector, flow immediately results no matter how small the gradient. On the other hand, when the density gradient is parallel to but opposed to the body force, the fluid remains in a state of unstable equilibrium until a critical density gradient (more precisely, a critical Grashof number) is exceeded. The Grashof number gives the ratio of buoyancy to viscous forces.

Convection from the interfaces is produced by surface tractions due to surface tension gradients (which again can be due to thermal, solutal, or other effects). If the temperature gradient is parallel to the undisturbed interface, flow immediately results no matter how small the gradient. When the temperature gradient is normal to the undisturbed interface, convection appears provided that a critical Marangoni number is exceeded. This Marangoni number is defined as the ratio of surface tension gradient forces to viscous forces.

A priori information on which type of convection prevails under given circumstances can be obtained from an order of magnitude analysis (Napolitano (1981) [19]). Nevertheless, convection is presumably negligible for most PCM capacitors because of the low temperature gradients (associated to the high thermal conductances usually required) and of the reduced characteristics lengths of the enclosures when a metallic filler is used (see clause 6.2).

Convection due to shrinkage forces associated to phase change is normally small when solid and liquid densities are not too different.

2.   Gravity presses the denser phase against the lower wall of the container.

At the onset of the cool down the liquid remains in contact with the lower wall, be it cooled or heated, while the upper part of the cell is empty because of the void (ullage) which is usually provided for safe operation at high temperatures when using rigid containers (see clause 6.1). Thence, the temperature of the cooled wall is expected to be lower when the device is cooled from above (poor thermal conductance), that when cooled from below.

As soon as the cool down progresses, the solid, which is assumed to be denser than the liquid, makes contact with the lower wall enhancing the heat transfer to it, because the solid phase has normally a higher thermal conductivity than the liquid.

Reliable cooling data of PCM cells are not easily found in the literature since cooling is difficult to control precisely. Data reported in Figure 8-36b, Clause 8.5, do not support the above prediction, rather the average wall temperature is higher (not smaller) when the

solid is pressed by gravity against the cooled wall. Notice, however that according to Table 5-9, clause 5.3, liquid 1-Heptene is more conductive than the solid.

During heat up, the insulation is similar. Since the frozen PCM is usually denser than the liquid, the solid falls to the bottom of the cell. When heating up from below, the solid PCM remains close to the heated face, with a thin liquid layer amid them, whereas when heated from above a void space or, at most, a thick gap filled with the liquid appears between the heated face and the solid PCM. Thence, the heated wall temperature is expected to be higher when the device is heated from above than when it is heated from below. This effect has been observed experimentally, see for instance, in clause 8.3 the tests corresponding to Figure 8-14. Melting time is barely affected by the orientation of the gravity vector.

Metallic fillers (see clause 6.2) have the two-fold effect of increasing the thermal contact conductance between container and PCM, and of impeding liquid motion. Migration of the liquid by capillary pumping toward selected parts of the container can be achieved by varying the cross sectional area of the filler cells as in the PCM device shown in clause 8.4.

5.1.4   Bubble formation

Bubbles can affect PCM operation in several ways: the thermal conductivity will be altered; bubbles in the liquid phase will cause stirring actions; small bubbles in the solid phase can take up some of the volume shrinkage, thereby avoiding the formation of large cavities.

There are several types of bubbles likely to occur during PCM performance under microgravity: PCM vapor bubbles, cavities or voids from volume shrinkage, and gas bubbles.

The most persistent bubbles seem to be those formed by dissolved gases. During solidification, dissolved gases can be rejected just as any other solute at the solid-liquid interface. During the reverse process of melting, bubbles previously overgrown in the solid can be liberated. In an one-g field, bubbles would be more likely to float to the top and coalesce. Under microgravity, bubbles would be trapped in the frozen solid.

In order to reduce the amount of dissolved gases it is suggested to boil the PCM in liquid form under reduced pressure. Another method would be to purge the liquid with a less soluble gas.

5.2   Possible candidates

Possible PCM candidates have been classified as follows:

— Paraffins. Table 5-2.

— Non-Paraffin Organics. Table 5-3.

— Salt Hydrates. Table 5-4.

— Metallic. Table 5-5.

— Fused Salt Eutectics. Table 5-6.

— Miscellaneous. Table 5-7.

— Solid-Solid. Table 5-8.

In each table, the PCMs are arranged in order of increasing melting temperatures.

Data given in this preliminary list deal only with chemical formula, melting temperature, heat of fusion, and density.

All the PCMs that either are dangerous, have undesirable freezing behavior, or that, according to several authors, do not show sufficient merit, have been excluded from these tables.

Table 5-2: PARAFFINS

Name	Chemical Formula	Melting Temperature [K]	Heat of Fusion, $h_f x 10^{-3}$ [J.kg^{-1}]	Density, ρ [kg.m^{-3}]
2,4-Dimethylpentane	C_7H_{16}	153,8	67	673 (293 K)
1-Heptane	C_7H_{14}	154		697 (293 K)
n-Heptane	C_7H_{16}	182,4	129	684 (293 K)
n-Dodecane	$C_{12}H_{26}$	263,4	141	749 (293 K)
n-Tridecane	$C_{13}H_{28}$	267,5	215	756 (293 K)
n-Tetradecane	$C_{14}H_{30}$	278,9	228 [b]	763 (293 K)
n-Pentadecane	$C_{15}H_{32}$	283	205 [b]	768 (293 K)
n-Hexadecane	$C_{16}H_{34}$	291,2	237 [b]	773 (293 K)
n-Heptadecane	$C_{17}H_{36}$	295	213 [b]	778 (293 K)
n-Octadecane	$C_{18}H_{38}$	301,2	243 [b]	777 (301 K)
n-Nonadecane	$C_{19}H_{40}$	305,1	171	777 (305 K)
n-Eicosane	$C_{20}H_{42}$	309,8	247	789 (293 K)
n-Heneicosane	$C_{21}H_{44}$	313,5	161	792 (293 K)
n- Docosane	$C_{22}H_{46}$	317,4	158	794 (293 K)
n-Tricosane	$C_{23}H_{48}$	320,6	129	778 (321 K)
n-Tetracosane	$C_{24}H_{50}$	323,9	162	766 (343 K)
n-Pentacosane	$C_{25}H_{52}$	326,7	164	769 [b]
Paraffin Wax		327,6 [b]	146 [b]	880 [b]
n-Hexacosane	$C_{26}H_{54}$	329,4	256 [b]	803 (293 K)
n-Heptacosane	$C_{27}H_{56}$	332,5	159	805 (293 K)
n-Octacosane	$C_{28}H_{58}$	334,4	164	807 (293 K)
n-Nonacosane	$C_{29}H_{60}$	336,7		
n-Triacontane	$C_{30}H_{62}$	338,8	240 [b]	763 (373 K)
n-Hentriacontane	$C_{31}H_{64}$	340,9	251 [b]	775 (351 K)
n-Dotriacontane	$C_{32}H_{66}$	342,7		811 (293 K)
n-Tritriacontane	$C_{33}H_{68}$	344,2 [b]		812 (293 K)

NOTE   COMMENTS: All paraffins are chemically inert and stable below 773 K. They exhibit negligible supercooling and low volume change on melting. Many are commercially available at reasonable cost. No-Toxic. Non-Corrosive.

[a]   All data in this table, unless otherwise stated, are from Weast (1976) [25]. Most of these data supersede those previously given by Hale, Hoover & O'Neill (1971) [13].

[b]   From Hale, Hoover & O'Neill (1971) [13].

Table 5-3: NON-PARAFFIN ORGANICS [a]

Name	Chemical Formula	Melting Temperature [K]	Heat of Fusion, $h_f \times 10^{-3}$ [J.kg^{-1}]	Density, ρ [kg.m^{-3}]
1-Chloropropane	C_3H_7Cl	150,2 [b]	84 [c]	891 (293 K) [b]
Methyl Ethyl Ketone	C_4H_8O	186,6 [b]	111 [d]	805 (293 K) [b]
Ethyl Acetate	$C_4H_8O_2$	189,4 [b]	118 [d]	900 (293 K) [b]
Methyl Propyl Ketone	$C_5H_{10}O$	195,2 [b]	104 [d]	809 (293 K) [b]
Ethyl Myristate	$C_{16}H_{32}O_2$	285,3 [b]	184	857 (298 K)
Acetic Acid	C_2H_4O2	289,8	187	1050 (293 K)
Polyethylene Glycol 600	$HO(C_2H_4O)_nH$	293-298	146	1100 (293 K)
d-Lactic Acid	$C_3H_6O_3$	299	184	1249 (288 K)
Diphenyloxide	$(C_6H_5)_2O$	301		1073 (293 K)
Methyl Palmitate	$C_{17}H_{34}O_2$	302	205	
1-3 Methyl Pentacosane	$C_{26}H_{54}$	302	197	
Camphenilone	$C_9H_{14}O$	312	205	
Docasil Bromide	$C_{22}H_{45}Br$	313	201	
Caprylone	$C_{15}H_{30}O$	313	259	
Heptadecanone	$C_{17}H_{34}O$	314	201	
1-Cyclohexylo-octadecane		314	218	
	$C_{24}H_{48}$			
4-Heptadecanone	$C_{17}H_{34}O$	314	197	
8-Heptadecanone	$C_{17}H_{34}O$	315	201	
Cyanamide	HNCNH	317	209	
				1073 (291 K)
Methyl Eicosanate	$C_{21}H_{42}O_2$	318	230	1282 (293 K)
Elaidic Acid	$C_{18}H_{34}O_2$	320	218	851 (352 K)
	$C_{17}H_{34}O$			
3-Heptadecanone	$C_{17}H_{34}O$	321	218	
2-Heptadecanone		321	218	805 (321 K) [b]
Oxazoline Wax-ES-254		323		
9-Heptadecanone	$C_{17}H_{34}O$	324	213	
Methyl Behenate	$C_{23}H_{46}O_2$	325	234	
	$C_{26}H_{52}O_2$	327	218	
Ethyl Lignocerate	$H_4P_2O_6$	328	213	
Hypophosphoric Acid	$C_{57}H_{110}O_6$	329	191	862 (353 K)
Trymyristin	$C_{45}H_{86}O_6$	306-330	201-213	885 (333 K) [b]

Name	Chemical Formula	Melting Temperature [K]	Heat of Fusion, h_fx10^{-3}[J.kg^{-1}]	Density, ρ [kg.m^{-3}]
Myristic Acid	$C_{14}H_{28}O_2$	331	199	858 (333 K)
	$C_{28}H_{56}O_2$			
Ethyl Cerotate	$C_{17}H_{34}O_2$	333	226	
Heptadecanoic Acid		342,6	199	847 (342 K)
Oxazoline Wax-TS-970		347		
Acetamide	C_2H_5ON	354	241	1159 (293 K) [b]

NOTE   COMMENTS: Most of these materials are flammable. Many of the long-chain acids exhibit polymorphism (two or more crystalline forms). The flash point is usually low. Impurities may greatly affect melting point. Elevated temperatures decompose many of these compounds.

[a]   All data in this table, unless otherwise stated, are from Weast (1976) [25]. Most of these data supersede those previously given by Hale, Hoover & O'Neill (1971) [13].

[b]   From Weast (1976) [25].

[c]   From Bledjian, Burden & Hanna (1979) [6].

[d]   From Keville (1976) [15].

Table 5-4: SALT HYDRATES

Name	Chemical Formula	Melting Temperature [K]	Heat of Fusion, h_fx10^{-3} [J.kg^{-1}]	Density, ρ [kg.m^{-3}]
Calcium Chloride Hexahydrate	$CaCl_2.6H_2O$	302,6	170	
Lithium Nitrate Trihydrate	$LiNO_3.3H_2O$	303,03	296	1550 (solid)
Sodium Hydrogen Phosphate Dodecahydrate	$Na_2HPO_4.12H_2O$	309	280	1520 (293 K)
Ferric Cloride Hexahydrate	$FeCl_3.6H_2O$	310	226	
Ferric Nitrate Enneahydrate	$Fe(NO_3)_3.9H_2O$	320,4		1684 (293 K)
Magnesium Sulfate Heptahydrate	$MgSO_4.7H_2O$	321,6	202	
Sodium	$Na_2S_2O_3.5H_2O$	322	200	1690 (solid)

Name	Chemical Formula	Melting Temperature [K]	Heat of Fusion, h_fx10^{-3} [J.kg^{-1}]	Density, ρ [kg.m^{-3}]
Thiosulfate Pentahydrate				
Lithium Acetate Dihydrate	$LiC_2H_3O_2.2H_2O$	331	251-377	
Magnesium Chloride Tetrahydrate	$MgCl_2.4H_2O$	331	178	
Sodium Hydroxide Monohydrate	$NaOH.H_2O$	337,5	272	1720
Barium Hydroxide Octahydrate	$Ba(OH)_2.8H_2O$	351	301	2180
Aluminium Potassium Sulfate Dodecahydrate	$AlK(SO_4)_2.12H_2O$	364	184	
Magnesium Chloride Hexahydrate	$MgCl_2.6H_2O$	390	167	1560

NOTE   COMMENTS: Corrosive. Small volume change upon melting. Supercooling to a marked extent, which can be minimized with suitable nucleating agents. Most of the materials tested have incongruent melting points and subsequent lack of easy reversibility.

From Hale, Hoover & O'Neill (1971) [13].

Table 5-5: METALLIC

Name	Chemical Formula	Melting Temperature [K]	Heat of Fusion, $h_f x 10^{-3}$ [J.kg^{-1}]	Density, ρ [kg.m^{-3}]
Gallium-Gallium-Antimony Eutectic	Very Small Amounts of GaSb in Ga Matrix	303		
Gallium	Ga	303,2	80,3	5903 (298 K)
Cerrolow Eutectic [a]	49 Bi + 21 In + 18 Pb + 12 Sn	331	90,9	8800 (293 K)
Cerrobend Eutectic [a]	50 Bi + 26,7 Pb + 13,3 Sn + 10 Cd	343	32,6	9400 (solid)
Bismuth-Lead-Indium Eutectic	52 Bi + 26 Pb + 22 In	343	29	8000-10000
Bismuth-Lead-Tin Eutectic	52,2 Bi + 32 Pb + 15,8 Sn	369		
Bismuth-Lead Eutectic	55,5 Bi + 44,5 Pb	398		10460

[a]   Cerrolow and Cerrobend are registered trademarks of CERRO Co., New York, N.Y.

NOTE   COMMENTS: Low volume change on melting. These materials are of interest when the volume is a consideration. High thermal conductivity, filler not required.

From Hale, Hoover & O'Neill (1971) [13].

Table 5-6: FUSED SALT EUTECTICS

Name	Chemical Formula	Melting Temperature [K]	Heat of Fusion, h_fx10⁻³ [J.kg⁻¹]	Density, ρ [kg.m⁻³]
	31 Na_2SO_4 + 13 NaCl + 16 KCl + 40 H_2O	277	234	
	32 Na_2SO_4 + 14 NaCl +12NH_4Cl + 42 H_2O	284		
	37 Na_2SO_4 + 17 NaCl + 46 H_2O	291		
	25 Na_2SO_4 + 21 $MgSO_4$ + 54 H_2O	294-297		
	19 Na_2SO_4 + 17 $MgSO_4$ + 64 H_2O	294-297		
	21 Na_2SO_4 + 19 $MgSO_4$ + 60 H_2O	294-297		
	20 $LiNO_3$ + 61 NH_4NO_3 + 19 $AgNO_3$	325		
	79 $AlCl_3$ + 17 NaCl + 4 $ZrCl_2$	341	234	
	66 $AlCl_3$ + 20 NaCl + 14 KCl	343	209	
	24 $LiNO_3$ + 71 NH_4NO_3 + 5 NH_4Cl	359		
	60 $AlCl_3$ + 26 NaCl + 14 KCl	366	213	
	66 $AlCl_3$ + 34 NaCl	366	201	
HTS [a]	40 $NaNO_2$ + 7 $NaNO_3$ + 53 KNO_3	415		

[a]   Registered Trademark of E.I. duPOINT DE NEMOURS Co., Inc.

NOTE   COMMENTS: Components can be varied using several eutectics to allow a choice of values for the malting point and heat of fusion. The variations in melting temperatures reported by different investigators are due to the influence of moisture during preparation. These materials are corrosive.

From Hale, Hoover & O'Neill (1971) [13].

Table 5-7: MISCELLANEOUS

Name	Chemical Formula	Melting Temperature [K]	Heat of Fusion, h_fx10⁻³ [J.kg⁻¹]	Density, ρ [kg.m⁻³]
Water	H_2O	273,2	333,4	999,8 (273,2 K)
TRANSIT HEET SERIES [a]		222-505	230-301	1600

[a]   Registered Trademark of ROYAL INDUSTRIES, Santa Ana, Cal.

NOTE   From Hale, Hoover & O'Neill (1971) [13].

Table 5-8: SOLID-SOLID

Name	Temperature [K]		Heat of Fusion, $h_f \times 10^{-3}$ [J.kg⁻¹]	Heat of Transition, $h_t \times 10^{-3}$ [J.kg⁻¹]	Density, ρ [kg.m⁻³]	Molar Mass
	Melting	Transition				
Diaminopentaerythritol	352-357	341	31,7	184		105,14
2-Amino-2-Methyl-1,3-Propanediol	354-357	351	32	264		135,12
2-Methyl-2-Nitro-1,3-Propanediol		352		201		
Trimethylolethane		354	46	192		
2-Hydroxymethil-2-Methyl-1,3-Propanediol	470	354		192	1160	
Monoaminopentaerythritol		359		192		
Tris (Hydroxymethil) Acetic Acid		397		205		
2-Amino-2-Hydroxymethyl-1,3-Propanediol		404		285		
	411-419	425	25	289		121,14
2,2-bis (Hydroxymethyl) Propionic Acid	425-428	457	26,8	301		134,13
Pentaerythritol	531		37,2			136,15

NOTE   COMMENTS: Soft, waxy solids that can be extruded under considerably less pressure than ordinary crystals. They have unusually high vapor pressures for solid. Volume changes are in the range of 10 to 50%. Supercooling is not an inherent property of solid state transitions. Transition temperatures are fairly high.
From Hale, Hoover & O'Neill (1971) [13].

5.3   Selected candidates

Data concerning several selected PCM candidates are presented in the following. All of these PCMs have reasonably large heat of fusion and, according to literature searches, their characteristics seem to be attractive. Several among them have been used in existing systems (see clause 8).

The candidates are listed as follows:

— Paraffins Table 5-9.

— Non-Paraffin Organics Table 5-12.

— Salt Hydrates Table 5-17.

— Metallic and Miscellaneous Table 5-18.

Information given in these tables includes: chemical formula, density, specificheat, surface tension, thermal conductivity, thermal diffusivity, vapor pressure, viscosity, melting and boiling temperature, heat of fusion, thermal expansion coefficient (and isothermal compressibility) volume change on melting, flash point, autoignition temperature, supercooling, cost and compatibility.

Above *Italics* were used to indicate properties whose temperature dependence is given graphically in Figure 5-3 to Figure 5-6, Clause 5.3, for a limited number of PCMs.

Costs per unit mass have been deduced from price quotations by the producers, for containers of given volume. High purity products are sold in small amounts. The fact that the cost is quoted indicates that the product is commercially available to the stated purity and, thence, the producer should be contacted.

Table 5-9: PARAFFINS

NAME	SYNONYMS	CHEMICAL FORMULA
2,4-DIMETHYL-PENTANE, see Table 5-10		C_7H_{16}
1-HEPTENE, see Table 5-10	α-HEPTYLENE	C_7H_{14}
n- HEPTANE, see Table 5-10		C_7H_{16}
n-DODECANE, see Table 5-10		$C_{12}H_{26}$
n-TETRADECANE, see Table 5-11		$C_{14}H_{30}$
n-HEXADECANE, see Table 5-11	CETANE	$C_{16}H_{34}$
n-OCTADECANE, see Table 5-11		$C_{18}H_{38}$
n-EICOSANE, see Table 5-11		$C_{20}H_{42}$

Table 5-10: PARAFFINS

NAME	2,4-DIMETHYL-PENTANE	1-HEPTENE	n- HEPTANE	n-DODECANE
SYNONYMS		α-HEPTYLENE		
CHEMICAL FORMULA	C_7H_{16}	C_7H_{14}	C_7H_{16}	$C_{12}H_{26}$
MOLAR MASS	100,21	98,19	100,21	170,34
DENSITY, ρ [kg.m^{-3}]	673(293 K)[a]	697(293 K)[a]	684(293 K)[a]	749(293 K)[a]
SPECIFIC HEAT, cx10^{-3} [J.kg^{-1}.K^{-1}]		1,800 [1 b] 1,214 [s]		2,2 (298 K) [1 c] 1,62 (250K) [s]
SURFACE TENSION, σx10^2 [N.m^{-1}]	1,815 (293 K) [d] 1,766 (298K)	2,042 (293 K) [e] 1,993 (298K)	2,030 (293 K) [d] 1,980 (298K)	2,491 (298 K) [d]
THERMAL CONDUCTIVITY, k [W.m^{-1}.K^{-1}]		0,104 [1 b] 0,06 [s]	0,129 (293 K) [e]	0,15 [c]
THERMAL DIFFUSIVITY, αx10^8 [m^2.s^{-1}]				
VAPOR PRESSURE, p_v [Pa]	133 (225 K) [a] 13332 (298,5 K)	50662 (344 K) [b]	35370 (338 K) [f]	133 (320,8 K) [a] 13332 (419,2 K)
VISCOSITY, μx10^3 [Pa.s]	0,375 (288 K) [d] 0,360 (293 K)	0,35 (293 K) [e] 0,34 (298 K)	0,4412 (288 K) [d] 0,3967 (298 K)	2,26 (273 K) [c]
MELTING TEMPERATURE [K]	153,8 [a]	154 [a]	182,4 [a]	263,4 [c]
BOILING TEMPERATURE [K]	353,5 [a]	366,6 [a]	371,4 [a]	489,3 [c]
LATENT HEAT OF FUSION, h_fx10^{-5} [J.kg^{-1}]	0,67 [a]	1,29 [a]	1,41 [a]	2,15 [a]
COEFF. OF THERMAL EXPANSION, β [K^{-1}]				
VOLUME CHANGE ON MELTING				Less than +10% [c]
FLASH POINT [K]	260,9 [d]		272,0 (TOC) [d,g]	346,9 (TCC) [d,h]
AUTOIGNITION TEMPERATURE [K]				
SUPERCOOLING	ΔT = 15 K [b]	ΔT = 5 K to 8 K [b]	ΔT = 5 K [f]	

NAME		2,4-DIMETHYL-PENTANE	1-HEPTENE	n- HEPTANE	n-DODECANE
COST (Purity, %)	MERCK (1981) [18] [DM.kg⁻¹]	42500 (≥ 99,5%)	2400 (98%)	110 (≥ 99%) 41800 (≥ 99,7%)	660 (99%) 38200 (≥ 99,5%)
	FLUKA (1978) [11] [SF.kg⁻¹]	650 (≥ 99%) 8600 (≥ 99,5%)	470 (~99%)	19 (≥ 99%) 2700 (≥ 99,7%)	220 (~99%) 4900 (≥ 99,5%)
COMPATIBILITY		COMPATIBLE WITH: Al and Al/SS couple. [b]		COMPATIBLE WITH: Al, SS, Mg, Al/SS couple, and Mg/SS couple. [f]	
COMMENTS		Organic solvent. [d]		Organic solvent, volatile, flammable. Unpleasant sensory effects may develop after breathing air. Containing more than 2x10⁻³ kg.m⁻³. Flammability limits in air 1,10%–6,70%v. Min. ignition temperature in air 496 K. [d,i]	Organic solvent, liquid, colorless, flammability limits in air at 298 K 0,61%–4,7% v. [d]
		Generally nontoxic. Toxicity varies with the volatility for all paraffin hydrocarbons. Exposed to flame or heat can react with oxidizing materials.			

[l] Liquid.

[s] Solid.

All data in this table, unless otherwise stated, are from Hale, Hoover & O'Neill (1971) [13].

[a] From Weast (1976) [25].

[b] From Bledjian, Burden & Hanna (1979) [6].

[c] From DORNIER SYSTEM (1971) [9].

[d] From Riddick & Bunger (1970) [21].

[e] From Vargaftik (1975) [24].

[f] From Keville (1976) [15].

[g] Tag Open Cup flash point tester.

[h] Tag Closed Cup flash point tester.

[i] From Windholz (1976) [27].

Table 5-11: PARAFFINS

NAME		n-TETRADECANE	n-HEXADECANE	n-OCTADECANE	n-EICOSANE
SYNONYMS			CETANE		
CHEMICAL FORMULA		$C_{14}H_{30}$	$C_{16}H_{34}$	$C_{18}H_{38}$	$C_{20}H_{42}$
MOLAR MASS		198,38	226,45	254,51	282,54
DENSITY, ρ [kg.m^{-3}]		763 (293 K) [a]	773 (293 K) [a]	777 (301 K) [a]	798 (293 K) [a]
SPECIFIC HEAT, cx10^{-3} [J.kg^{-1}.K^{-1}]		2,07 (278,9 K) [l] 1,56 (250 K) [s]	2,21 (298 K) [l c] 1,52 (250 K) [s]	2,16 [s]	2,01 [l] 2,21 [s]
SURFACE TENSION, σx10^2 [N.m^{-1}]		2,743 (283 K)	2,747 (293 K)	2,745 (303 K)	2,90 (293 K) [e]
THERMAL CONDUCTIVITY k [W.m^{-1}.K^{-1}]		0,15	0,15 (289,8 K)	0,15 (301,2 K)	0,15
THERMAL DIFFUSIVITY, αx10^8 [m^2.s^{-1}]			8,7		
VAPOR PRESSURE, p_v [Pa]		133 (349,4 K) [a] 13332 (451,5 K)	133 (378,3 K) [a] 13332 (481,5 K)	133 (392,6 K) [a] 13332 (509 K)	133 (471,2 K)
VISCOSITY, μx10^3 [Pa.s]		2,92 (283 K) [c]	3,454 (293 K)	3,060 (313 K) [e]	4,29 (311 K)
MELTING TEMPERATURE [K]		278,9 [a]	291,2 [a]	301,2	309,8
BOILING TEMPERATURE [K]		525,6	560 [c]	591,1	616 [a]
LATENT HEAT OF FUSION, h_fx10^{-5} [J.kg^{-1}]		2,28	2,37	2,43	2,47
COEFF. OF THERMAL EXPANSION, β [K^{-1}]					3x10^{-4}
VOLUME CHANGE ON MELTING		Less than +10% [c]	Of the order of +8% [c]		
FLASH POINT [K]					
AUTOIGNITION TEMPERATURE [K]					
SUPERCOOLING		NONE OBSERVED	NEGLIGIBLE	NEGLIGIBLE	NONE OBSERVED
COST	MERCK (1981) [18]	37500 (≥ 99,5%)	540 (99%) 37 00 (≥ 99%)	650 (98%) 36800 (≥ 99,3%)	1400 (98%)

NAME		n-TETRADECANE	n-HEXADECANE	n-OCTADECANE	n-EICOSANE
(Purity, %)	[DM.kg⁻¹]				
	FLUKA (1978) [11] [SF.kg⁻¹]	260 (≥ 99%) 5100 (≥ 99,5%)	210 (≥ 99%)	200 (≥ 98%) 640 (≥ 99%)	480 (≥ 97%)
COMPATIBILITY		Noncorrosive to most structural materials			Compatible with most structural materials, noncorrosive.
COMMENTS		Liquid, colorless.		Crystal, colorless.	White, waxy solid.
		Generally nontoxic. Toxicity varies with the volatility for ell paraffin hydrocarbons. Exposed to flame or heat can react with oxidizing materials.			

l Liquid.

s Solid.

All data in this table, unless otherwise stated, are from Hale, Hoover & O'Neill (1971) [13].
a From Weast (1976) [25].

c From DORNIER SYSTEM (1971) [9].

e From Vargaftik (1975) [24].

Table 5-12: NON-PARAFFIN ORGANICS

NAME	SYNONYMS	CHEMICAL FORMULA
1-CHLORO-PROPANE, see Table 5-13	n-PROPYL CHLORIDE	$CH_3CH_2CH_2Cl$
METHYL ETHYL KETONE, see Table 5-13	2-BUTANONE, ETHYL METHYL KETONE	$CH_3CH_2COCH_3$
ETHYL ACETATE, see Table 5-13	ACETIC ACID ETHYL ESTER, ACETICETHER, VINEGAR NAPHTHA	$CH_3CO_2CH_2CH_3$
METHYL PROPYL KETONE, see Table 5-13	2- PENTANONE, ETHYL ACETONE	$CH_3CH_2CH_2COCH_3$
OXAZOLINE WAX-ES-254, see Table 5-14		
TRISREARIN, see Table 5-14	GLYCEROL TRIOCTADECA-NOATE, GLICEROL TRISTEARATE, STEARIN	$C_{57}H_{111}O_6$
MYRISTIC ACID, see Table 5-14	TETRADECA-NOIC ACID	$C_{13}H_{27}COOH$
STEARIC ACID, see Table 5-14	OCTADECANOIC ACID	$C_{17}H_{35}COOH$
ACETIC ACID, see Table 5-15	VINEGAR, GLACIAR ACETIC, ETHANOICOR METHANE CARBOXYLIC ACID	CH_3COOH
POLYETHYLENE GLYCOL 600, see Table 5-15	α-HYDRO-ω-HYDROXYPOLY(Oxy-1,2-ETHANEDIYL), CARBOWAX, NYCOLINE, MACROGOL, PLURACOL E, POLY G, POLYGLYCOL E, SOLBASE, PEG	$HO(C_2H_4O)nH$
ELAIDIC ACID, see Table 5-15	9-OCTADECENOIC ACID (trans)	$C_{17}H_{33}COOH$
OXAZOLINE WAX-TS-970, see Table 5-16		
ACETAMIDE, see Table 5-16	ACETIC ACID AMIDE, ETHANAMIDE	CH_3CONH_2
METHYL FUMARATE, see Table 5-16		$(CHCO_2CH_3)_2$

Table 5-13: NON-PARAFFIN ORGANICS

NAME	1-CHLORO-PROPANE	METHYL ETHYL KETONE	ETHYL ACETATE	METHYL PROPYL KETONE
SYNONYMS	n-PROPYL CHLORIDE	2-BUTANONE, ETHYL METHYL KETONE	ACETIC ACID ETHYL ESTER, ACETIC ETHER, VINEGAR NAPHTHA	2- PENTANONE, ETHYL ACETONE
CHEMICAL FORMULA	$CH_3CH_2CH_2Cl$	$CH_3CH_2COCH_3$	$CH_3CO_2CH_2CH_3$	$CH_3CH_2CH_2COCH_3$
MOLAR MASS	78,54	72,12	88,12	86,14
DENSITY, ρ [kg.m^{-3}]	891 (293 K) [a]	805 (293 K) [a]	900 (293 K) [a]	809 (293 K) [a]
SPECIFIC HEAT, cx10^{-3} [J.kg^{-1}.K^{-1}]				
SURFACE TENSION, σx10^2 [N.m^{-1}]	2,178 (293 K) [b] 2,048 (303 K)	2,69 (273 K) [b] 2,397 (297,8 K)	2,375 (293 K) [b] 2,255 (303 K)	
THERMAL CONDUCTIVITY, k [W.m^{-1}.K^{-1}]			0,0092 (273 K) [c] 0,0166 (373 K)	
THERMAL DIFFUSIVITY, αx10^8 [m^2.s^{-1}]				
VAPOR PRESSURE, p_v [Pa]	133 (204,7 K) [a] 13332 (270,5 K)	65568 (338 K) [d]	68701 (338 K) [d]	21025 (338 K) [d]
VISCOSITY, μx10^3 [Pa.s]	0,372 (288 K) [b] 0,318 (303 K)	0,423 (288 K) [b] 0,365 (303 K)	0,473 (288 K) [b] 0,400 (303 K)	
MELTING TEMPERATURE [K]	150,2 [a]	186,6 [a]	189,4 [a]	195,2 [a]
BOILING TEMPERATURE [K] [e]	319,6 [a]	352,6 [a]	350,1 [a]	375 [a]
LATENT HEAT OF FUSION, h_fx10^{-5} [J.kg^{-1}]	0,84 [f]	1,11 [d]	1,18 [d]	1,04 [d]
COEFF. OF THERMAL EXPANSION, β [K^{-1}]				
VOLUME CHANGE ON MELTING				
FLASH POINT [K]		272,0 (TCC) [b,g]	268,7 (TCC) [b,g]	
AUTOIGNITION				

NAME		1-CHLORO-PROPANE	METHYL ETHYL KETONE	ETHYL ACETATE	METHYL PROPYL KETONE
TEMPERATURE [K]					
SUPERCOOLING		ΔT = 5 K [f]	ΔT = 11 K [d]		
COST (Purity, %)	MERCK (1981) [18] [DM.kg^{-1}]	520 (98%)	58 (99%) 35500 ($\geq$ 99,5%)	66 (99%) 86 ($\geq$ 99,8%)	140 (98%)
	FLUKA (1978) [11] [SF.kg^{-1}]	89 (>98%)	10 ($\geq$ 99,5%)	12 ($\geq$ 99,5%)	61 (>98%)
COMPATIBILITY		Incompatible with: Al/SS couple. [f]	Compatible with: Al, SS, Mg and Mg/SS couple. Incompatible with Al/SS couple. [d]	Compatible with: Al, SS, Mg, Al/SS couple and Mg/SS couple. [d]	
COMMENTS		Organic solvent. Colorless liquid. Relatively safe. Flammability limits in air are 2,60% and 11,10% v, the latter value at elevated temperature. [b,h]	Organic solvent. Flammable. Acetone-like odor, low hazard with normal handling. Low toxicity. Irritation prevented below 0,59x10^{-3} kg.m^{-3} in air. Flammability limits in air 2,05%–11,00% v. Minimum ignitium temperature in air 778 K. [b,h]	Organic solvent. Clear, volatile, flammable liquid, fruity odor, pleasant taste when diluted. Ignition temperature 700 K. Explosive limits in air 2,2%–11,5% v. Slowly decompose by moisture, then acquires an acid reaction. [b,h]	Organic solvent. Colorless liquid. [h]

NOTE   All data in this table, unless otherwise stated, are from Hale, Hoover & O'Neill (1971) [13].

[a] From Weast (1976) [25].

[b] From Riddick & Bunger (1970) [21].

[c] From Vargaftik (1975) [24].

[d] From Keville (1976) [15].

[e] Measured at a pressure of about 10^5 Pa, unless otherwise indicated.

[f] From Bledjian, Burden & Hana (1979) [6].

[g] Tag Closed Cup flash point tester.

[h] From Windholz (1976) [27].

Table 5-14: NON-PARAFFIN ORGANICS

NAME	OXAZOLINE WAX-ES-254	TRISTEARIN	MYRISTIC ACID	STEARIC ACID
SYNONYMS		GLYCEROL TRIOCTADECANOATE, GLICEROL TRISTEARATE, STEARIN	TETRADECANOIC ACID	OCTADECANOIC ACID
CHEMICAL FORMULA		$C_{57}H_{111}O_6$	$C_{13}H_{27}COOH$	$C_{17}H_{35}COOH$
MOLAR MASS	723	891,46	228,37	284,47
DENSITY, ρ [kg.m^{-3}]		862 (353 K)	858 (333 K)	847 (342 K)
SPECIFIC HEAT, cx10^{-3} [J.kg^{-1}.K^{-1}]			2,26 [l] 1,59 [s]	
SURFACE TENSION, σx10^2 [N.m^{-1}]				3,93 (358 K)
THERMAL CONDUCTIVITY, k [W.m^{-1}.K^{-1}]	APPEARS TO BE QUITE LOW			
THERMAL DIFFUSIVITY, αx10^8 [m^2.s^{-1}]	ESTIMATED VERY LOW			
VAPOR PRESSURE, p_v [Pa]		133 (378,4 K)	133 (415 K) [a] 13332 (523,5 K)	133 (446,7 K) [a] 13332 (564 K)
VISCOSITY, μx10^3 [Pa.s]		18,5 (348 K)		11,6 (343 K)
MELTING TEMPERATURE [K]	323	329	331	342,6
BOILING TEMPERATURE [K] [e]			523,6 (1,33x10^4 Pa) [a]	505 (2x10^3 Pa) [a]
LATENT HEAT OF FUSION, h_fx10^{-5} [J.kg^{-1}]	ESTIMATED LARGE	1,91	1,99	1,99
COEFF. OF THERMAL EXPANSION, β [K^{-1}]				8,1x10^{-10}
VOLUME CHANGE ON MELTING				
FLASH POINT [K]				469
AUTOIGNITION				668

NAME		OXAZOLINE WAX-ES-254	TRISTEARIN	MYRISTIC ACID	STEARIC ACID
TEMPERATURE [K]					
SUPERCOOLING		ΔT = 2 K to 3 K	NONE OBSERVED	NONE OBSERVED	NONE OBSERVED
COST (Purity, %)	MERCK (1981) [18] [DM.kg⁻¹]			72 (97%) 580 (99%)	83 (95%) 3760 (99%)
	FLUKA (1978) [11] [SF.kg⁻¹]		41 (~95%) 4800 (≥ 99%)	25 (~97%) 99 (99%) 4200 (≥ 99,5%)	1105 (99%) 4200 (≥ 99,5%)
COMPATIBILITY		Very inert, compatible with many materials. Exhibits container separation with quartz and pyrex.	Compatible with Al.	Compatible with many structural materials including Aluminium.	Compatible with many structural materials. Exhibits container separation in pyrex.
COMMENTS		A commercial wax. Probably flammable.	White crystalline solid.	White crystals. Toxicity apparently low.	White, amorphous solid. Slight flammability when exposed to flame or heat. Very slight toxicity. Slowly evaporates at 363 K - 373 K. [h]

NOTE   All data in this table, unless otherwise stated, are from Hale, Hoover & O'Neill (1971) [13].

[a] From Weast (1976) [25].

[e] Measured at a pressure of about 10^5 Pa, unless otherwise indicated.

[h] From Windholz (1976) [27].

Table 5-15: NON-PARAFFIN ORGANICS

NAME	ACETIC ACID	POLYETHYLENE GLYCOL 600	ELAIDIC ACID
SYNONYMS	VINEGAR, GLACIAR ACETIC, ETHANOIC OR METHANE CARBOXYLIC ACID	α-HYDRO-ω-HYDROXYPOLY (Oxy-1,2-ETHANEDIYL), CARBOWAX, NYCOLINE, MACROGOL, PLURACOL E, POLY G, POLYGLYCOL E, SOLBASE, PEG	9-OCTADECENOIC ACID (trans)
CHEMICAL FORMULA	CH_3COOH	$HO(C_2H_4O)nH$	$C_{17}H_{33}COOH$
MOLAR MASS	60,05 [a]	570-630	282,46
DENSITY, ρ [kg.m^{-3}]	1050 (293 K)	1100 (293 K)	851 (352 K)
SPECIFIC HEAT, cx10^{-3} [J.kg^{-1}.K^{-1}]	1,96 [1] 2,04 [s]	2,26 [s]	
SURFACE TENSION, σx10^2 [N.m^{-1}]	2,742 (293 K)	4,43	
THERMAL CONDUCTIVITY, k [W.m^{-1}.K^{-1}]	0,18 (298 K) [1]	0,16 (323 K)	
THERMAL DIFFUSIVITY, αx10^8 [m^2.s^{-1}]	8,39		
VAPOR PRESSURE, p_v [Pa]	133 (255,8 K) [a] 13332 (336 K)	6,9x10^{-4} (373 K)	133 (444,3 K) [a] 13332 (561 K)
VISCOSITY, μx10^3 [Pa.s]	1,314 (288 K) [b] 1,040 (303 K)	11,5 (293 K)	
MELTING TEMPERATURE [K]	289,8	293-298	320
BOILING TEMPERATURE [K] [e]	391,3		561 (1,33x10^4 Pa) [a]
LATENT HEAT OF FUSION, h_fx10^{-5} [J.kg^{-1}]	1,87	1,46	2,18
COEFF. OF THERMAL EXPANSION, β [K^{-1}]	1,071 (298 K)	7,5x10^{-3}	
VOLUME CHANGE ON MELTING	+15,6%		

NAME		ACETIC ACID	POLYETHYLENE GLYCOL 600	ELAIDIC ACID
FLASH POINT [K]		313 (TCC) [b,g]	519	
AUTOIGNITION TEMPERATURE [K]		839		
SUPERCOOLING		ONE PHASE SUPERCOOLING, $\Delta T \cong 15$ K	NONE OBSERVED	NONE OBSERVED
COST (Purity, %)	MERCK (1981) [18] [DM.kg^{-1}]	52 ($\geq$ 99,8%)	53	
	FLUKA [11] (1978) [SF.kg^{-1}]	11 (>99,8%)	13	2750 (~95%) 10000 ($\geq$ 99%)
COMPATIBILITY		Compatible with: Al, Ti, Ta, Zr, precious metals, SS, Fluorocarbons, graphite and glass-ceramics.	Compatible with: Al.	
COMMENTS		Organic solvent. clear, colorless. Vinegar odor, burns the skin, caustic, irritating. Heated to decomposition emits toxic fumes. Exposed to heat or flame can react with oxidizers. Min. Ignition temperature in air 823 K. [b,h]	In chemical formula above n ranges from 12,5 to 13,9. colorless viscous liquid. Slight flammability, exposed to heat or flame can react with oxidizing materials. Non-toxic. Slightly hygroscopic, characteristic odor. [h]	White leaflets. [h]

NOTE   All data in this table, unless otherwise stated, are from Hale, Hoover & O'Neill (1971) [13].

[a] From Weast (1976) [25].

[b] From Riddick & Bunger (1970) [21].

[e] Measured at a pressure of about 10^5 Pa, unless otherwise indicated.

[g] Tag Closed Cup flash point tester.

[h] From Windholz (1976) [27].

Table 5-16: NON-PARAFFIN ORGANICS

NAME	OXAZOLINE WAX-TS-970	ACETAMIDE	METHYL FUMARATE
SYNONYMS		ACETIC ACID AMIDE, ETHANAMIDE	

NAME	OXAZOLINE WAX-TS-970	ACETAMIDE	METHYL FUMARATE
CHEMICAL FORMULA		CH_3CONH_2	$(CHCO_2CH_3)_2$
MOLAR MASS	970	59,07	144,12
DENSITY, ρ [kg.m^{-3}]		1159 (293 K)	1045 (378,6 K)
SPECIFIC HEAT, cx10^{-3} [J.kg^{-1}.K^{-1}]			
SURFACE TENSION, σx10^2 [N.m^{-1}]		3,93 (358 K)	2,567 (379 K)
THERMAL CONDUCTIVITY, k [W.m^{-1}.K^{-1}]	ESTIMATED VERY LOW		
THERMAL DIFFUSIVITY, αx10^8 [m^2.s^{-1}]	ESTIMATED VERY LOW	330	
VAPOR PRESSURE, p_v [Pa]		133 (338 K) [a] 13332 (431 K)	
VISCOSITY, μx10^3 [Pa.s]		2,182 (364,1 K) [b] 1,461 (384,8 K)	
MELTING TEMPERATURE [K]	347	354	375
BOILING TEMPERATURE [K] [e]		495	465
LATENT HEAT OF FUSION, h_fx10^{-5} [J.kg^{-1}]	ESTIMATED LARGE	2,41	2,42
COEFF. OF THERMAL EXPANSION, β [K^{-1}]			
VOLUME CHANGE ON MELTING		+8,15%	+18% to +20%
FLASH POINT [K]			
AUTOIGNITION TEMPERATURE [K]			
SUPERCOOLING	NONE OBSERVED	NONE OBSERVED	NONE OBSERVED
COST (Purity, %)	MERCK (1981) [18] [DM.kg^{-1}]		119 (99%)	

NAME		OXAZOLINE WAX-TS-970	ACETAMIDE	METHYL FUMARATE
	FLUKA (1978) [11] [SF.kg⁻¹]		44 (≥ 99%)	
COMPATIBILITY		Very inert, compatible with many materials. Exhibits container separation with quartz and pyrex.	Compatible with: Al.	
COMMENTS		A commercial wax. Probably flammable.	At normal state: white slightly yellow, deliquescent, fine crystal. Mousy odor except odorless when pure. Excellent solvent for both organic and inorganic compounds. Mild irritant. When heated to decomposition emits toxic cyanide fumes (decomposition point unavailable). [b,h]	White crystalline solid. Vigorous convection noted in melt. Compounds appear to have peculiar surface tension properties.

NOTE   All data in this table, unless otherwise stated, are from Hale, Hoover & O'Neill (1971) [13].

[a] From Weast (1976) [25].

[b] From Riddick & Bunger (1970) [21].

[e] Measured at a pressure of about 10^5 Pa, unless otherwise indicated.

[h] From Windholz (1976)[27].

Table 5-17: SALT HYDRATES

NAME	BARIUM HYDROXIDE OCTAHYDRATE	DISODIUM HYDROXIDE HEPTAHYDRATE	LITHIUM NITRATE TRIHYDRATE	SODIUM HYDROGEN PHOSPHATE DODECA-HYDRATE
SYNONYMS				
CHEMICAL FORMULA	$Ba(OH)_2.8H_2O$	$2NaOH.7H_2O$	$LiNO_3.3H_2O$	$Na_2HPO_4.12H_2O$
MOLAR MASS	315,51	206,1	123	138,01
DENSITY, ρ [kg.m⁻³]	2180 (289 K)		1430 [l] 1550 [s]	1520 (293 K)
SPECIFIC HEAT,	1,17 [s]	0,815 (288,7 K) [l]		1,94 (323 K);

NAME	BARIUM HYDROXIDE OCTAHYDRATE	DISODIUM HYDROXIDE HEPTAHYDRATE	LITHIUM NITRATE TRIHYDRATE	SODIUM HYDROGEN PHOSPHATE DODECA-HYDRATE
cx10^{-3} [J.kg^{-1}.K^{-1}]		0,447 (288,7 K) [s]		1,69 (273,2 K)
SURFACE TENSION, σx10^2 [N.m^{-1}]				
THERMAL CONDUCTIVITY, k [W.m^{-1}.K^{-1}]				476 (322 K); 0,514 (305 K)
THERMAL DIFFUSIVITY, αx10^8 [m^2.s^{-1}]			18	
VAPOR PRESSURE, p_v [Pa]		133 (283,15 K) 372,4 (288,65 K)		
VISCOSITY, μx10^3 [Pa.s]				
MELTING TEMPERATURE [K]	351	288,7	303,03	309
BOILING TEMPERATURE [K]				
LATENT HEAT OF FUSION, h_fx10^{-5} [J.kg^{-1}]	3,01	2,716	2,96	2,8
COEFF. OF THERMAL EXPANSION, β[K^{-1}]				43,5 x 10^{-5} [l] 8,8 x 10^{-5} [s]
VOLUME CHANGE ON MELTING			+8%	+5,1%
FLASH POINT [K]				

NAME	BARIUM HYDROXIDE OCTAHYDRATE	DISODIUM HYDROXIDE HEPTAHYDRATE	LITHIUM NITRATE TRIHYDRATE	SODIUM HYDROGEN PHOSPHATE DODECA-HYDRATE
AUTOIGNITION TEMPERATURE [K]				
SUPERCOOLING	NEGLIGIBLE	MAXIMUM $\Delta T = 3\ K$	Without a catalyst, up to 30 K of supercooling can be expected. An effective catalyst: $Zn(OH)NO_3$.	NONE OBSERVED
COST				
COMPATIBILITY	Corrosive to Aluminium.		Compatible with Aluminium, quartz, and pyrex. Non-wetting effects have not been observed.	Corrosive to Aluminium. Corrosion of Aluminium by basic salt hydrates can be eliminated in some cases by inhibitors, such as sodium silicate (water glass).
COMMENTS	A salt hydrate with 54,31% mass of anhydrous salt. Very alkaline. Breathing dust or contact with skin is harmful.	A salt hydrate with 38,83% mass of anhydrous salt.	Clear, colorless liquid or crystalline solid. A salt hydrate with 56,5% mass of anhydrous salt.	White crystals with 39,36% mass anhydrous salt. Very alkaline. Contact should be avoided.

[l]   Liquid.

[s]   Solid.

NOTE   After Grodzka (1969) [12], Hale, Hoover & O'Neill (1971) [13], DORNIER SYSTEM (1971) [9].

Table 5-18: METALLIC AND MISCELLANEOUS

NAME	METALLIC		MISCELLANEOUS	
	CERROBEND EUTECTIC	GALLIUM	TRANSIT HEET	WATER
SYNONYMS				
CHEMICAL FORMULA	50 Bi + 26,7 Pb + 13,3 Sn + 10 Cd	Ga		H_2O
MOLAR MASS		69,72		18,016
DENSITY, ρ [kg.m^{-3}]	9400 [s]	6093 (305,5 K) 5903 (298 K)	1600	999,8 (273,15 K) [1] 916,8 (273,15 K) [s]
SPECIFIC HEAT, cx10^{-3} [J.kg^{-1}.K^{-1}]	0,167	0,397 [1] 0,34 [s]	3,4 [1] 1,76 [s]	4,21 [1] 2,04 [s]
SURFACE TENSION, σx10^2 [N.m^{-1}]		73,5 (303 K)		7,56 (273,2 K)
THERMAL CONDUCTIVITY, k [W.m^{-1}.K^{-1}]	19	33,7		0,567 (273,2 K) [1] 2,2 (273,2 K) [s]
THERMAL DIFFUSIVITY, αx10^8 [m^2.s^{-1}]		ESTIMATED VERY HIGH		13,5 [1] 8,43 [s]
VAPOR PRESSURE, p_v [Pa]		133 (1622 K)		610,4 (273,2 K)
VISCOSITY, μx10^3 [Pa.s]		1,612 (370,8 K)		1,79 (273 K)
MELTING TEMPERATURE [K]	343	302,93	AVAILABLE IN RANGE 222 to 505	273,15
BOILING TEMPERATURE [K]		2256		373,2
LATENT HEAT OF FUSION, h_fx10^{-5} [J.kg^{-1}]	0,326	0,803	2,3	3,334
COEFF. OF THERMAL	6,6 x 10^{-5}	1,2 x 10^{-4} [1] 5,8 x 10^{-5} [s]		1,125 x 10^{-4}

	METALLIC		MISCELLANEOUS	
NAME	**CERROBEND EUTECTIC**	**GALLIUM**	**TRANSIT HEET**	**WATER**
EXPANSION, β [K^{-1}]				
VOLUME CHANGE ON MELTING	+1,7%	–3,2%		–9,06%
FLASH POINT [K]				NONE
AUTOIGNITION TEMPERATURE [K]				NONE
SUPERCOOLING	Slight, about $\Delta T = 1$ K	Variable from 12 K to 30 K. Depends on purity.		Variable, depends upon impurities and rate of cooling.
COST				
COMPATIBILITY	Compatible with Aluminium.	Compatible with Titanium, fused quartz, ceramics, Titania, Zirconia, Beryllia, Alumina, Tungsten, Graphite and Tantalum. Aluminium and anodized Aluminium are attacked.		Compatible (destilled or deionized water) with: Al and Al-Alloys; Cu and Cu-Alloys; Ni; Ti and Ti-Alloys; Mg; W; Zr and Zr-Alloys; Be up to 533 K; ZN up to 322 K; graphite; hidrocarbons, silicone and urethane rubbers; neoprene; nylon; polyethylene; polypropylene; polystyrene; acrylics.
COMMENTS	Cerrobend is a registered trademark of Cerro Co., New York, N.Y. A low melting eutectic.	Is a gray-white metal. The presence of Li and Bi as impurities tend to decrease supercooling. Appear to be non-poisonous.	Transit Heet is a registered trademark of Royal Industries, Santa Ana, California.	Clear, colorless liquid. Non-toxic. Non-flammable.

[l]   Liquid.

[s]   Solid.

NOTE   After Grodzka (1969) [12], Hale, Hoover & O'Neill (1971) [13], DORNIER SYSTEM (1971) [9].
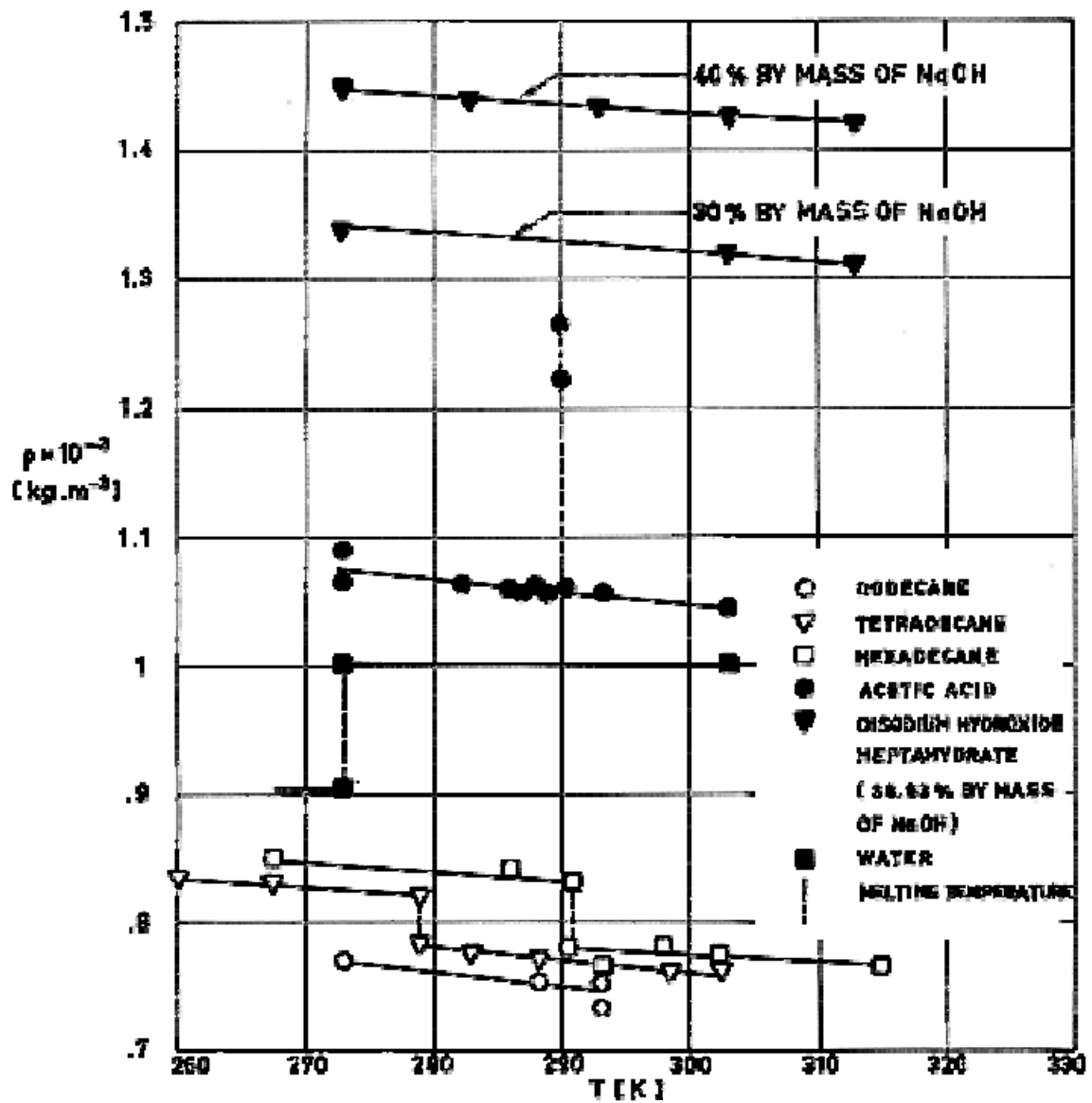
Note: non-si units are used in this figure

Figure 5-3: Density, ρ, vs. temperature T, for several PCMs. From DORNIER System (1971) [9].
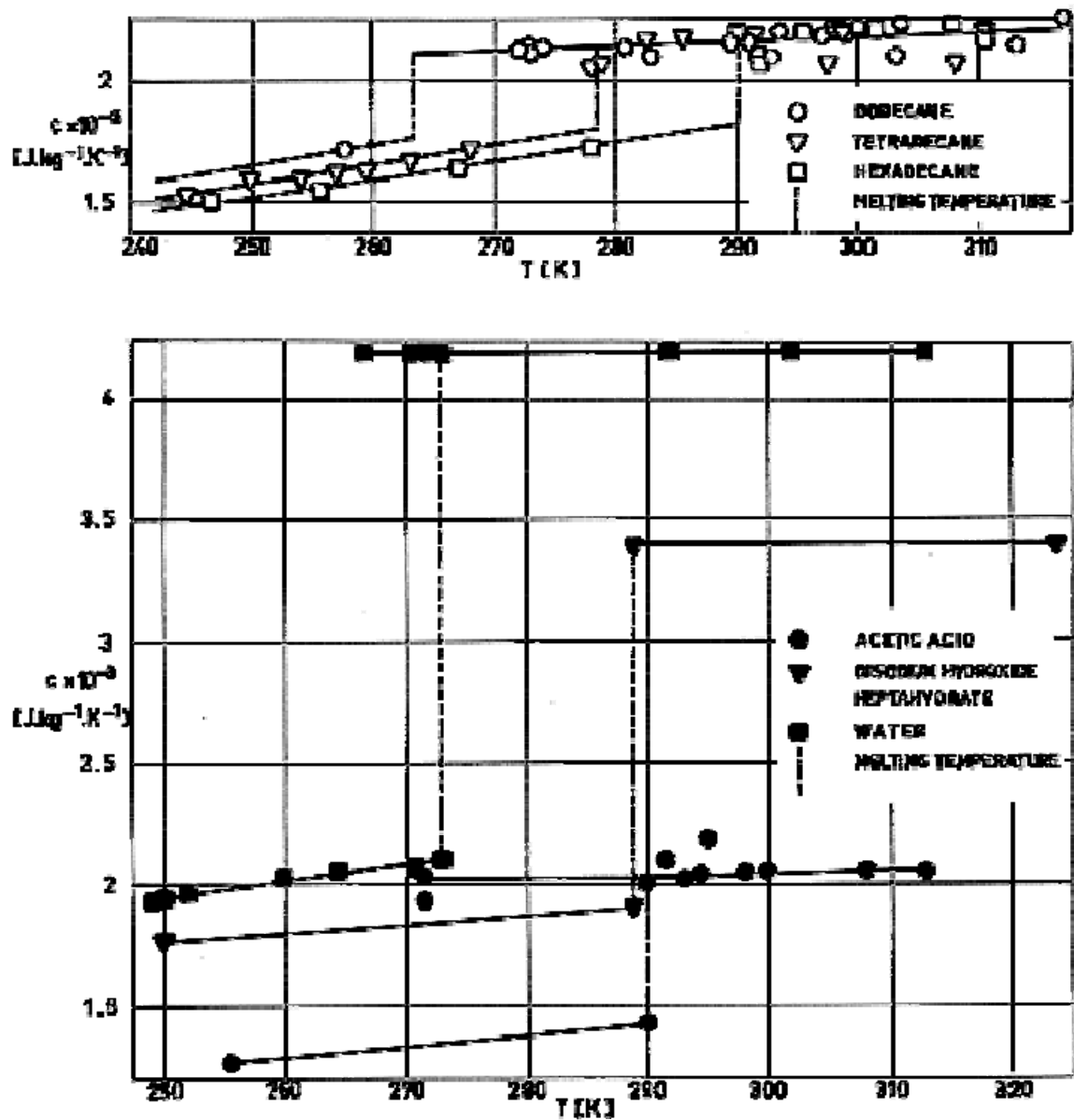
Note: non-si units are used in this figure

Figure 5-4: Specific heat, *c*, vs. temperature *T*, for several PCMs. From DORNIER System (1971) [9].
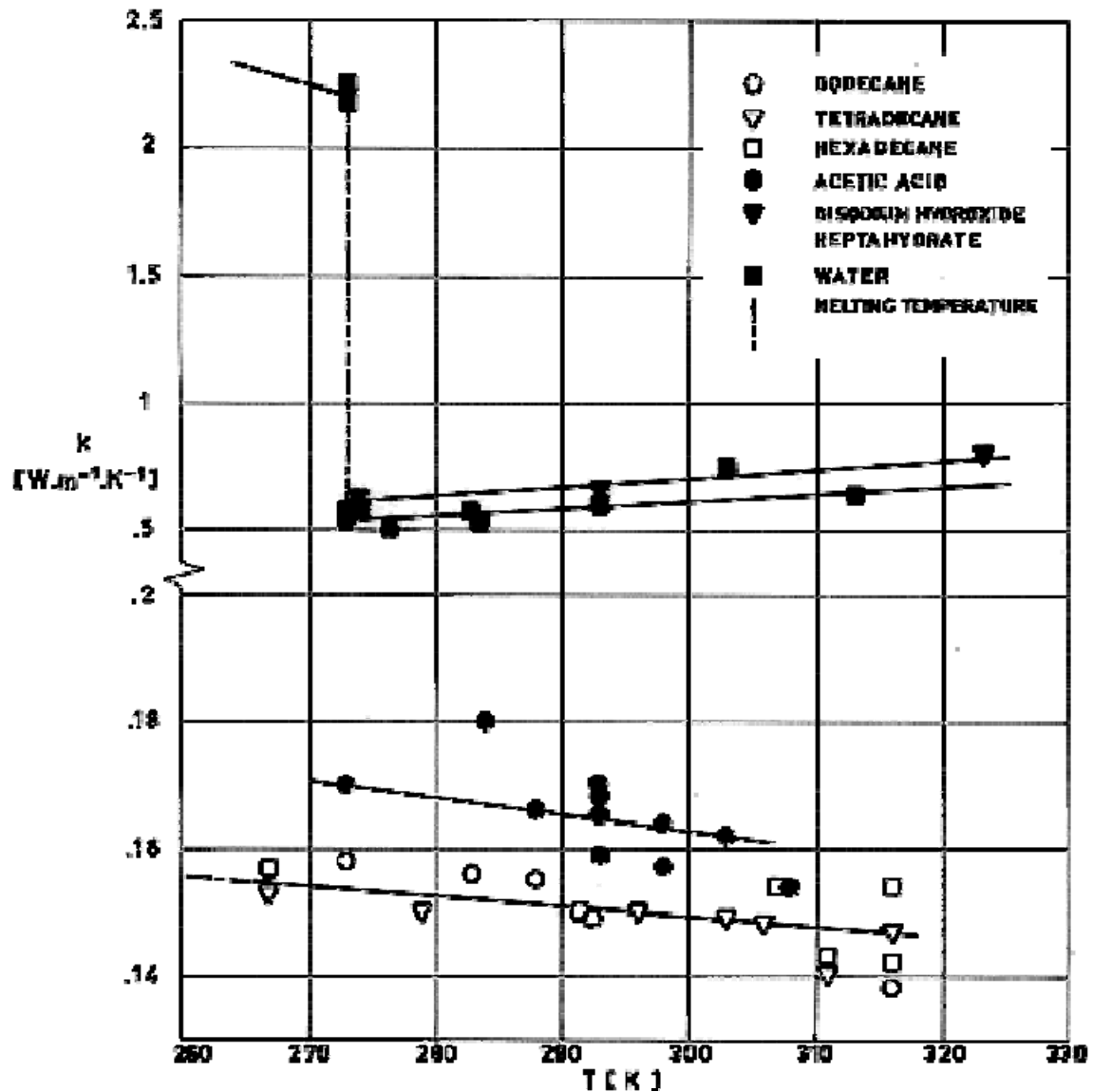
Note: non-si units are used in this figure

Figure 5-5: Thermal conductivity, *k*, vs. temperature *T*, for several PCMs. From DORNIER System (1971) [9].
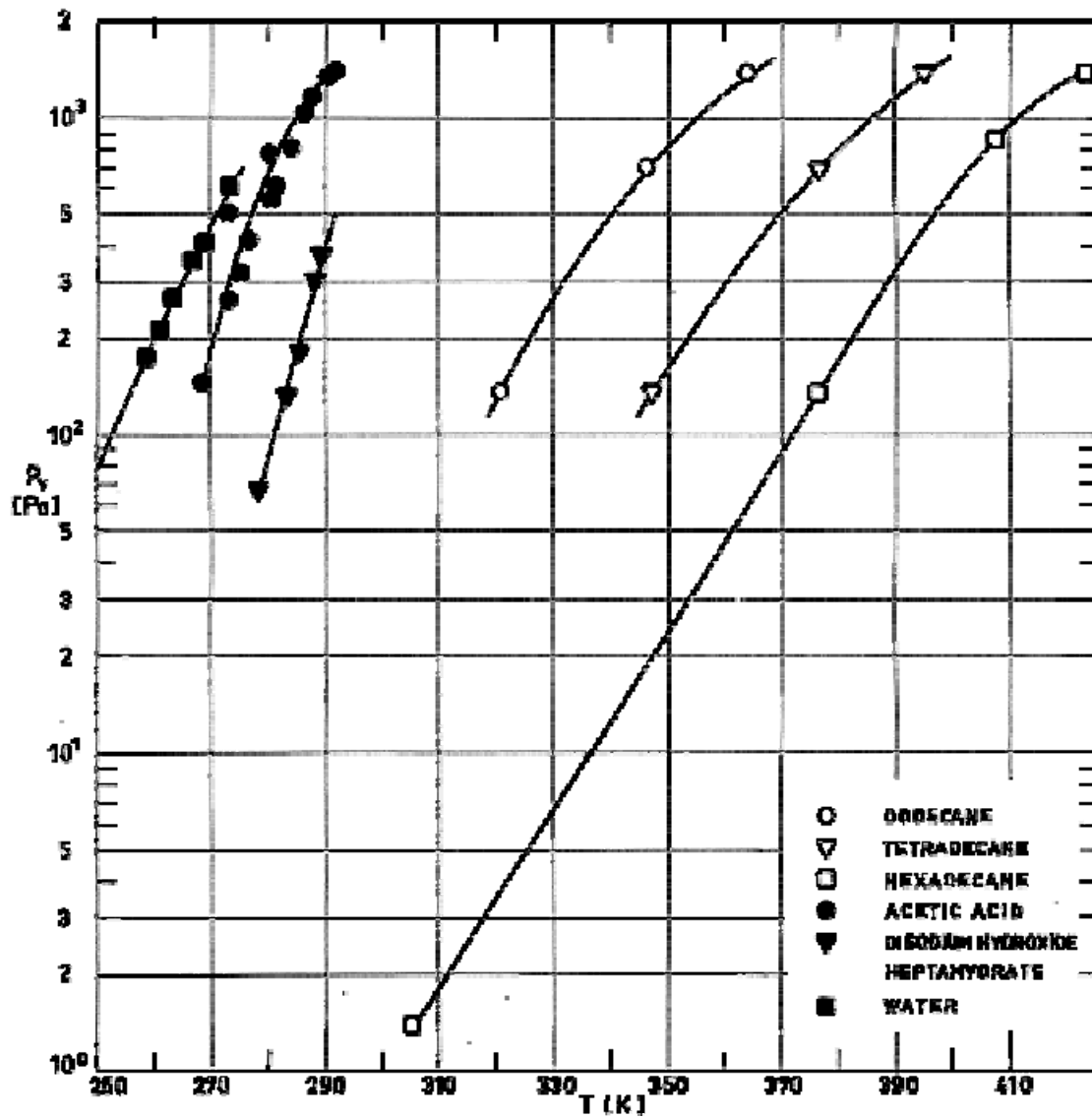
Figure 5-6: Vapor pressure, p_v, vs. temperature T, for several PCMs. From DORNIER System (1971) [9].

Note: non-si units are used in this figure

Figure 5-7: Viscosity, μ, vs. temperature T, for several PCMs. From DORNIER System (1971) [9].

Note: non-si units are used in this figure
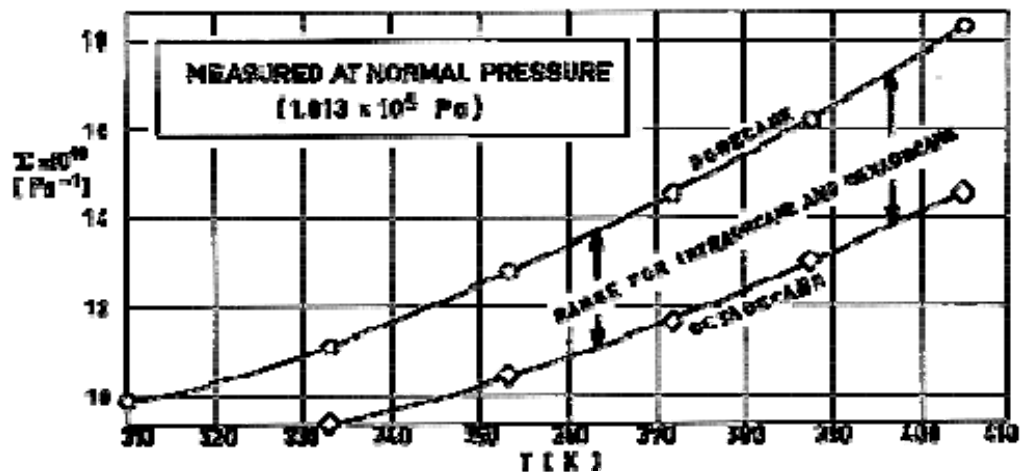
Figure 5-8: Isothermal compressibility, χ, vs. temperature T, for several PCMs. From DORNIER System (1971) [9].

6
PCM technology

6.1   Containers

Containers of PCMs differ primarily in their outer shape (circular or rectangular), and in the flexible element which may be used for compensating the volume variation of the material during the phase change.

The flexible elements of the container may be: metallic bellows, metallic membranes, or rubber diaphragms.

1.   Elastic bellows placed between the cold plate and the opposite wall is prestressed in tension during the filling process. After filling is complete, this bellows exerts a compressive load on the liquid PCM. When solidification occurs, the bellows further contract and still maintain a compressive load on the PCM. The major advantage of a bellows-type container is that no void or gas volume is left in the container, thence the heat transfer within the container is not decreased by the presence of such voids.

2.   Metallic membranes should be prestressed prior to installation, and have a negative deflection in the load-free state. The initial deflection of the metallic membrane will depend on the filling level of the PCM in the container. When a rigid container is used it is necessary to provide a void or gas volume for expansion of PCM during melting.

A significant problem in designing the rigid container is the sizing of the void volume. If the container were totally vacuum-tight and evacuated prior to flight, the void volume required would merely be the volume change upon expansion of the PCM. Nevertheless air will enter in the void volume, prior to launch, when the PCM is still in the solid phase, by effusion through the minute holes existing in joints and seams of the container. Regardless of the pressure of this gas, when complete melting occurs a large pressure could appear inside the container because of the volume changes associated with the melting process. Therefore, the inner volume of the container should be large enough to keep the pressure of trapped gases below reasonable limits.

6.2   Fillers

The use of fillers with PCM offers distinct advantages, the primary one being the improvement of the thermal conductivity of the PCMs which, unless the metallic, have low conductivities.

When fillers are not used, the temperature at the heated surface of the PCM may rise far above its melting point, with solid material still available but thermally isolated from the heated surface.

On the other hand when a metal filler is used, thermal gradients in the PCM bulk are considerably reduced, because of the high thermal conductivity of the filler.

The fillers which, according to reported tests, are the most widely used are:

- Aluminium: as powder, foam, wool, fins, or honeycomb.

- Copper foam.

- Alumina (Al$_2$O$_3$) as powder or foam.

The reported results indicate that aluminium honeycomb offers the largest system improvement compared to other fillers tested.

An important type of filler which deserves more attention than that paid up to the moment is formed by aluminium fins. In some cases fins are used in preference to honeycomb because of the problems associated with contact conductances between the honeycomb and the cold plate. Fins can be welded to the cold plate whereas honeycomb is usually attached to it with epoxy, which results in an undesirably high contact resistance.

6.3 Containers and fillers

6.3.1 Materials and corrosion

Containers and fillers of PCM cells are made of metals because they provide a high thermal conductivity to the cell.

Four different metals are currently used for these purposes: Aluminium, Cooper, Titanium and Stainless Steel.

The compatibility of PCM with these metals is limited by the corrosion induced by the PCM itself or by impurities in it.

The primary mode of material corrosion of concern in PCM technology is chemical corrosion. Generally, salt hydrates, metalics, and fused salt eutectics are the most corrosive materials.

Corrosion can be reduced by appropriate inhibitors. These inhibitors can be classified in the following two basic categories:

1. Oxide films such as those which appear on aluminium, titanium, and stainless steel. The protective layer of oxide is inert to many PCM.

2. Additives which form protective coatings, constituted by compounds absorbed directly on the metal surface, providing physical protection against the corrosive attack. Among these additives, long chain aliphatic acids and aqueous solutions of sodium bicarbonate and phosphate are the most widely used. Normally small amounts of these substances are added to the PCM.

Relevant physical properties of the metallic materials mentioned above are presented in Table 6-1. PCM which are compatible with these metals are listed in Table 6-2.

Table 6-1: Physical Properties of Several Container and Filler Materials

	ALUMINIUM	COPPER	TITANIUM	STAINLESS STEEL
DENSITY, ρ [kg.m^{-3}]	2700	8910	4540	7530-8010
MODULUS OF ELASTICITY, Ex10^{-10} [Pa]	6,96	11,7	11	20
SPECIFIC HEAT, c [J.kg^{-1}.K^{-1}]	894	422	519	460-500
TENSILE STRENGTH, σ_{ult}x10^{-8} [Pa]	1,8-2,3	2,2-3,4	3-4,2	2,76-22,7
THERMAL CONDUCTIVITY, k [W.m^{-1}.K^{-1}]	113-238	391	7-14	13-37
LINEAR THERMAL EXPANSION COEFFICIENT, βx10^6 [K^{-1}]	23,8	17,7	9-11	11-20,3

NOTE   After Wilkins & Jenks (1948) [26], Hodgman (1953) [14], Hale, Hoover, & O'Neill (1971) [13], DORNIER SYSTEM (1972) [10].

Table 6-2: Compatibility of PCM with Several Container and Filler Materials

	ALUMINIUM	COPPER	TITANIUM	STAINLESS STEEL
PARAFFINS	Compatible	Compatible		All stainless steels are moderate to excellent in corrosion resistance. Corrosion resistance of all stainless steels depends upon its chromium content. Chrome as a pure metal is very active, but it occurs as an oxide in stainless steel, usually FeO.Cr$_2$O$_3$. The reason stainless steels are so inert to many environments is due to the formation of this oxide. Since the alloy vary so widely in corrosion resistance, it would be advisable to consult data for specific alloys.
NON-PARAFFIN ORGANICS	Compatible with: Acetic Acid, Benzoic Acid, Elaidic Acid, Ethylene Glycol, Methyl Fumarate, Myristic Acid, Oxazoline Waxes, Polyethylene, Glycol, Stearic Acid, Tristearin.	Compatible with: Acetic Acid, Formic Acid.	Compatible with: Acetic Acid, Chloroacetic Acid, Salicylic Acid, Stearic Acid, Succinic Acids.	
SALT-HYDRATES	Non-compatible	Non-compatible	Compatible with: Magnesium sulfate, Sodium Sulfate.	
METALLICS			Compatible with: Gallium.	
FUSED SALT EUTECTICS	Compatible with most Fused Salt Eutectics.		Compatible with: Potasium Chloride, Sodium Chloride.	
MISCELLANEOUS	Compatible with Distilled or Deionized Water.	Compatible with Distilled Water.	Compatible with Water.	
COMMENTS	-Non-compatible with PCMs which are strong acids or bases. -Compatible with oxidizing PCMs only if oxide film is presented.	-Compatible with most non-oxidizing salt solutions. -The attack by mineral and organic acids is dependent	-Compatible with most inorganic and organic salts.	

	ALUMINIUM	COPPER	TITANIUM	STAINLESS STEEL
	-Compatible with most inorganic PCMs and with organic sulfides.	largely upon the presence of an oxidizing agent on solution.		

NOTE   After Wilkins & Jenks (1948) [26], Hale, Hoover, & O'Neill (1971) [13], DORNIER SYSTEM (1972) [10].

6.3.2   Exixting containers and fillers

6.3.2.1   Container and fillers developed by dornier system

DORNIER SYSTEM, Germany, has developed and tested the following fillers:

—   Fully Machined Filler.

—   Honeycomb Filler.

—   Honeycomb Filler with Heat Conduction Fins.

The mesh size of the honeycomb used is $3,175 \times 10^{-3}$ m, and the foil thickness $5,08 \times 10^{-5}$ m (perforated). The density is 129,3 kg.m^{-3}. The choice of the honeycomb core is affected by the required heat conduction. material is aluminium alloy.

Additional fins lead to an increased heat conduction. The fully machined filler being expensive, is used only in exceptional cases of high heat conduction requirements.

The containers developed by DS have been the following:

—   Container with machined wall profile and welded top and bottom. (Figure 6-1).

—   Container fully machined with welded top. (Figure 6-2).

—   Machined wall profile with adhesive bonded top and bottom. (Figure 6-3).

The material used has been aluminium alloy in all cases. The honeycomb filler has been adhesive-bonded to the container.
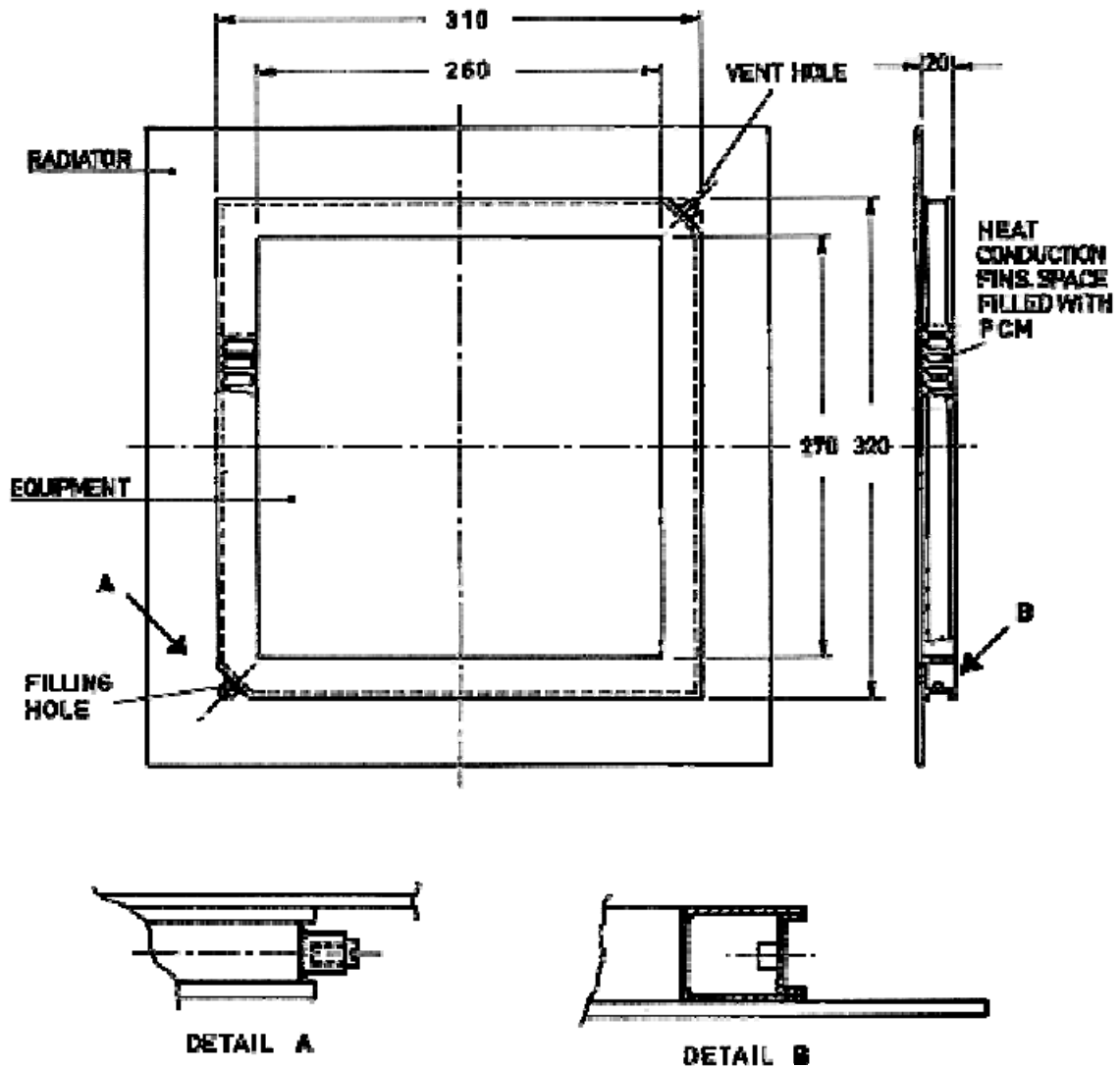
Figure 6-1: Container with machined wall profile and welded top and bottom. Honeycomb filler with heat conduction fins. All the dimensions are in mm. From DORNIER SYSTEM (1972) [10].
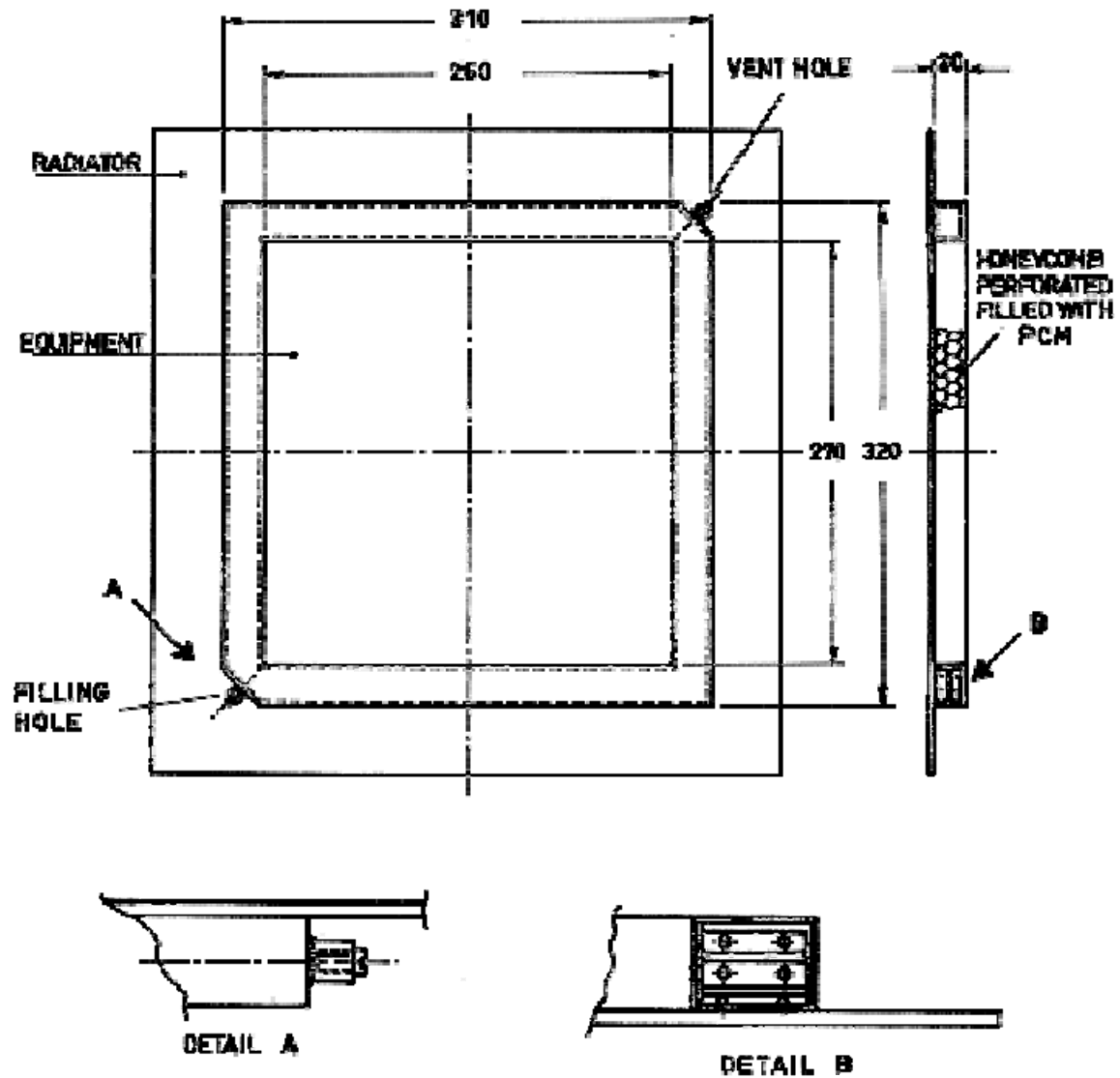
Figure 6-2: Fully machined container with welded top. Honeycomb filler. All the dimensions are in mm. From DORNIER SYSTEM (1972) [10].
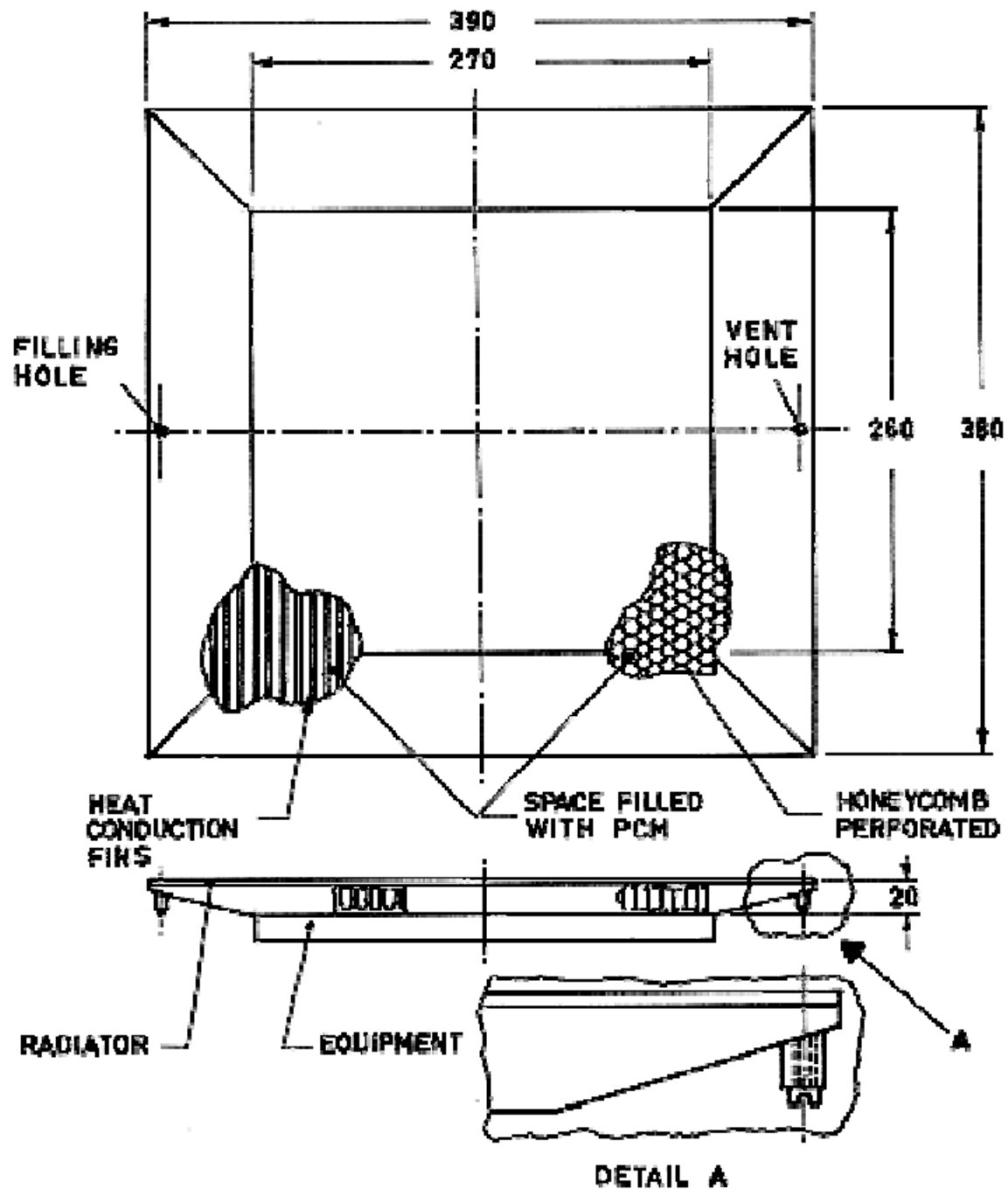
Figure 6-3: Machined wall container profile with top and bottom adhesive bonded. Alternative filler types are honeycomb or honeycomb plus fins. All the dimensions are in mm. From DORNIER SYSTEM (1972) [10].

7
PCM performances

7.1 Analytical predictions

7.1.1 Introduction

Several input data should be taken into account when the use of a PCM capacitor is being considered. In the simplest case, these data should be:

1. The heat transfer rate, q_0, from the heat source.

2. The heat rejection rate, q_R, to the sink.

3. The maximum energy which can be stored in the PCM package.

4. The time history for heating and cooling.

5. the temperature level.

6. Constraints of size, mass, and material compatibility.

A trade-off study of the multiple possible choices requires a simple analytical model for relating the properties of the PCM and filler, and the dimensions of the package, to the above data. An extremely simple analytical model is presented in this clause. The mentioned model is based on the following assumptions.

1. The temperature field is one-dimensional, it depends on the coordinate through the PCM Package, x, and on time, t.

2. The system is controlled by melting. This means that the variation of the internal energy of the system is mainly due to melting. This is so because, in most cases, the ratio $h_f/c(T_0-T_M)$ is much larger than one.

3. PCM properties are constant although different from solid to liquid.

4. Non-steady effects appear through changes in the position of the melting (or freezing) front. This front is supposed to be planar and infinitely thin.

5. Conduction of heat through the PCM-filler system takes place according to the "parallel thermal conduction model". In this model heat is transferred simultaneously although separately through two different paths, one exhibiting the characteristics of the PCM and the other one those of the filler, without any interaction between both paths.

7.1.2 Heat transfer relations

Let us consider the system sketched in Figure 7-1 below, which consists of:

    1.   the components whose temperature are controlled,

    2.   a PCM package, and

    3.   a radiator.
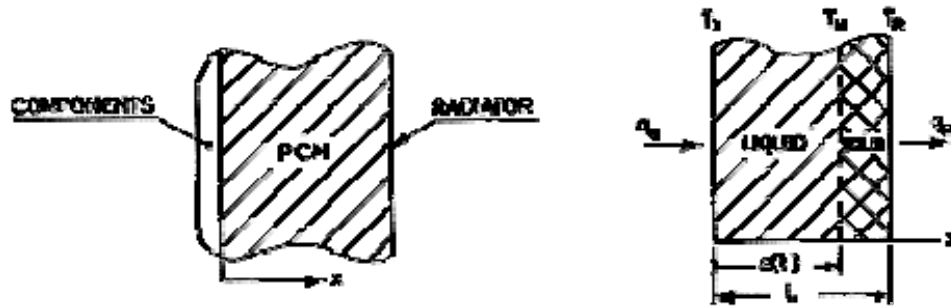
Figure 7-1: Sketch of the PCM package showing the solid-liquid interface.

When it is assumed that the system is one-dimensional, the temperature -which depends only on the gravitational variable, *x*, and on the time, *t*- will obey the following differential equation:

$$\rho \frac{\partial (cT)}{\partial t} = -\frac{\partial}{\partial x}\left(k \frac{\partial T}{\partial x} \right)$$

[7-1]

Note: non-si units are used in this figure

The value of ρ, *c* and *k* should by those corresponding to the liquid phase when $0 \leq x \leq s(t)$, and those corresponding to the solid otherwise.

The boundary conditions are:

at $x = 0$; $T = T_0$

at $x = s(t)$; $T = T_M$, and

$$k_s \frac{\partial T}{\partial x}\bigg|_{x=s(t)} = k_l \frac{\partial T}{\partial x}\bigg|_{x=s(t)} + \rho h_f \frac{ds(t)}{dt}$$

[7-2]

Note: non-si units are used in this figure

at $x = L$; $T = T_R$

Notice that, once T_0 and T_R are assumed to be constant, the configuration only depends on *t* through the position of the solid-liquid interface, whose temperature is obviously constant.

When the ratio $c(T_0 - T_M)/h_f$ is much lower than one,

$$\frac{c(T_0 - T_M)}{h_f} << 1$$

[7-3]

Note: non-si units are used in this figure

the rate of variation, by mere conduction, of the internal energy of the system, which is of the order $\rho c(T_0 - T_M)$, is much smaller than the rate of variation by melting, of the order of ρh_f, so that the system is melting-controlled; the freezing (or melting) front reaches very soon its operating position, and a steady-state appears after a short time.

From the above differential equation, with $\partial T / \partial t = 0$, it is deduced that:

$$\frac{dT}{dx} = \text{Constant}$$

[7-4]

Note: non-si units are used in this figure

although the constant may take different values on either side of the melting front. In the liquid side:

$$\left(\frac{dT}{dx}\right)_l = -\frac{q_0}{k_l}$$

[7-5]

Note: non-si units are used in this figure

while in the solid side:

$$\left(\frac{dT}{dx}\right)_s = -\frac{q_R}{k_s}$$

[7-6]

Note: non-si units are used in this figure

In addition, the position of the interface at the time t, is given by the differential equation:

$$\frac{ds(t)}{dt} = \frac{1}{\rho h_f}\left[k_l \frac{T_0 - T_M}{s(t)} - k_s \frac{T_M - T_R}{L - s(t)}\right]$$

[7-7]

Note: non-si units are used in this figure

with the initial condition $s(0) = 0$.

The maximum temperature of the components for a given PCM package is that required to melt all the PCM. In such a case, the temperature distribution across the PCM is a straight line, and the temperature of the components is given by:

$$T_0 = T_M - L\left(\frac{dT}{dx}\right)_l = T_M + \frac{q_0 L}{k_l}$$

[7-8]

Note: non-si units are used in this figure

Once fixed the maximum temperature which the components can withstand, the above equation gives the required thickness, *L*, of a given PCM.

When a filler material is integrated into the PCM package to improve its thermal conductivity, the heat transfer rate has two components, that through the PCM and that through the filler. Assuming that the PCM is completely molten, and using a parallel thermal conduction model, the following expression results:

$$q_0 A_T = k_F \frac{T_0 - T_M}{L} A_F + k_l \frac{T_0 - T_M}{L} A_{PCM}$$

[7-9]

Note: non-si units are used in this figure

where the first term in the right-hand side gives the heat transfer contribution of the filler, and the second one the contribution of the PCM.

Introducing an apparent conductivity of the PCM package, k_T, defined as: $k_T A_T = k_F A_F + k_l A_{PCM}$, the maximum temperature of the components will be:

$$T_0 = T_M + \frac{q_0 L}{k_T}$$

[7-10]

Note: non-si units are used in this figure

In addition, assuming again that the material is completely molten, the maximum energy stored by the PCM package will be given by:

$$E_{\max} = \rho_l L h_f A_{PCM} + \left(\rho_F A_F c_F + \rho_l A_{PCM} c_l\right)\frac{(T_0 - T_M)L}{2}$$

[7-11]

Note: non-si units are used in this figure

Now, by means of [7-10] and [7-11], and the additional equations:

$$A_T = A_F + A_{PCM}$$

[7-12]

$$M_T = M_F + M_{PCM} + M_C$$

[7-13]

$$M_{PCM} = \rho_l L A_{PCM}$$

[7-14]

$$M_F = \rho_l L A_F$$

[7-15]

it is possible to obtain the following relevant physical magnitudes of the PCM slab as a function of the ratio A_F/A_T:

— Thickness, L, of the PCM slab.

— Total thermal conductivity, k_T.

— Mass of the PCM, M_{PCM}.

— Total mass, M_T.

— Excursion temperature, $\Delta T = T_0 - T_M$.

provided that the following data have been fixed:

— Phase change material.

— Filler material.

— Container mass, M_C.

— Total cross section, A_T.

— Required maximum heat storage, E_{max}.

— Heat transfer rate from the components whose temperature are controlled, q_0.

Values of these physical magnitudes, as calculated by using the simplified analytical model, have been plotted versus the ratio A_F/A_T in Figure 7-2 and Figure 7-3. Notice that for very low values of this ratio, the excursion temperature, $T_0 - T_M$, could be large, and being large the ratio $c(T_0 - T_M)/h_f$, the steady-state assumption could not be valid. Nevertheless, it is hoped that the simplified analytical model can be used in all cases of practical interest.
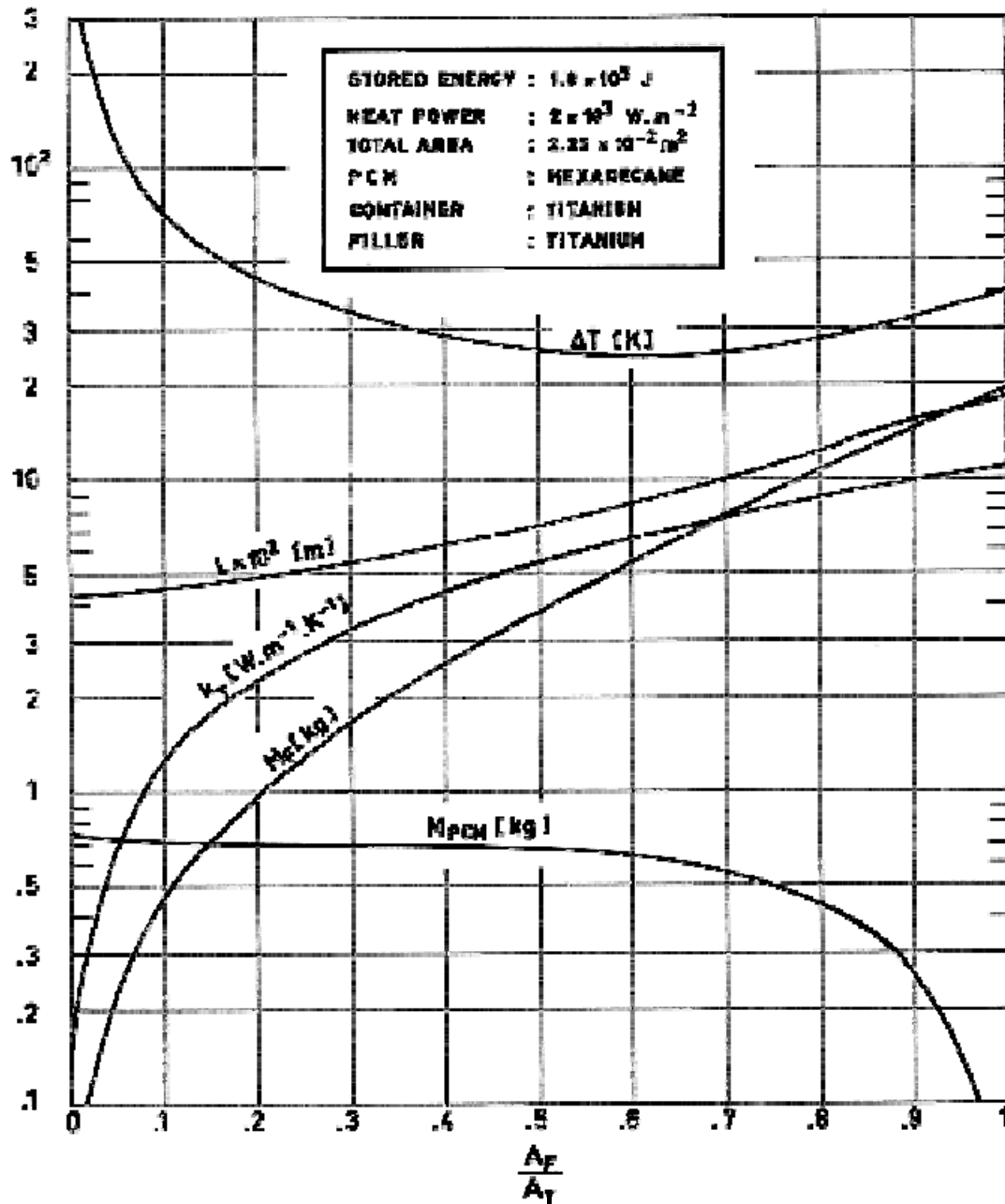
Note: non-si units are used in this figure

Figure 7-2: PCM mass, M_{PCM}, filler mass, M_F, package thickness, L, temperature excursion, ΔT, and total conductivity, k_T, as functions of the ratio of filler area to total area, A_F/A_T. Calculated by the compiler.
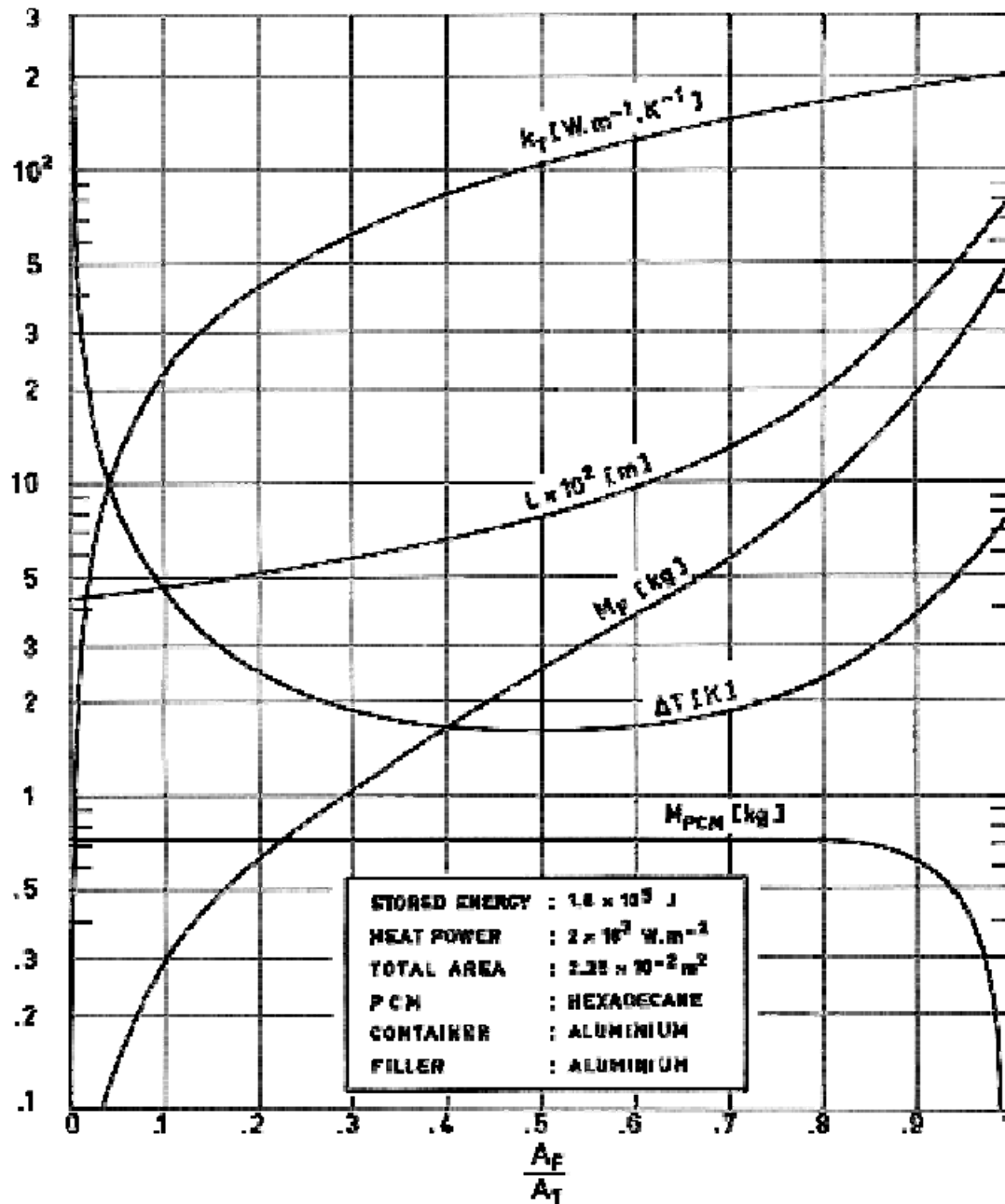
Note: non-si units are used in this figure

Figure 7-3: PCM mass, M_{PCM}, filler mass, M_F, package thickness, L, temperature excursion, ΔT, and total conductivity, k_T, as functions of the ratio of filler area to total area, A_F/A_T. Calculated by the compiler.

8
Existing systems

8.1 Introduction

PCM capacitors from several developers are described, as thoroughly as possible, in this clause.

As a general rule, only devices developed after around 1972 have been enclosed. The paper by Abhat & Groll (1974a) [1] could be helpful for a survey of previous effort.

Most of the described devices are (or were) in the development stage; only those in clause 8.5 have been flight tested, and none of them seems to be commercially available with the exception of Trans Temp Systems, clause 1.1

The lastly mentioned products have not been developed with spacecraft applications in sight, nevertheless they are worth being included because they take advantage of PCM technology for more or less mundane applications.

8.2 Dornier system

Developer	Dornier System GmbH, Friedrichshafen, Federal Republic of Germany		
Model	1	2	3
Heat Storage [J]	$5,4 \times 10^5$ (150 W.h)	$1,08 \times 10^5$ (30 W.h)	$1,368 \times 10^6$ (380 W.h)
Heat Storage per Unit Mass [J.kg^{-1}]	$1,35 \times 10^5$	$1,35 \times 10^5$	$1,52 \times 10^5$
Thermal Conductance [W.K^{-1}]			
Operational Temperature Range [K]	293-313	293-313	
Filling Temperature [K]			
Phase Change Temperature [K]			
Temperature Stability [K]	±3 (During Eclipse)		
Shape	Box-Shaped		
Overall Dimensions [m]	0,360x0,180x0,059	0,150x0,150x0,035	0,500x0,500x0,035
Container		Fully machined container in the shape of a hollow box with welded lid.	Machined wall profile with adhesive bonded top and bottom faces.
Filler		Two different fillers were envisaged: 1) Honeycomb core with cell axes normal to	Honeycomb 3×10^{-3} m from flat to flat, with a foil thickness of 5×10^{-5} m. Density 129,3 kg.m^{-3}. Honeycomb faces are perforated. Cell axes are

Developer	Dornier System GmbH, Friedrichshafen, Federal Republic of Germany		
Model	**1**	**2**	**3**
		the lid, Figure 8-2b. 2) Special matrix with cells parallel, and cover sheets or fins normal to the lid, Figure 8-2c. Filler adhesive bonded to the container.	perpendicular to top and bottom faces. Honeycomb adhesive bonded to the container.
Inner Volume [m^3]			
Ullage [%]			
Mass of Container & Filler [kg]			
Mass of PCM [kg]			
Overall Mass [kg]	4	0,80	9
PCM		Octadecane	
Container Materials		Aluminium alloy AlMg$_3$ (Al alloy 5302)	
Filler Materials		Aluminium alloy	
Other Materials		Bonding film REDUX (CIBA-GEIGY (UK) Limited, Duxford, Cambridge, CB2 4QA, England).	
Thermal Performances	No data given. The device has been developed, manufactured and tested	No data given. According to the developer, this device has been space qualified by long	No data given. The device has been developed, manufactured and tested according to specifications established for ATC

Developer	Dornier System GmbH, Friedrichshafen, Federal Republic of Germany		
Model	**1**	**2**	**3**
	according to specifications established for HLS (geostationary communications satellite).	time tests (about 2000 melting and freezing cycles during six months).	(geostationary satellite).
Lifetime	5 years (to be qualified).	1 year.	5 years (to be qualified).
Applications	Temperature control of a power supply unit during eclipse.	Temperature control of electronic equipment with different power profiles. Orbits near the Earth and transfer orbits.	1) Temperature control of high dissipation heat producing transmitters, Figure 8-3a. 2) Temperature control of 4 high dissipation heat producing transmitters under variable power profile, Figure 8-3b.
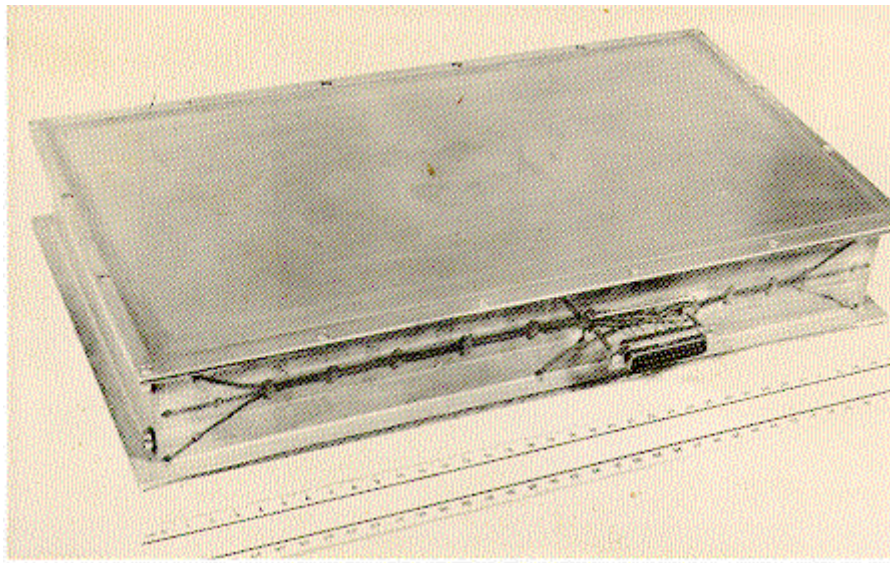
Figure 8-1: PCM capacitor for eclipse temperature control developed by Dornier System.
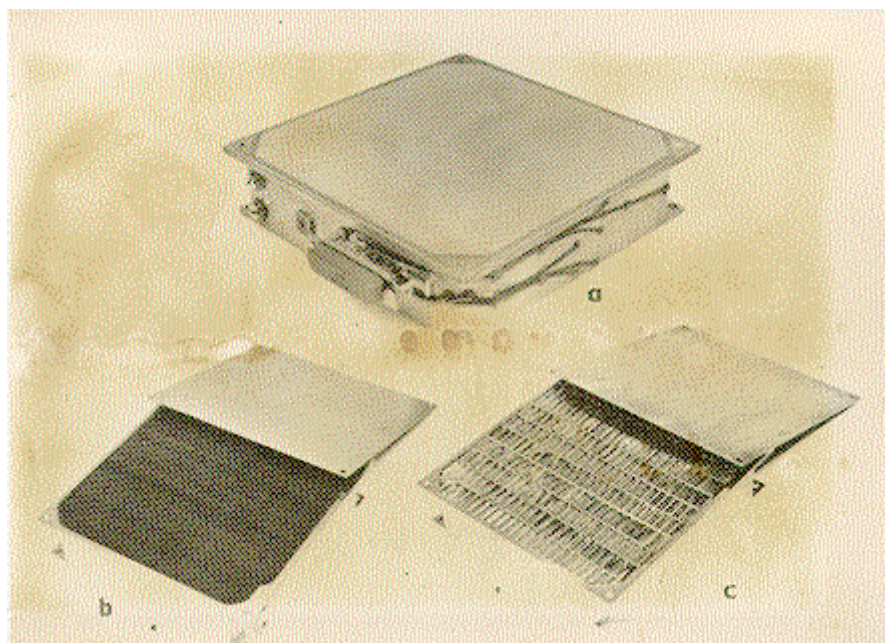
Figure 8-2: 30 W.h PCM capacitors developed by Dornier System. a) Complete PCM capacitor. b) Container and honeycomb filler with cells normal to the heat input/output face. c) Container, honeycomb filler with cells parallel to the heat input/output face, and cover sheets.
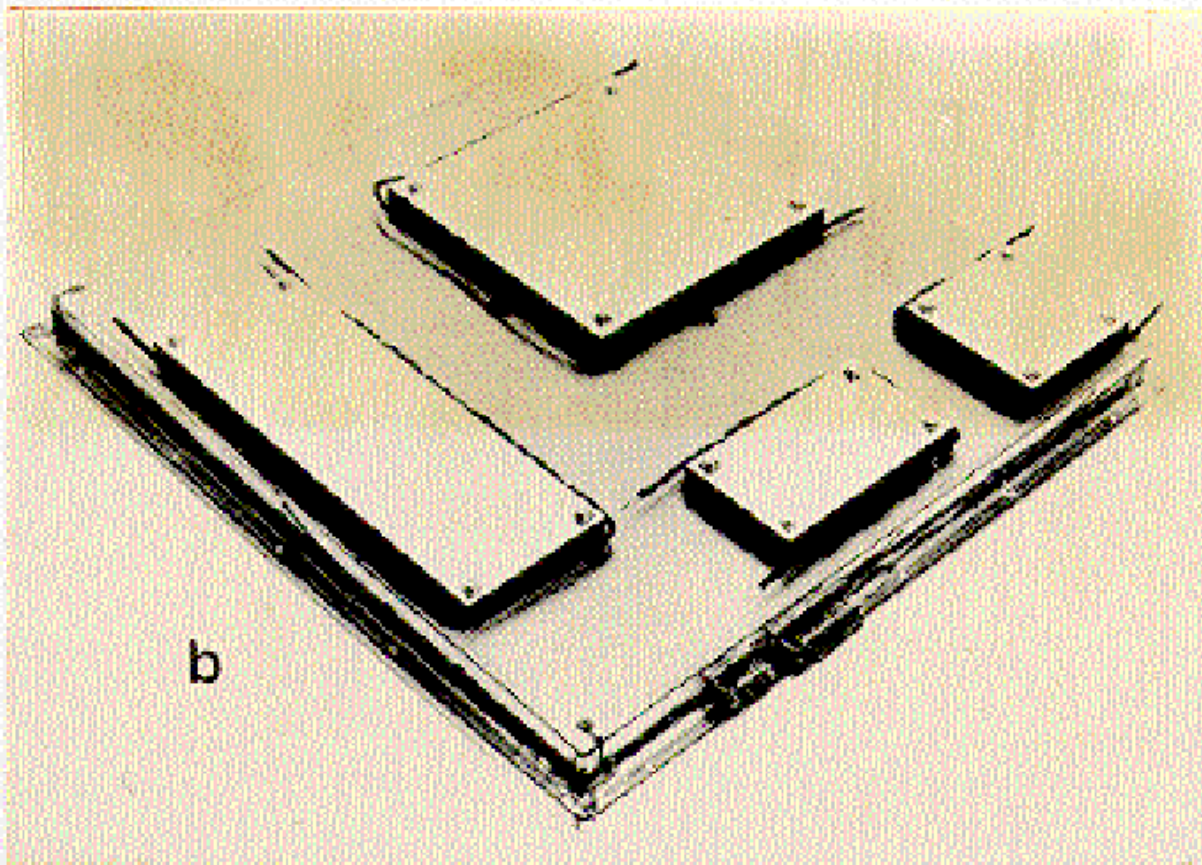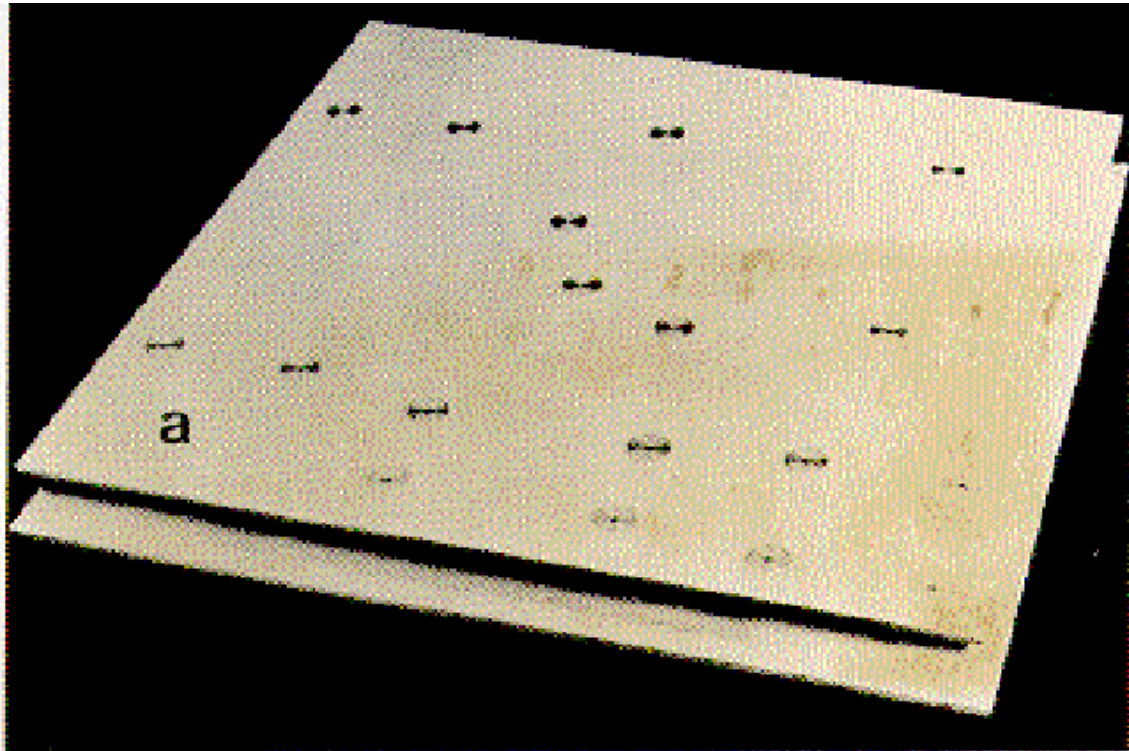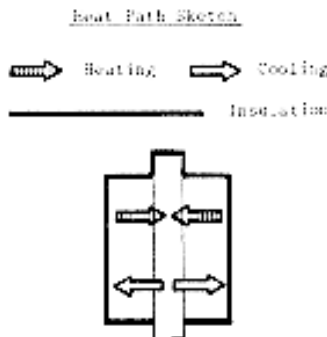
Figure 8-3: PCM mounting panels developed by Dornier Syatem. b) Shows the arrangement used for thermal control of four different heat sources.

Reference: DORNIER SYSTEM (1972) [10].

Developer	**Dornier System GmbH, Friedrichshafen, Federal Republic of Germany**	
Heat Storage [J]	8,64x10⁴ (24 W.h)	
Heat Storage per Unit Mass [J.kg⁻¹]	8,64x10⁴	
Thermal Conductance [W.K⁻¹]	20, based on the temperature gradient within the PCM device. 7,5, gravity parallel to the cells of the PCM device which is attached to an axial heat pipe. 2,5, gravity normal to the cells of the PCM device. In the last two cases, the thermal conductance of the heat pipe and the contact conductance between heat pipe and PCM device are presumably included.	
Operational Temperature Range [K]	308-313	
Filling Temperature [K]		
Phase Change Temperature [K]	309,8	
Temperature Stability [K]	±0,5	
Shape	Hexagonal Prism	
Overall Dimensions [m]	0,80 (diameter)x0,120	
Container	Consists of two parts, each of them half-enclosing the condense of the axial heat pipe. Thermal contact between the container and the heat pipe is achieved by pressure, through screws which hold together both parts of the container. 34 axial blind holes are bored in each part. These holes are partially filled with the PCM.	
Filler	Nonbored-out material left as integral part of the container.	
Inner Volume [m³]		
Ullage [%]	25 at operational temperature.	

Developer	Dornier System GmbH, Friedrichshafen, Federal Republic of Germany
Mass of Container & Filler [kg]	
Mass of PCM [kg]	
Overall Mass [kg]	1
PCM	Eicosane
Container Materials	Aluminium
Filler Materials	
Other Materials	
Thermal Performances	Results given by Koch, Lorschiedter, Strittmatter & Pawlowski (1976) [16] are: Temperature vs. time under heating (and under intermittent heating on-off) at selected points of the system which consists of a flat plate aluminium heat pipe with acetone, an axial titanium heat pipe with ethanol, and the PCM device. The flat plate is heated, on one side by a resistance heating foil. Results from ground tests and for flight tests, under six minutes near zero gravity, are given. Ground tests were performed with the axes of the cells (and axial heat pipe) in either vertical or horizontal position.
Lifetime	
Applications	Temperature stabilization of a heat pipe condenser. The device operates in the "unique mode" absorbing heat through melting. The complete system was flown as a part of the International Heat Pipe Experiment (IHPE) on 4 Oct. 1974 within a NASA sounding rocket programme (see McIntosh, Ollendorf & Harwell (1975) [17]). This particular experiment was designated as GfW-Heat Pipe Experiment, and has been reported by Koch, Lorschiedter, Strittmatter & Pawlowski (1976) [16].

TESTS

The system consisted of three components:

1. A flat plate aluminium heat pipe with acetone as working liquid.

2. An axial titanium heat pipe with ethanol.

3. The PCM device.

The flat plate circular heat pipe has a diameter of 0,15 m and a thickness of 9×10^{-3} m. Inside screens of $2,25 \times 10^{-4}$ m mesh size served as capillary structures.

The flat plate was heated on one side by a resistance heating foil fed by a battery. On the opposite side there was a cone-shaped condensation surface, into which the cone-shaped heating surface of the axial

heat pipe was fitted. This second heat pipe passed over into a transport and cooling zone with an outside diameter of 1,27x10-2 m via a cross section reduction. The total length amounted to about 0.6 m. The axial heat pipe was provided with a titanium screen structure and a spiral artery.

In the following, only tests relevant to the PCM device are considered. Additional information can be found in Koch, Lorschiedter, Strittmatter & Pawlowski (1976) [16].

Tests performed were

1. Component tests. Thermal tests, vibration tests and vacuum tests, which were carried out before integration.

   Tests with the PCM device indicated that 30 W could be stored during 30 min, which is well above the nominal heat storage (24 W.h) given in the previous page.

   The maximum temperature difference within the device was 1,5 K for 30 W heat transfer rate.

   The temperature difference between the axial heat pipe and the PCM device was either 12 K or 4 K depending on whether the gravity action was normal or parallel to the symmetry axis, respectively. This difference can be explained on the basis of the discussion in clause 5.1.3. The contact surface between the container and the PCM is smaller when the axes of the cells are horizontal and, the temperature gradient becomes larger.

   As it can be seen in Figure 8-6, the above mentioned temperature differences, 12 K and 4 K, are partially due to the conductance of the axial heat pipe, which is not given in the paper and which, although admittedly large, hardly can be an order of magnitude larger than the thermal conductance of such a massive metallic container. Thence the values 2,5 $W.K^{-1}$ and 7,5 $W.K^{-1}$, given in the previous page under Thermal Conductance, are probably too small.

2. System tests. The aim of the ground system tests was to determine the heating up time of the whole system and the temperature at selected points, once the steady state conditions are reached. Heating up times around 20 min are quoted by the authors. Data in Figure 8-6a indicate that the time for complete melting seems to be of the order of 90 min for 28 W transfer rate. The heating up time of the system with a pre-heated PCM device is much shorter, of the order of 4 min.

The system was launched aboard a Black Brant Sounding Rocket from White Sands, New Mexico, on 4 Oct. 1974. The flight provided 6 min of near zero gravity during which a total of 10 separate heat pipe experiments were performed.

According to Koch et al (1976) [16] the temperature differences under zero gravity were much higher than under normal gravity. Nevertheless, evidence of thermal contact between the PCM and the container walls exits since the wall temperature increased by 1,2 K within 100 s, whereas the estimated increase under no contact (detached needles of eicosane) would be of the order of 7 K within 100 s. Figure 8-6c lacks the required resolution to substantiate these contentions and, in any case, the experimental time looks unduly short to carry out this type of experiments.
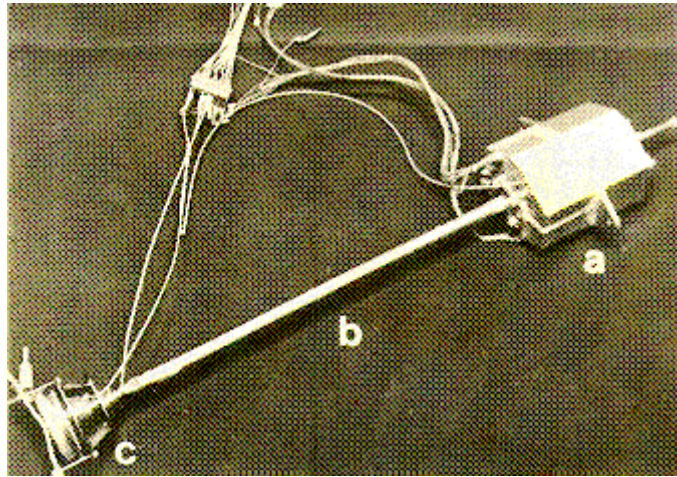
Figure 8-4: Thermal control system formed by, from right to left, a: PCM capacitor, b: axial heat pipe and, c: flat plate heat pipe. This system was developed by Dornier System for the GfW-Heat Pipe Experiment. October 1974.
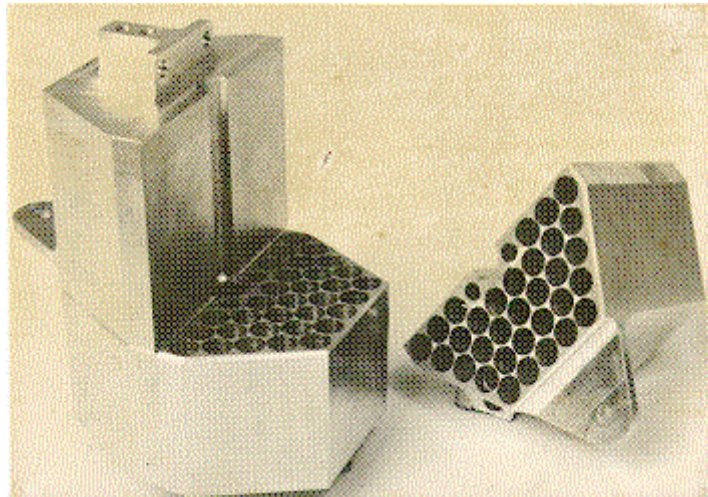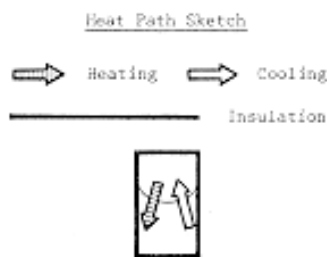
Figure 8-5: PCM capacitor shown in the above figure.
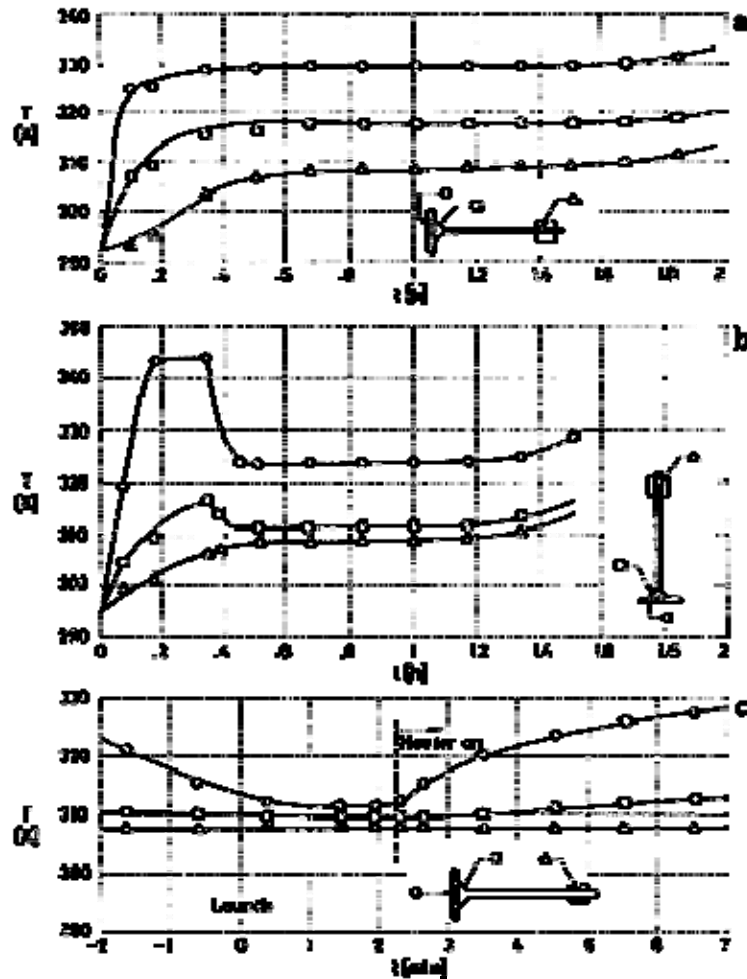
Note: non-si units are used in this figure

Figure 8-6: Temperature, *T*, as selected points in the complete system vs. time, *t*, during heat up. a) Ground tests. Symmetry axis in horizontal position. *Q* = 28 W. b) Ground tests. Symmetry axis in vertical position. *Q* = 28 W. The high temperatures which appear at start-up are due to pool boiling in the evaporator of the axial heat pipe. c) Flight experiment under microgravity conditions. *Q* not given. notice time scale.

References: DORNIER SYSTEM (1972) [10], McIntosh, Ollendorf & Harwell (1975) [17], Koch, Lorschiedter, Strittmatter & Pawlowski (1976) [16].

Developer	Dornier System GmbH, Friedrichshafen, Federal Republic of Germany	
Heat Storage [J]	$1{,}152 \times 10^5$ (32 W.h)	
Heat Storage per Unit Mass [J.kg^{-1}]	$1{,}152 \times 10^5$	Heat Path Sketch
Thermal Conductance [W.K^{-1}]		
Operational Temperature Range [K]	273-333	
Filling Temperature [K]		
Phase Change Temperature [K]	331	
Temperature Stability [K]	±2	
Shape	Circular Cylinder	
Overall Dimensions [m]	0,80 (diameter)x0,150	
Container		
Filler		
Inner Volume [m^3]		
Ullage [%]		
Mass of Container & Filler [kg]		
Mass of PCM [kg]		
Overall Mass [kg]	1	
PCM	Myristic Acid	
Container Materials		
Filler Materials		
Other Materials		
Thermal Performances	Results given in the reference are: Temperature excursions at the surface of the rate gyros under the extreme ambient temperatures 273 K and 333 K.	

Developer	Dornier System GmbH, Friedrichshafen, Federal Republic of Germany
	Temperature excursions at the surface of the rate gyros under changing ambient temperatures between 273 K and 333 K every 2 h. The aim of these tests was to demonstrate the reliable operation of the rate gyros during preflight phase (4 h) and flight phase (4 min) under different range environmental conditions as in Kiruna and Sardinia.
Lifetime	
Applications	Temperature stabilization of 8 W rate gyros within a 3-axis attitude control system. This device was developed for the rate gyros of the sounding rocket ESRO S-93.
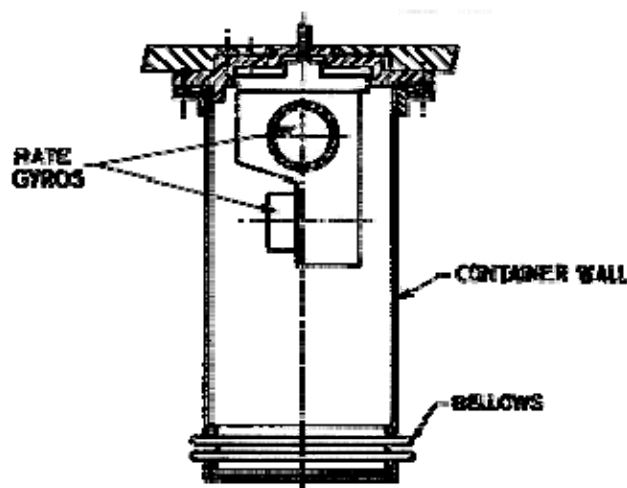
Figure 8-7: PCM capacitor developed by Dornier System for temperature control of two rate gyros onboard the Sounding Rocket ESRO "S-93".
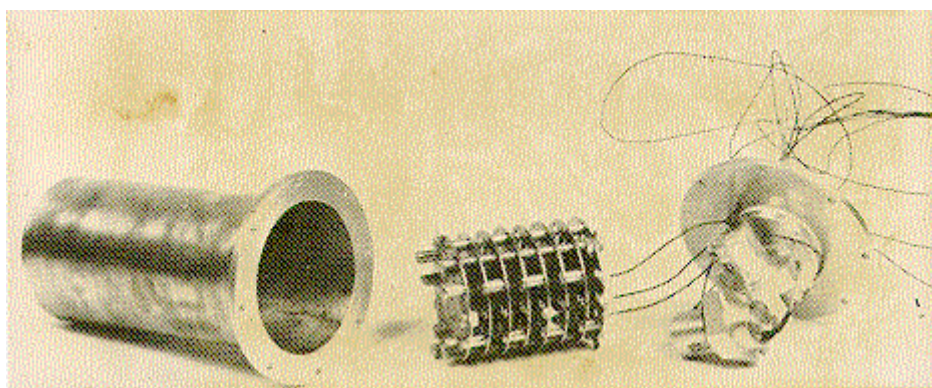
Figure 8-8: Test model of the above PCM capacitor. In the figure are shown, from right to left, the two rate gyros, the filler and the container.
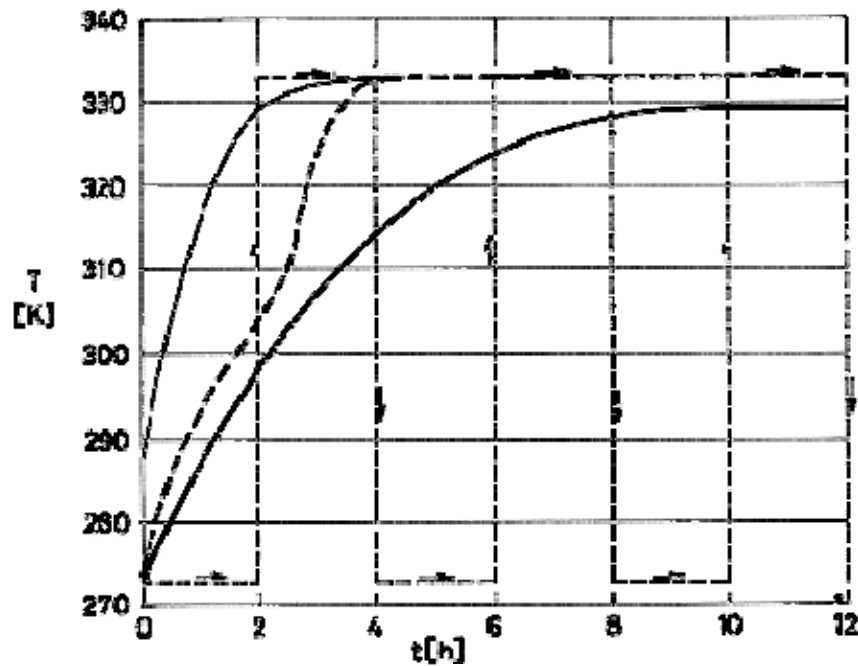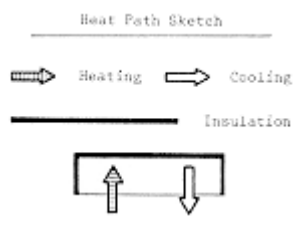
Figure 8-9: Temperature, *T*, at the surface of the rate gyros, vs. time, *t* . ▬▬ Ambient temperature, *T*$_R$ = 273 K. ▬▬ Ambient temperature, *T*$_R$ = 273 K. ▬ ▬ Ambient temperature changing between 273 K and 333 K. ▬ ▬ This curve shows the history of the ambient temperature used as input for the last curve above. References: DORNIER SYSTEM (1972) [10], Striimatter (1972) [22].

8.3   Ike

Developer	Institut für Kernenergetik of the University of Stuttgart (IKE) Federal Republic of Germany	
Heat Storage [J]	$1,8\times10^5$ (50 W.h)	Heat Path Sketch
Heat Storage per Unit Mass [J.kg^{-1}]	$8,5\times10^4$	
Thermal Conductance [W.K^{-1}]		
Operational Temperature Range [K]	223-373	
Filling Temperature [K]	373	
Phase Change Temperature [K]	300	
Temperature Stability [K]	±5	
Shape	Box-Shaped	
Overall Dimensions [m]	0,293x0,291x0,0195	
Container	Hollow box 0,0165 m deep and having $1,5\times10^{-3}$ m thick walls. A flange $1,5\times10^{-3}$mx$1,5\times10^{-3}$m is left all along the perimeter of the box to support the lid. The lid, $1,5\times10^{-3}$m thick, is electron beam welded along the box perimeter. Three 6×10^{-3} m diameter openings were provided, two in one side and the other in the opposite side for filling and evacuating purposes, respectively.	
Filler	1. 10^{-3}m thick compartment walls left as integral parts of the box during machining. The box contains 22 compartments each 0,143 mx0,025 mx0,0165 m. The compartment walls are perforated with two rows of staggered 4×10^{-3}m diameter holes. Distance between holes in the same row is 0,026 m. 2. Honeycomb, $8,1\times10^{-3}$m from flat to flat (outer). Wall thickness $0,35\times10^{-3}$m. Slanted faces of each cell are perforated with 2×10^{-3}m diameter holes, two in each face, 0,013 m apart. Each half honeycomb layer runs along the length and width of the compartment.	
Inner Volume [m^3]	$1,1\times10^{-3}$	
Ullage [%]	0 at 373 K; 9,5 at 305 K; 14 at 300 K	

Developer	Institut für Kernenergetik of the University of Stuttgart (IKE) Federal Republic of Germany
Mass of Container & Filler [kg]	1,354 (box, lid, filler, epoxy)
Mass of PCM [kg]	0,770
Overall Mass [kg]	2,124
PCM	Octadecane 99% pure
Container Materials	Aluminium alloy $AlMg_3$ (Al alloy 5302)
Filler Materials	Aluminium alloy $AlMg_3$ for compartment walls. Aluminium-Manganese alloy for honeycomb. The honeycomb layers were epoxy-bonded using Eccobond 58-C to the box, to each other and to the lid inner face.
Other Materials	Eccobond 58-C epoxy (Emerson, Cuming Europe, Oevel, Belgium).
Thermal Performances	Results given in the reference are: Measured temperature (for given heat transfer rates and a heat storage capacity of $1,8x10^5$ J) both at the center of the heat input/output face and average of that face. Average temperature was also calculated. Measured and computed time for complete melting. Measured temperature and heat storage capacity for that time.
Lifetime	
Applications	Space radiator augmentation.

TESTS

The only input/output face was instrumented with five thermocouples laid in grooves in the outside face. Five more thermocouples were placed outside the opposite insulated face. The thermocouples were spot-welded to the box walls at the point were each groove ends (Figure 8-10).

Figure 8-10: Location of the thermocouples in the input/output face. The thermocouples placed on the opposite face do not appear in the figure since they are projected in the same positions as those in the input/output face. All the dimensions are in mm.

A heater-cum-calorimeter unit provided heating and cooling of the PCM capacitor.

Only heating data are reported.

The heat input/output profile was (50 W.h heat storage):
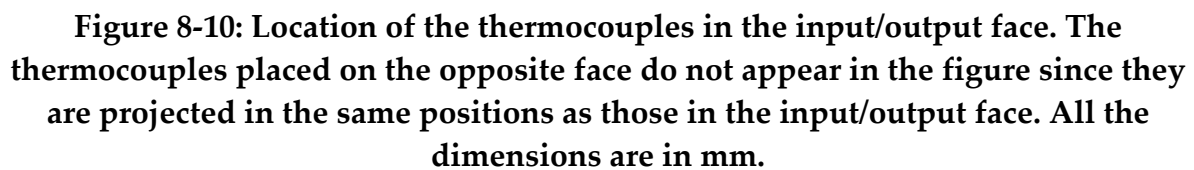
— 100 W heat transfer rate heating for half an hour, followed by 100 W cooling during the same time.

— 50 W heating for 1 h followed by 50 W cooling for 1 h.

— 25 W heating for 2 h and 25 W cooling for 2 h.

— 17 W heating for 3 h and 17 W cooling for 3 h.

Initial temperatures for heating (cooling) were approximately 5 K below (above) PCM melting point.

The above cycle was repeated twice, heating from below. A couple more test at the high end of the power cycle were then done with the cell vertical and with the cell horizontal heated from above. Differences were small.

NUMERICAL MODELLING

The SINDA lumped capacity network computer programme was used. An additional capacitance, equal to the mass of PCM at the node times the latent heat of fusion, is introduced to account for the phase change of the melting/freezing nodes.

The spatial location of the melting/freezing front at a given moment is first calculated assuming no phase change (and temperature independent PCM properties). Nodes whose temperatures have just exceeded the melting temperature form the front. The additional capacitance is then introduced in these nodes for subsequent computation and kept in them provided that the resulting temperature deviates from the melting temperature less than a given value, ΔT_M, the so called melting range. In this case $\Delta T_M = 1K$.

Three different network models were used.

Model A. Quasi-unidimensional modeling. 2 nodes in the container walls and 20 each in the PCM and in the filler. Heat transfer from the flat faces of the honeycomb to the PCM is neglected leading to wall temperature below experimental and much higher times for complete melting (Figure 8-13).

Model B. Two slightly different sets of honeycomb cells exits: those in contact with the container large faces through flat faces (Wax 1 set), and those contacting through the ideal mid plane of the cell (Wax 2 set). Similarly, two sets of filler nodes were used. The model requires 50 nodes; 2 for the container walls, 12 for each set of waxes and 12 for each set of fillers. Conduction from the flat faces of the honeycomb to the PCM is accounted for.

Model C. The two sets of filler nodes result to be similar in nature, they exhibit the same capacitance, and the same filler-filler and filler-wax conductance. Thence, both sets can be assembled into a single set. This reduces the number of nodes to 38.

Models B and C accurately predict the wall temperature and the time for complete melting (Figure 8-13).
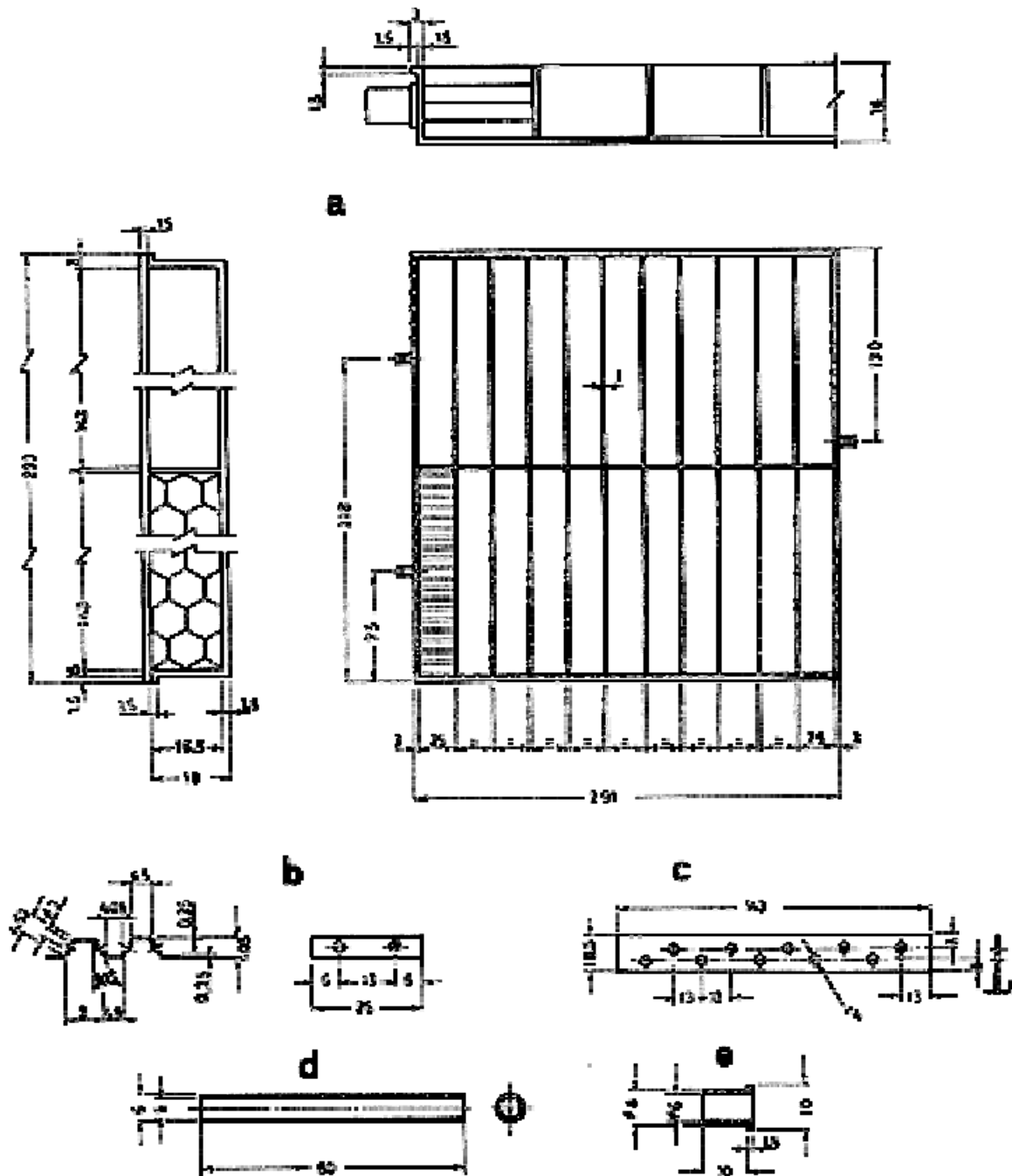
Note: non-si units are used in this figure

Figure 8-11: Prototype PCM capacitor developed by IKE. All the dimensions are in mm. a: Box. b: Honeycomb half layer. c: Perforations in compartment walls. d: pinch tube. e: Extension of the pinch tube.
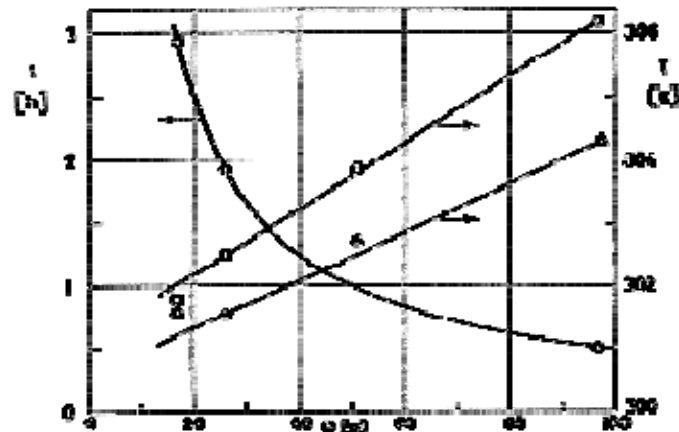
Figure 8-12: Time, *t*, for nominal heat storage and temperature, *T* of the heat transfer face vs. heat input rate, *Q* . ○ Time for nominal heat storage. □ Measured average wall temperature at time *t* . △ Measured temperature at the center of the heat transfer face at time *t*.
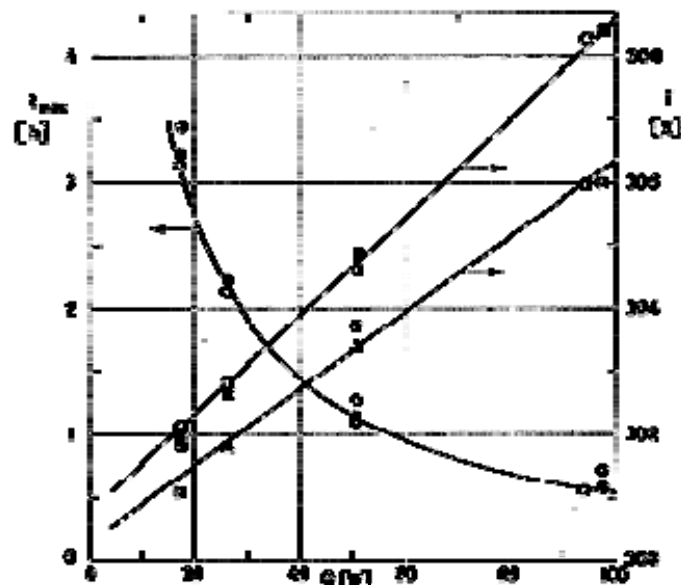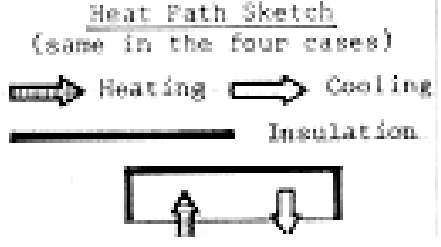
Figure 8-13: Time, *t_{max}*, for complete melting and temperature, *T*, of the heat transfer face vs. heat input rate, *Q*.
Time for complete melting: ○ measured. ◖ calculated by model A. ● Calculated by models B or C.
Average wall temperature at time *t_{max}* : □ measured. ◫ calculated by model A. ■ Calculated by models B or C. △ Measured temperature at the center of the heat transfer face at *t_{max}*.

Reference: Abhat & Groll (1974a) [1].

Developer	Institut für Kernenergetik of the University of Stuttgart (IKE) Federal Republic of Germany			
Model	**1**	**2**	**3**	**4**
Heat Storage [J]	$1,8 \times 10^5$ (50 W.h)			
Heat Storage per Unit Mass [J.kg^{-1}]				
Thermal Conductance [W.K^{-1}]	<2,1	<2,5	<5	<9,3
Operational Temperature Range [K]			Heat Path Sketch (same in the four cases) Heating ⟹ Cooling Insulation	
Filling Temperature [K]	328			
Phase Change Temperature [K]	300			
Temperature Stability [K]	See Figure 8-16			
Shape	Box-Shaped			
Overall Dimensions [m]	0,156x0,140x0,013	0,157x0,153x0,013	0,157x0,150x0,013	0,157x0,150x0,013
Container	Hollow box, 0,01 m deep and having $1,5 \times 10^{-3}$ m thick walls. A lid, $1,5 \times 10^{-3}$ m thick, is epoxy-bonded to the box through a flange 3×10^{-3} mx3×10^{-3} m left around the open end of the box. Three openings 6×10^{-3}m diameter are provided, two in the one side and the other in the opposite for filling and evacuating purposes, respectively.			Same as 3 but lid is electron beam welded to the box.
Filler	None.	10^{-3} m thick compartment walls, 0,03 m apart, left as integral parts of the box during machining. The walls are	Compartment walls plus honeycomb 0,012 m from flat (outer). Each cell face was perforated with one 3×10^{-3} m diameter hole. Cell	Same as 3 but comb 0,01 m from flat to flat and cell axis parallel to the lid.

Developer	Institut für Kernenergetik of the University of Stuttgart (IKE) Federal Republic of Germany			
		perforated with 4×10^{-3} m diameter holes. 0,01375 m apart.	axis perpendicular to the lid.	
Inner Volume [m³]	210×10^{-6}	225×10^{-6}	$202,5 \times 10^{-6}$	$196,5 \times 10^{-6}$
Ullage [%]	0 at 328 K			
Mass of Container & Filler [kg]				
Mass of PCM [kg]	0,160	0,165	0,135	0,138
Overall Mass [kg]				
PCM	Octadecane 99% pure			
Container Materials	Aluminium alloy AlMg₃ (Al alloy 5302)			
Filler Materials	None	Aluminium alloy AlMg₃ for compartment walls.	Same as 2 plus AlMn alloy honeycomb layers diffusion bonded to each other and to the box. Lid epoxy bonded.	Same as 3 although honeycomb layers epoxy bonded to each other, to the box and to the lid.
Other Materials	Auromal K-70 silver-filled epoxy. Pin holes appeared after three months.		Eccobond 58-C epoxy (Emerson & Cuming Europe, Oevel, Belgium).	
Thermal Performances	Results given in the sources are: Measured wall and PCM temperatures. Time for complete melting deduced from these data. Maximum temperature at the heat input/output face for complete melting vs.heat transfer rate. Both measured and calculated. Transient effective thermal conductance of the device vs. heat transfer rate. Deduced from measurements.			
Lifetime				
Applications	Study of devices based on Aluminium container and fillers, and octadecane as PCM.			

TESTS

The two large faces were each instrumented with four thermocouples, laid in grooves cut in the box and lid surfaces and spot-welded at the positions shown in Figure 8-14.

Five thermocouples were placed within the box in models 1, 2 and 3.These thermocouples were enclosed in 2×10^{-3} m diameter aluminium tubes slitted around the region where the thermocouples bead was to be located, thus exposing the bead to the environment around it. The tubes passed through the box and were supported at its side walls.
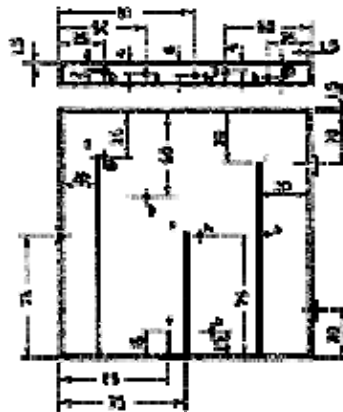
Note: non-si units are used in this figure

Figure 8-14: Location of the thermocouples in the heat input/output face (f) and within the box (b). The thermocouples placed on the opposite face do not appear in the figure since they are projected on the same positions as those in the input/output face. All the dimensions are in mm.

A heater-cum-calorimeter unit provided heating and cooling of the PCM capacitor. This unit was mechanically clamped to the capacitor at either large face, through a film of high thermal conduction grease. All faces other than that in contact with the calorimeter were insulated.

Only heating data are reported. Heating runs started at $298 \pm 0,5$ K (approximately 2 K below freezing point) and were continued until melting of the PCM, as detected from the temperature-time curves, Figure 8-16. The face temperature is the arithmetic average of the thermocouple readings at a given instant.

Most data were obtained while heating from below. Experiments were performed with model 3 with the device horizontal either heated from below or from above, and with the device vertical. Melting time was barely affected by the orientation of the device, but the heated wall temperature increased for high heat transfer rates when gravity caused a gap to occur between the PCM and the heat input face.

Visual observation of melting/freezing front and corrosion studies were performed by using a model with a plexiglas lid bolted to the box.

NUMERICAL MODELLING

The SINDA lumped capacity network computer programme was used. An additional capacitance is introduced to account for the phase change of the melting/freezing nodes.

The spatial location of the melting/freezing front at a given moment is first calculated assuming no phase change (and temperature independent PCM properties). Nodes whose temperatures have just exceeded the melting temperature form the front. The additional capacitance is then introduced in

these nodes for subsequent computations and kept in them provided that the resulting temperature deviates from the melting temperature less than a given value, ΔT_M, the so called melting range. In this case, $\Delta T_M = 1$ K.

Two different network models were considered.

Model A. Unidimensional network with 20 nodes in the PCM and 1 each in the container large faces. An effective thermal conductance is used on the basis of filler geometry and of a conduction path length corresponding to steady state conduction in the PCM without phase range.

This network model was used with models 1, 2 and 3.

Model B. Quasi-unidimensional network to allow for separate paths for heat flow from the container faces into PCM and filler, and from the filler to the PCM. 20 additional nodes are required to represent the filler material. This network model was used with model 3. Comparison of results from either network model indicated that lumping together of PCM and filler should not be recommended when a compact filler is used.

In addition, a two-dimensional model was developed, for model 4 devoided of the honeycomb, to study the temperature distribution in planes parallel to large faces.

In order to simplify the numerical modeling it has been assumed that. 1) Material properties are temperature independent. 2) Convection and gravity effects, shrinkage upon phase change and heat losses, are all absent. 3) Contact resistance between container and filler is zero.
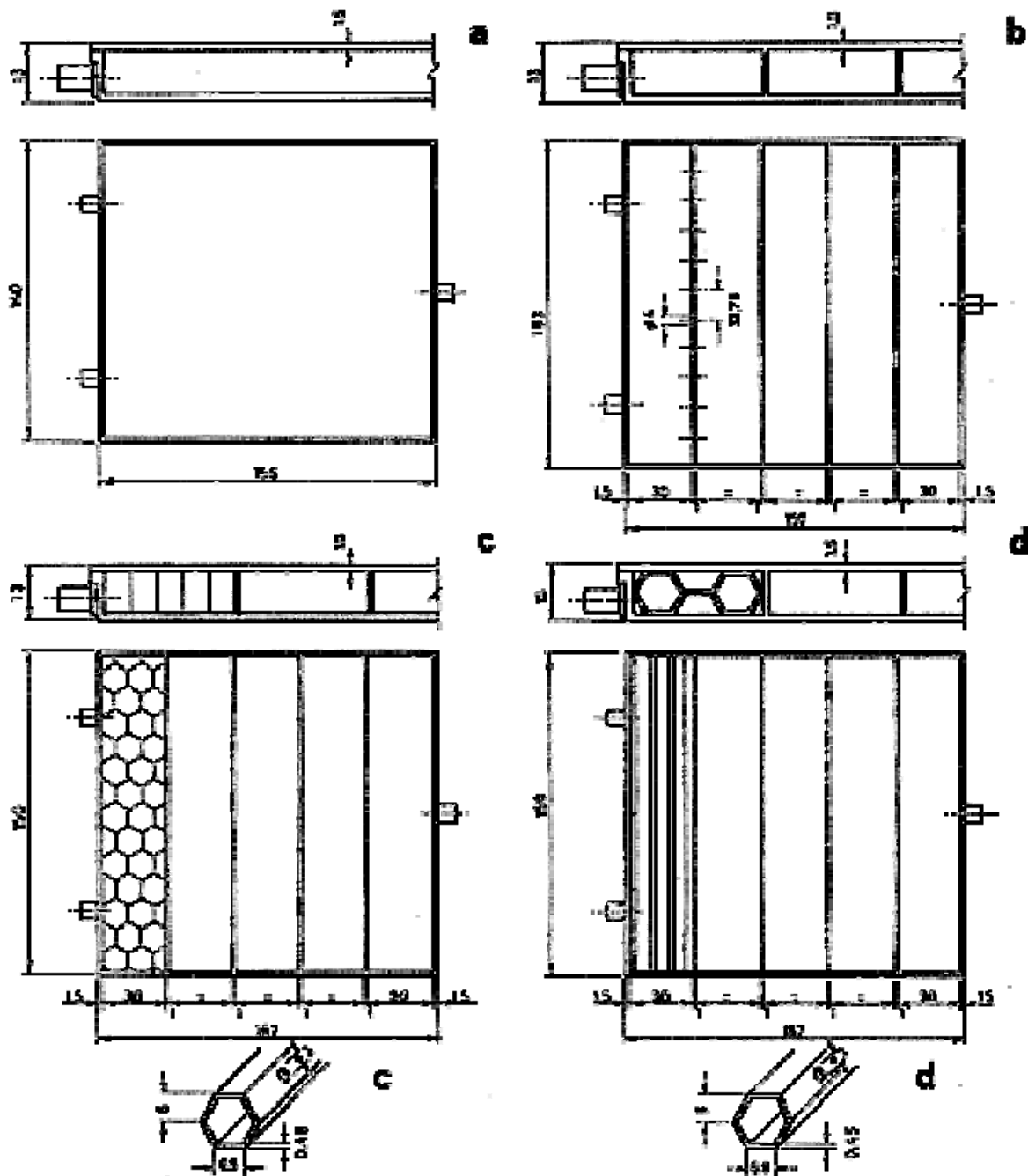
Note: non-si units are used in this figure

Figure 8-15: PCM capacitors with several fillers developed by IKE. All the dimensions are in mm. a: Model 1. b: Model 2. c: Model 3. d: Model 4.
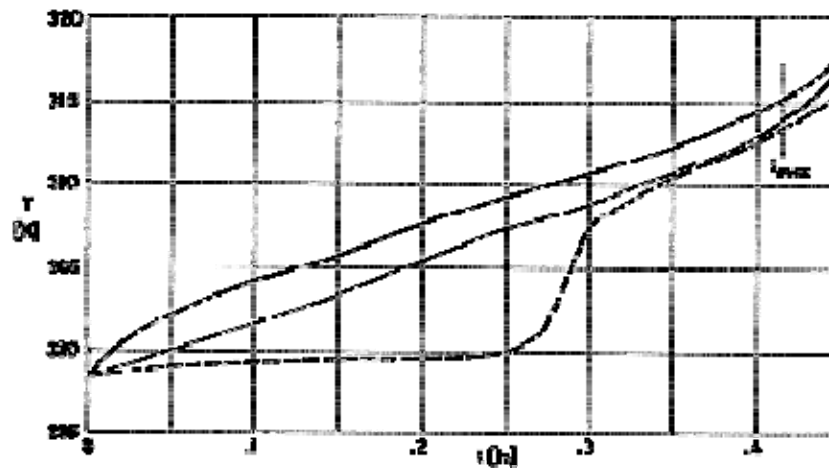
Note: non-si units are used in this figure

Figure 8-16: Measured temperature, *T*, at several points of the PCM capacitor vs. time *t*. Model 2. Heat up with a heat transfer rate *Q* = 30,6 W. Points are placed as follows (Figure 8-14): ▬▬ Upper left corner of the heat input/output face. ▬▬ Center of the insulated face. ▬ ▬ Center of the box, immersed in the PCM. Time for complete melting *t_{max}*, is shown by means of a vertical trace intersecting the curves.
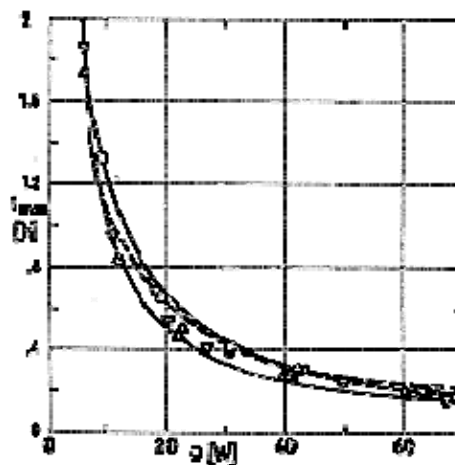
Note: non-si units are used in this figure

Figure 8-17: Time for complete melting, *t_{max}*, vs. heat input rate *Q* . Model 1. ○ Measured. Model 2. □ Measured. ▬▬ Calculated by using model A. Model 3. △ Measured. ▬▬ Calculated by using model A. ▬ ▬ Calculated by using model B. Model 4. ▽ Measured.
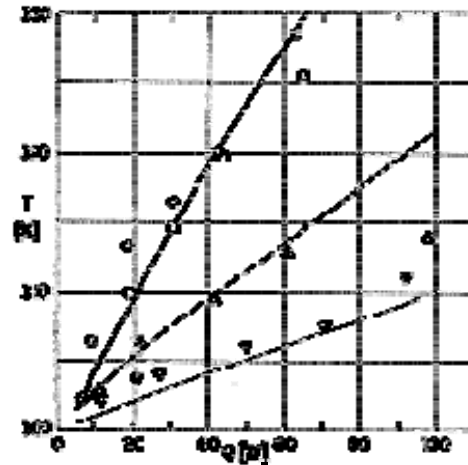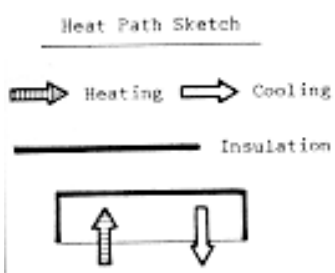
Figure 8-18: Largest measured temperature, *T*, of the heat input/output face vs. heat input rate, *Q* .Model 1. ○ Measured. Model 2.□ Measured. ━━━ Calculated by using model A. Model 3. △ Measured. ━━━ Calculated by using model A. ▬ ▬ Calculated by using model B. Model 4. ▽ Measured.

References: Abhat & Groll (1974a, 1974b) [1] & [2].

Developer	**Institut für Kernenergetik of the University of Stuttgart (IKE)** **Federal Republic of Germany**	
Heat Storage [J]	$3,6 \times 10^5$ (100 W.h)	Heat Path Sketch
Heat Storage per Unit Mass [J.kg^{-1}]	$1,51 \times 10^5$	
Thermal Conductance [W.K^{-1}]	6,7 W.K^{-1} no bonding epoxy (see Filler Materials below). 5,6 W.K^{-1} for $0,5 \times 10^{-3}$ m bond thickness.	
Operational Temperature Range [K]	263-323	
Filling Temperature [K]	331	
Phase Change Temperature [K]	301,3	
Temperature Stability [K]	See Figure 8-21	
Shape	Box-Shaped	
Overall Dimensions [m]	0,300x0,200x0,0425	
Container	Hollow box 0,04 m deep. All walls except the base are 10^{-3} m thick. The base (heat transfer and mounting face) is $1,5 \times 10^{-3}$ m thick. The lid, 10^{-3} m thick, is electron beam welded to the container all along its periphery. A flange 6×10^{-3} m x $1,5 \times 10^{-3}$ m, all around the base is placed for mounting purposes. The heat transfer area is 0,288 m x 0,188 m. Two 6×10^{-3} m diameter openings are provided in one of the side walls for evacuating and filling. During testing all the faces, except the base, are insulated with Styropor.	
Filler	1. 10^{-3} m thick compartment walls left as integral parts of the box during machining. The box contains 4 compartments each 0,1 m x0,925 m x0,04 m and 2 central compartments 0,084 m x0,0925 m x0,04 m each. The compartment walls are perforated with two rows of side-by-side 3×10^{-3} m diameter holes. Distance between holes in the same row is 0,0115 m and distance between rows is 0,015m. 2. Honeycomb $6,35 \times 10^{-3}$ m flat to flat (outer). Wall thickness $0,1 \times 10^{-3}$ m. Slanted faces of each cell are perforated with $1,5 \times 10^{-3}$ m diameter holes, two in each face, 0,013 m apart. Cell axes are parallel to the input/output face.	
Inner Volume [m^3]	$2,1 \times 10^{-3}$	

Developer	Institut für Kernenergetik of the University of Stuttgart (IKE) Federal Republic of Germany
Ullage [%]	0 at 331 K; 2,25 at 323 K; 9 at 301,3 K
Mass of Container & Filler [kg]	0,885
Mass of PCM [kg]	1,502
Overall Mass [kg]	2,387
PCM	Octadecane 99,5% pure
Container Materials	Aluminium alloy AlMg$_3$ (Al alloy 5302)
Filler Materials	Aluminium alloy 5302 for compartment walls. Aluminium alloy 5052 honeycomb DURACORE, 7,9-1/40,0040 (American Cynamid Co. Bloomingdale, Maryland, USA). The honeycomb is bonded to the walls, base, and lid using Eccobond 58-C. Bond layer thickness $0,5 \times 10^{-3}$ m.
Other Materials	Eccobond 58-C (Emerson & Cuming Europe, Oevel, Belgium). Styropor insulator (BASF Ludwighshafen, Germany). Pinch tubes are Aluminium.
Thermal Performances	Results given in the references are: Base and lid temperatures vs. time, for given heat flux. Both measured and computed. Time for complete melting is deduced from these data. Interface position (and molten fraction) vs. time for given heat flux. Computed. Temperature distribution throughout the device for different times. Computed. Base maximum temperature at complete melting vs. heat flux. Both measured and computed.
Lifetime	7 years estimated.
Applications	Survival of high power-dissipation equipment not operating during eclipse due to lack of power from the solar array. The PCM replaces the heat radiated during eclipse.

TESTS

The two large faces were each instrumented with five thermocouples (Figure 8-19). Those placed in the heat input/output face were embedded in grooves $0,5 \times 10^{-3}$ m deep and 10^{-3} m wide, and were spot-welded to the wall at the end point of each groove. No grooves were cut in the lid surface, the thermocouples simply lying on it.
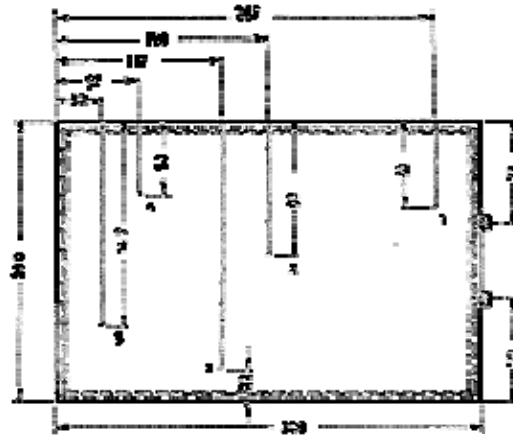
Figure 8-19: Location of the thermocouples in the heat input/output face. The thermocouples placed on the opposite face do not appear in the figure since they are projected on the same positions as those in the input/output face. Thermocouples are numbered for later reference. All the dimensions are in mm.

Heating was provided by a MINCO foil resistance heater (see ECSS-E-HB-31-01 Part 11, clause 4.5.2.8) glued along the whole heat input/output face. Cooling was done by using a calorimeter heldon that face across the heating foil.

Three different types of tests were performed.

1. Performance measurements. Heating, mostly at a rate of 83,3 W over a period of 72 min. The initial temperature was 299 ±0,5 K. Heating was stopped when the largest recorded temperature was 323 K.

    In most cases the PCM capacitor was heated from below, although several runs were carried out with the capacitor held vertical. No significant differences were detected.

2. Cool down. The PCM within the capacitor was frozen after each performance test in order to restore the initial conditions for a new performance test. The rate of cooling could not be accurately determined, while actual heating rates were measured within 2% accuracy. Thence, cooling data are not reported.

3. Space qualification tests.

    (a) Thermal soak tests. The PCM capacitor was cyclically subjected to the extreme limits of the qualification temperature range. To this aim was cooled to 263 K remaining at this temperature for 3 h. The temperature was then raised to 323 K and maintained for 3 h. The cycle was repeated three times.

    (b) Thermal cycle tests. Heating to 313 K for PCM melting. After 30 min the temperature was reduced to 283 K for freezing. After 30 min the temperature was increased again to 313 K. The heating and cooling times were nearly the same, the cycle period not exceeding 5 h.

    Tests 3.1 and 3.2 were performed in vacuum at 1,33 x 10^{-2} Pa. The reference temperature was that at the center of the heat input/output face.

    (c) Vibration tests. Random, sinusoidal, and constant acceleration.

    Following each of the space qualification tests a performance test was carried out to detect any degradation in performance because of the space qualification procedures. The results are reproducible although some scatter in the temperature was observed.

NUMERICAL MODELLING

The SINDA lumped capacity network computer programme was used. An additional capacitance in introduced to account for the phase change of the melting/freezing nodes. The network model used is similar to model C of the first numerical modeling in clause 5.3. A slab normal to the input/output face, whose width is equal to two honeycomb half-cells and whose height is equal to the container depth, was modeled, 6 nodes were used to reproduce each couple of contiguous half-cells along a normal to the input/output face, and the filler between them. There are 12 half-cells along a normal to the input/output face thence, a complete network consists of 42 nodes (2 nodes corresponding to the end faces). Nevertheless, fair results were obtained more economically by lumping together each couple of half-cells into one single node, plus another node for the dividing filler, so that only 26 nodes are required.

In order to simplify the numerical modeling, it has been assumed that convection and gravity effects, shrinkage upon phase change ad heat losses, are all absent.
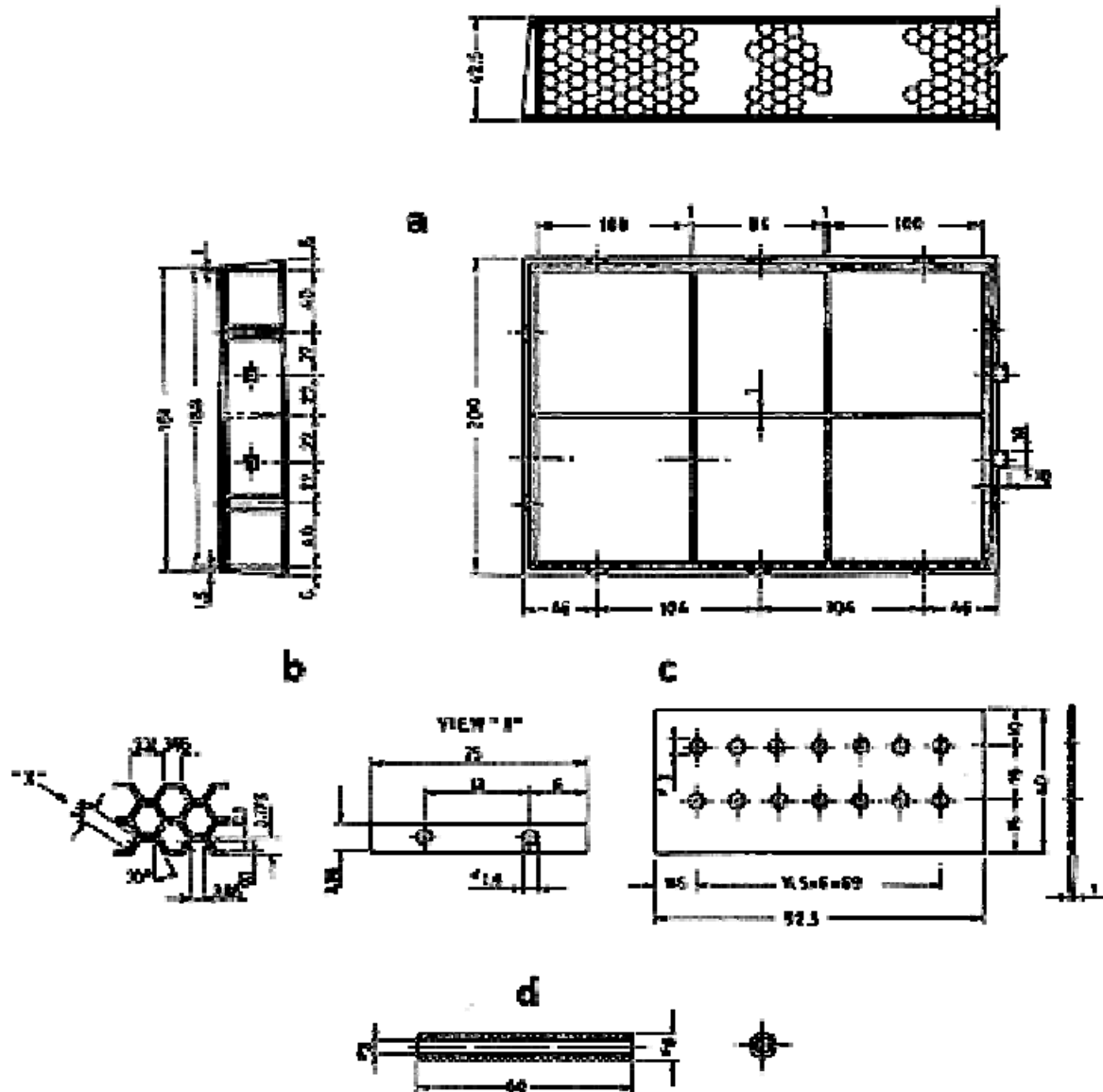
Note: non-si units are used in this figure

Figure 8-20: PCM capacitor developed by IKE for ESA (ESTEC). All the dimensions are in mm. a: Box. b: Honeycomb calls. c: Perforations in compartment walls. d: Pinch tube.

Note: non-si units are used in this figure
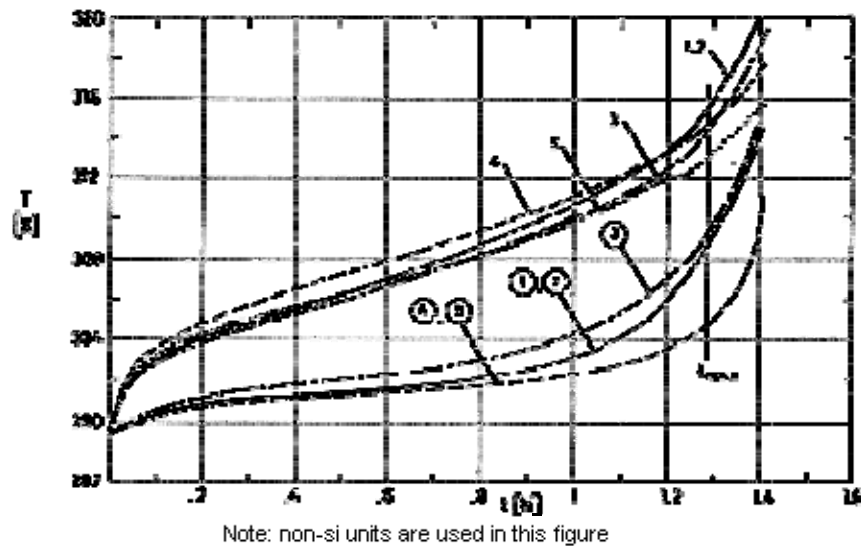
Figure 8-21: Measured temperature, *T* at several points in either of the large faces of the container vs. time, *t*. Heat up with a heat transfer rate *Q* = 86,4 W. Points 1 to 5 are placed in the heat input/output face as indicated in Figure 8-19. Circled points are in the same positions at the insulated face. Time for complete melting, *tmax*, is shown by means of a vertical trace intersecting the curves.
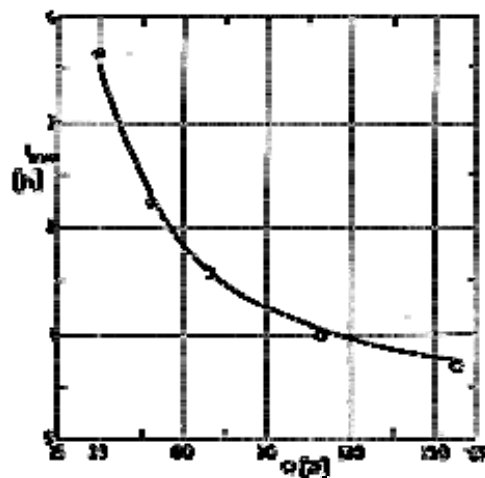
Figure 8-22: Time for complete melting, *tmax* vs. heat input rate, *Q* . ○ Measured. ▬▬ Calculated by using the 26 nodes model. Overall thermal conductances in the range 1,4 W.K⁻¹ to 5,6 W.K⁻¹.
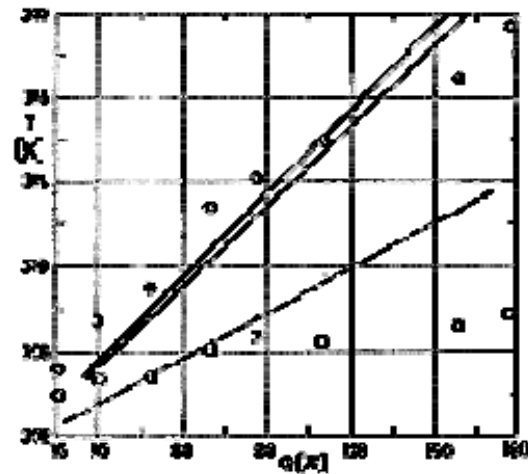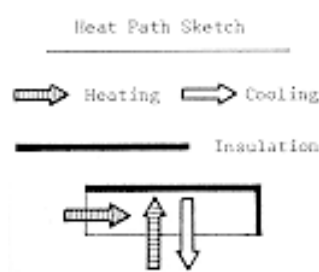
Figure 8-23: Average temperature, *T* of either of the large faces vs. heat input rate, *Q*. *t* = *t_{max}*. Heat input/output face. ○ Measured. ▬▬▬ Calculated by the 26 nodes model. Overall thermal conductance 5,6 W.K⁻¹ . ▬▬▬ Calculated as above. Overall thermal conductance 6,7 W.K⁻¹. Insulated face. □ Measured. ▬ ▬ Calculated as above. Overall thermal conductance 5,6 W.K⁻¹ and 6,7 W.K⁻¹.

Reference: Abhat (1975, 1976) [3] & [4].

8.4   B&k engineering

Developer	B&K Engineering, Inc., Towson, Maryland, USA	
Heat Storage [J]	$1,08x10^5$ (30 W.h) nominal. Measured values are within 87% to 92% the nominal.	Heat Path Sketch Heating Cooling Insulation
Heat Storage per Unit Mass [J.kg⁻¹]	$4x10^4$	
Thermal Conductance [W.K⁻¹]	8,0 (Calculated). 10,5 (Measured in the PCM device alone)	
Operational Temperature Range [K]	123-323	
Filling Temperature [K]	343	
Phase Change Temperature [K]	182,4	
Temperature Stability [K]	±0,2 (Component Test)	
Shape	Box-Shaped	
Overall Dimensions [m]	0,489x0,114x0,059	
Container	TIG welded aluminium rectangular box divided into two identical compartments by an aluminium center wall. This wall is perforated with twenty five holes $2,38x10^{-3}$m diameter. A saddle for attachment of the transporter heat pipe (TPHP) in the Heat Pipe Experiment Package (HEPP) is integral with the box.	
Filler	1. Compartment wall. 2. Honeycomb, $4,8x10^{-3}$m cell. Wall thickness $0,05x10^{-3}$ m. Each cell contains two holes $1,6x10^{-3}$ m diameter. 80% of the inner volume is filled with partially expanded core and the remaining with fully expanded core. The void density in the compartments is approximately 90%. Cell axis normal to the base which is in contact with radiator surface. The fully expanded honeycomb is located near the heat pipe (input) side. Under 0 g the liquid migrates towards the partially expanded honeycomb by capillary pumping. For 1 g testing the fully expanded honeycomb is placed at the top. The honeycomb is held in place with adhesive sheets, cutting through the sheets to establish metal to metal contact with the compartment wall and with top and bottom bases.	

Developer	B&K Engineering, Inc., Towson, Maryland, USA
Inner Volume [m³]	
Ullage [%]	0 at 343 K.
Mass of Container & Filler [kg]	1,980
Mass of PCM [kg]	0,753
Overall Mass [kg]	2,733
PCM	n-Heptane
Container Materials	6061-T6 aluminium alloy.
Filler Materials	6061-T6 aluminium alloy for compartment wall. 5052 aluminium alloy for the honeycomb.
Other Materials	Adhesive sheets Hysol EA 934 (The Dexter Corporation, Hysol Division, Clean, New York).
Thermal Performances	Results given in the reference are: Mean temperature vs. time under cooling for both PCM device and HEPP system. Mean temperature vs. time of component, for two different heat transfer rates. Heat storage, predicted and deduced from measurements of component test (under both heating and cooling), and from system test.
Lifetime	
Applications	Energy storage in the Heat Pipe Experiment Package (HEPP). The HEPP was developed for flight aboard TIROS-N spacecraft. It is now being considered for flight on the Long Duration Exposure Facility (LDEF) to be placed in orbit by the Space Shuttle (see Clark (1981)).

TESTS

The following tests were performed:

1.- Component Tests. The PCM capacitor was placed in a thermal vacuum test chamber (Figure 8-24) with a liquid nitrogen cooled wall ($T_W \cong 90$ K). The container was oriented at a 28° angle with respect to the vertical in order to duplicate the test orientation of the HEPP system. The fully expanded honeycomb filler was located at the top. An aluminium fin was attached to the container to simulate the HEPP radiator. This fin was cooled by a liquid nitrogen coolant loop. Heating up from the radiator was simulated by an electrical heater attached to the fin, and heat pipe inputs by an electrical heater attached to the heat pipe saddle. An MLI blanket was used to insulate the underside of the test assembly.

The whole test assembly was instrumented with 33 thermocouples (outside the container) and 5 strain gages. A quadripole mass spectrometer was interfaced with the thermal vacuum chamber as a leak detector.
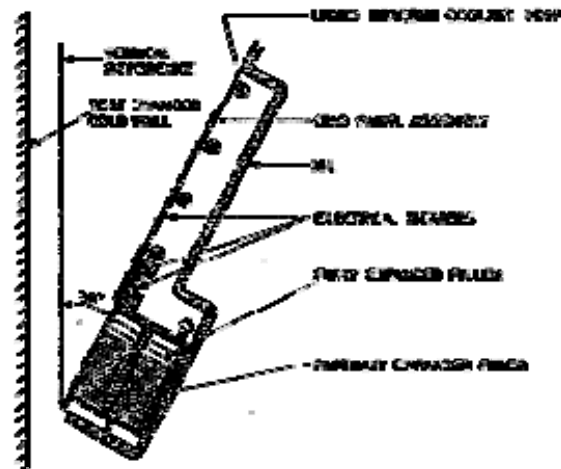
Figure 8-24: Set-up used for component tests.

The sequence of thermal tests was the following.

1.1.- Cool down by the liquid nitrogen-cooled wall. Curves of temperature vs. time were obtained and the heat storage for cool down was deduced from these data. Discrepancies in the freezing point from the nominal value were detected in these as well as in the system tests. These discrepancies are attributed to location or calibration of the thermocouples.

1.2.- Simulated heating loads from the heat pipe, 15, 25, 35 and 45 W heat transfer rates. The tests were stopped at complete melting, as indicated by the temperature readings. Curves of temperature vs. time were obtained and the heat storage for heating up was deduced from these data. The reference temperature in these curves is the average container temperature.

1.3.- Thermal cycling. 12 cycles lasting approximately 5 h each and including accelerated melting and freezing of the PCM. The temperature range was from 123 K to 313 K. These tests aimed at simulating space flight operation.

1.4.- Steady-state radiator calibration test. Test made in order to predict the heat rejection capability of the HEPP system.

1.5.- Simulated heating loads from the heat pipe, 15 and 45 W heat transfer rates. The results of these tests were compared with those performed in 1,2) above, for detecting the effects of possible degradation in the PCM characteristics, leakage from the cell,... None of these effects were observed.

1.6.- Thermal cycling, as in 1.3).

1.7.- Simulated heating loads from the heat pipe, as in 2).

2.- Systems Tests. The PCM device was integrated with the HEPP (Figure 8-26) for system testing. During these tests the device was subjected to various heat loads and melting/freezing cycles.

Components and system tests were performed by using different test systems. This could be the reason for the discrepancies observed in Figure 8-28.

NUMERICAL MODELLING

A network computer programme for the HEPP was prepared and subsequently verified during system tests. No details are given in the reference concerning such programme.

Figure 8-25: PCM capacitor developed by B & K Engineering for NASA. All the dimensions are in mm.

Figure 8-26: Schematic of the PCM capacitor in the TIROS-N cryogenic heat pipe experiment package (HEPP). From Ollendorf (1976) [20].

Note: non-si units are used in this figure
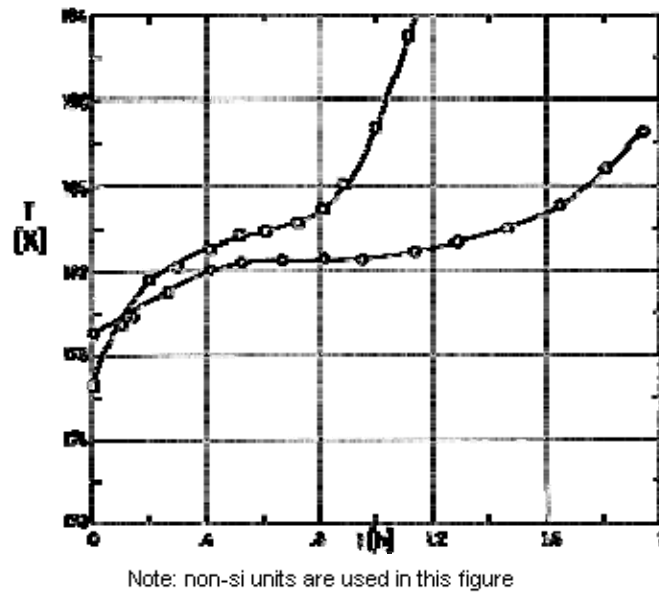
Figure 8-27: Average temperature, *T* of the container vs. time, *t* , during heat up for two different heat transfer rates. ○ *Q* = 25 W. □ *Q* = 45 W. Component tests data.
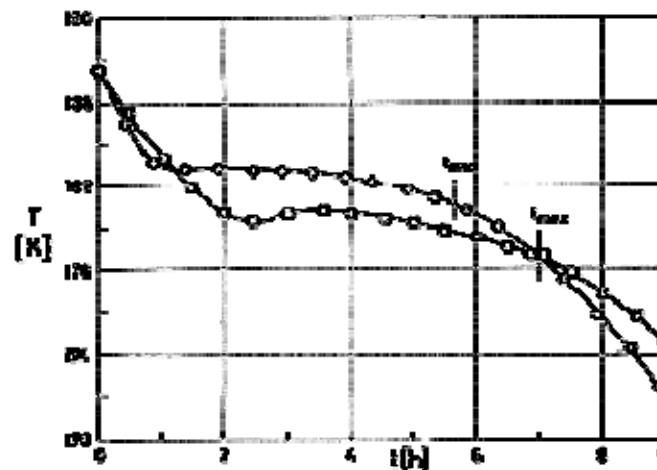
Figure 8-28: Average temperature, *T*, of the container vs. time, *t*, during cool down. Data from either component or system tests. ○ Component tests, *Q* = 6,1 W. Freezing interval *Δt* ≅ 4,5 h. □ System tests, *Q* = 5,2 W. Freezing interval *Δt* ≅ 5 h. Time for complete melting, t_{max}, is shown by means of a vertical trace intersecting the curves.
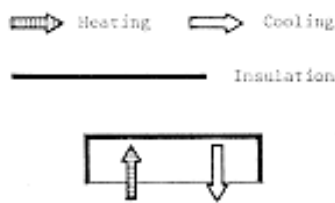
References: All data in this item, unless otherwise stated, are from Brennan, Suelau & McIntosh (1977) [7].

8.5 Aerojet electrosystems

Developer	Aerojet Electrosystems Company, Azusa, California, USA	
Heat Storage [J]	$2,16 \times 10^5$ (60 W.h). Estimated from Figure 8-32	Heat Path Sketch
Heat Storage per Unit Mass [J.kg^{-1}]		
Thermal Conductance [W.K^{-1}]		
Operational Temperature Range [K]	153-223	
Filling Temperature [K]		
Phase Change Temperature [K]	182,4 (n-Heptane); 187,1 (Methyl-ethyl ketone)	
Temperature Stability [K]	±0,2 (n-Heptane), ±1,6 (Methyl-ethyl ketone)	
Shape	Pie-Shaped	
Overall Dimensions [m]	0,457 (diameter)	
Container	Cylindrical. Divided into four separate quadrants comprising two compartments each. One of the compartments is placed near the central axis and the other radially outwards. The volume of both compartments is similar. The set of inner compartments is filled with one of the PCMs and the outer compartments with the other PCM. No hint is given to indicate which PCM is placed in either set of compartments and this is presumably immaterial. The container is placed in the rear side of a 0,4572 m magnesium alloy disc covered with SSMs (see ECSS-E-HB-31-01 Part 6, clause 5.2.6).	
Filler	No filler except compartment walls.	
Inner Volume [m³]		
Ullage [%]		
Mass of Container & Filler [kg]		
Mass of PCM [kg]	0,576 (n-Heptane); 1200 (Methyl-ethyl ketone). Estimated from Figure 8-32	
Overall Mass [kg]		

Developer	Aerojet Electrosystems Company, Azusa, California, USA
PCM	n-heptane and methyl-ethyl ketone. Sixteen PCMs were tested, with melting points between 177 K and 195 K. Most of them were rejected because of supercooling tendencies. Among those which were considered satisfactory, namely: n-heptane, methyl-ethyl ketone, ethyl acetate and methyl-propyl ketone, the two mentioned first were selected since their physical properties were the most favorable.
Container Materials	Magnesiun alloy HM 21 A (Mg - 0,6 Mn - 2,0 Th). Dow Chemical Co., The Metal Products Div., Midland, Michigan, USA.
Filler Materials	Magnesium alloy HM 21 A foe compartment walls.
Other Materials	
Thermal Performances	Results given in the reference are: PCM temperature and heat transfer rate vs. time for the input rate corresponding to the "Stooichiometric" day in orbit. This is the day when all the heat input is consumed in melting the available PCM and the same amount of material is completely refrozen during the cooling part of the day. In orbit the S day for the n-heptane was reached at 770 days after launch, and for MEK at 880 days after launch. Actual maximum diurnal temperature of the radiator for the first 880 days in orbit is also given.
Lifetime	Orbital flight experience up to 880 days in orbit has been reported (Figure 8-33).
Applications	Attenuation of the warming trend, due to radiator contamination, of a radiator cooled satellite.

TESTS

The following tests were performed:

1. PCM screening tests in laboratory flasks. These tests aimed at observing the melting and freezing characteristics of the candidate PCMs, and at devising methods for evacuating and filling the flasks with the pure fluid. The flasks were immersed in cooling or heating baths, as required.

    Shrinkage of the solidifying material away from the flask wall was noticed even when a conductive metal mesh was used as filler.

2. Corrosion tests. Determination of the corrosion rate of various magnesium alloys, aluminium alloys and stainless steel. Single alloys, welded specimens and dual specimen couples were tested. The results are reported in the reference as uniform reduction of the test coupon thickness per year, and pit growth per year. Both uniform corrosion rate and

pit growth were less than 3 mils (7,62x10⁻⁵ m) per year for all the tested combinations of the PCM and metals except methyl-ethyl ketone with the aluminium-stainless steel couple.

3. Calorimeter tests to measure the exact melting point, heat of fusion and supercooling behavior of the candidate PCMs. These tests showed about the same supercooling for a given fluid as in 1), in spite of the much lower cooling rate achieved with the calorimeter.

4. "Beaker" tests. A magnesium alloy container or beaker (Figure 8-29) whose geometry does not duplicate that of the prototype PCM capacitor, was used to measure the structural effects associated with extreme temperature cycling at worst case gravitational orientations of a PCM filled container. Temperature differences within the container and between container and PCM were found to agree with calculated values.

The container was placed either horizontal, heated from below, or inclined 30° to the horizontal. In this last case, the heater was placed either as in Figure 8-29 or on the top, near a vapor filled region.
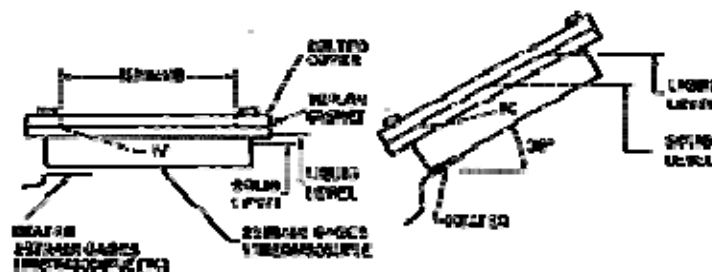
Figure 8-29: Set up used for the "Beaker" tests.

The strains, measured by gages affixed to the container walls, were the same with an empty as with a PCM filled container and, in any case, less than those for one atmosphere (1,013x10⁵ Pa) differential across the container walls.

There was no significant effect of the gravity vector orientation on the heat transfer to or from the PCM. Although a conductive metal mesh brush was used in some tests, the thermal conductance requirements were fulfilled without filler in any case and, thence, the final prototype does not have any filler.

5. "Canteen" tests. The canteen is a quadrant of the actual PCM capacitor (Figure 8-30). These tests aimed at studying the structural integrity of the container and the behavior of the PCM capacitor under conditions corresponding to the stoichiometric day. Leak tests were also performed.

A vacuum chamber at 1,33x10⁻⁴ Pa was used for the tests. The container was tested in both horizontal and vertical positions, and heated up or cooled down from the base (simulating the radiator). The model was exposed to three thermal cycles between 158 K and 223 K, after which temperature was lowered to 3 K below the PCM melting point and the material frozen. Loss of an SSM of the radiator was simulated by a 4 W heat input rate on a 2,54x10⁻² m x 2,54x10⁻² m area for a minimum of 30 min. The temperature was then raised to ambient and the container leak tested.

Strains were measured at four points on the container walls, again yielding similar results for the empty and for the PCM filled container. Temperatures were measured at eleven points, on the walls and within. Temperature differences between the container and the PCM were less than 0,6 K.

6. Radiator qualification tests. Thermal cycling, in a vacuum of 1,33x10⁻⁴ Pa, simulating worst case ground storage up to 338 K, and worst case orbital conditions between 153 K and 223 K.

Temperatures followed the same profiles as under 5) above when the heat fluxes of the *S* day were simulated.

No SSM was cracked or delaminated. Leak rates obtained through the use of monitoring mass spectrometers were found to be below 10^{-10} m³ (standard) per second.

Random vibration tests in three mutually perpendicular axes at 20 g did not produce measurable leaks or visible damage to any surface, including mirrors.

NUMERICAL MODELLING

A computer thermal model of the whole satellite was available. This model, which contains about 300 nodes, was used in conjunction with a thermal transient orbital programme to determine diurnal temperature profiles. A phase change subroutine was written which would handle the amount of energy absorbed or given up as latent heat of fusion. Additional nodes were incorporated to the radiator model to represent the PCM.
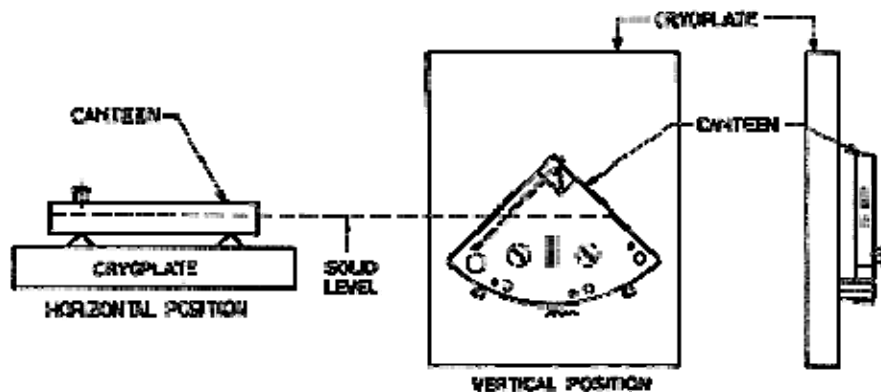
Figure 8-30: Set up used for the "Canteen" tests. ▤▤▤ Strain gage. ∿∿∿ Temperature sensor.
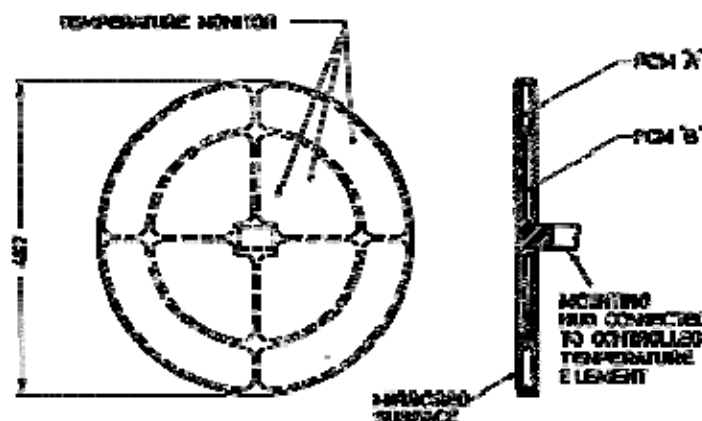
Figure 8-31: PCM capacitor developed by Aerojet ElectroSystems Company. The outer diameter is given in mm.
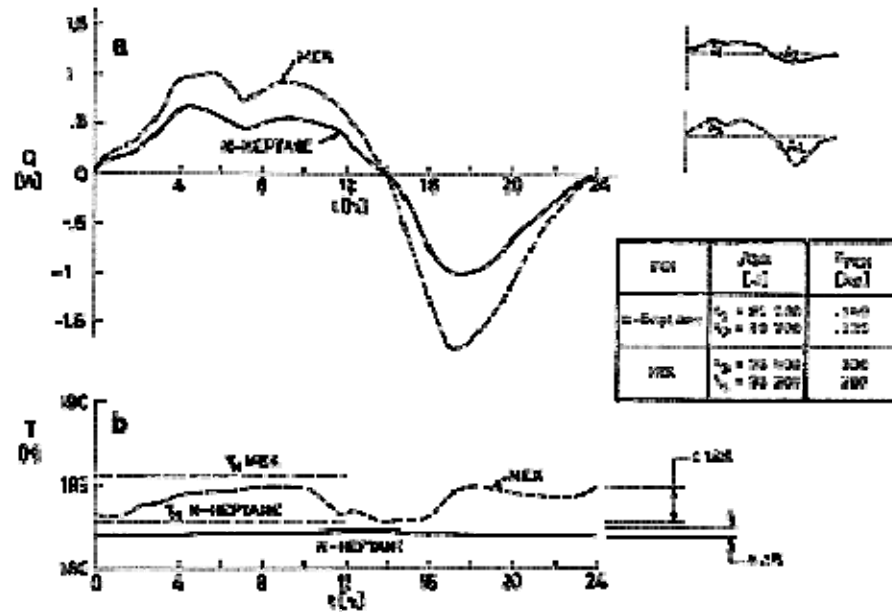
Note: non-si units are used in this figure

Figure 8-32: "Canteen" simulation of the S day. a) Heat transfer rate, *Q* vs. time, *t*. b) PCM temperature, *T*, vs. time *t*. Data in the insert table estimated by the compiler through area integration and the value of *h_f* in Tables 8-9 and 8-10.
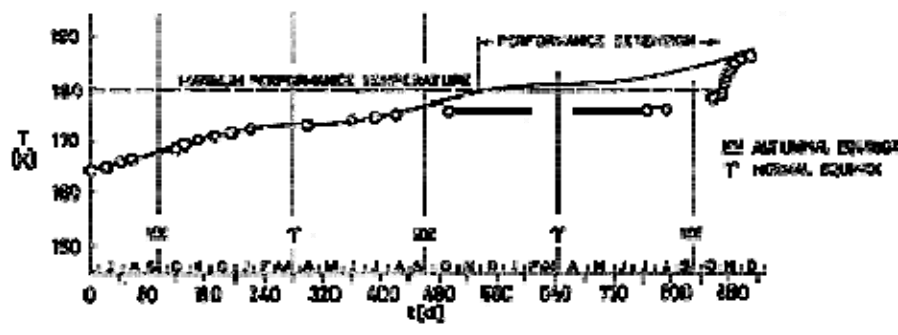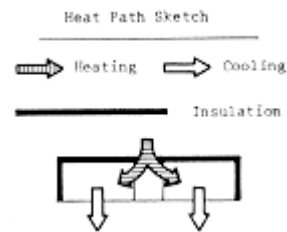
Figure 8-33: Maximum diurnal temperature, *T* of the radiator vs. orbital time, *t*. ▬▬ Predicted with no-phase change. ○ Measured. Phase-change attenuated the warming trend of the radiator for eleven months (performance extension).

Reference: Keville (1976) [15].

Developer	**Aerojet Electrosystems Company, Azusa, California, USA**	
Heat Storage [J]	$3,3 \times 10^5$ (92 W.h)	Heat Path Sketch
Heat Storage per Unit Mass [J.kg^{-1}]		
Thermal Conductance [W.K^{-1}]	Above 4 during cooling, and above 2,5 during heating.	
Operational Temperature Range [K]	133-344	
Filling Temperature [K]	340-345	
Phase Change Temperature [K]	154	
Temperature Stability [K]		
Shape	Pie-Shaped	
Overall Dimensions [m]	0,3454 (diameter)x0,0699	
Container	Cylindrical, divided into four separate quadrants for higher reliability, structural integrity and thermal conductance. The cylindrical wall is $1,52 \times 10^{-3}$m thick, the base $6,35 \times 10^{-3}$ m thick, and the opposite face $3,56 \times 10^{-3}$ m thick. Four filling ports, one for each quadrant are provided in the thinner planar face. Cooling takes place through a gas cooled heat exchanger in the shape of a spiral coil brazed to a circular heat-distributing plate in contact with the base. The coil tube has an outer diameter of $6,35 \times 10^{-3}$ m with a $0,71 \times 10^{-3}$ wall thickness. Heating is provided, via conduction, through a mounting hub connected to the element to be controlled.	
Filler	1. Compartment walls. 2. Honeycomb, $12,7 \times 10^{-3}$m flat to flat, wall thickness $0,43 \times 10^{-3}$ m. The honeycomb is brazed to the inner side of the base, to which the gas cooling coils are externally brazed. The cell axis is parallel to the cylinder axis. A container with no filler was also tested, but it did not meet the thermal conductance requirements for the flight model.	
Inner Volume [m³]	$4 \times 0,936 \times 10^{-3} = 3,744 \times 10^{-3}$	
Ullage [%]	0 at 345 K; 20 at 154 K (liquid); 30 at 154 K (solid)	
Mass of Container & Filler [kg]	1,531 for the test container (and filler) consisting of one quarter-section of the flight unit.	
Mass of PCM [kg]	$4 \times 0,664 = 2,656$	

Developer	Aerojet Electrosystems Company, Azusa, California, USA
Overall Mass [kg]	
PCM	1-heptene. Sixteen PCMs were tested, with melting points between 149 K and 156 K, but only three (1-heptene, 2, 4 dimethyl pentane and chloroprapane) crystallized upon cooling with only slight supercooling tendency. Chloropropane proved to be incompatible with stainless steel in contact with aluminium (a stainless steel ball in an aluminium seat was used to seal the container). Among the other two, 1-Heptene exhibits higher heat of fusion and lower degree of supercooling.
Container Materials	Aluminium alloy
Filler Materials	Aluminium alloy
Other Materials	
Thermal Performances	Results given in the reference are: Container average temperature vs. time for a nominal heat transfer rate of ±2,5 W, with or without filler, and in three orientations in the gravitational field.
Lifetime	
Applications	Energy storage in an active cooling system for a satellite borne infrared detector.

TESTS

The following tests were performed:

1. PCM screening tests in a cylindrical stainless steel container. The temperature of a thermocouple immersed in 0,013 kg of PCM was monitored while heating or cooling the container at a rate of about 2 K.min^{-1}. All the PCMs tested except the three already mentioned under PCM in the [table](#) corresponding to the second heat path sketch of clause 8.5, failed to exhibit a temperature plateau, because of supercooling, even if cooled 60 K to 70 K below their reported triple points.

2. Compatibility and thermal stability tests of the three selected PCMs.Chloropropane did not pass these tests because of incompatibility with stainless steel in contact with aluminium.

3. Melting/freezing thermal tests. These tests were performed with the twofold aim of verifying the adequacy of the structural and thermal design of the container and of checking the numerical modeling.

The tests were made by use of a quadrant of the flight unit. Thermocouples and strain gages were used to measure the temperature distributions and the strains during the thermal tests (Figure 8-34). Three thermocouples were mounted on the face to which the gas coils were brazed (12, 17, 14); three on the face containing the filling port (6, 7, 8); one on each of the sides (9, 10); one on the rim (11), and one near the heater on the mounting hub interface (26).

Four more temperature readings were required for the overall thermal balance of the system. Two immersion thermocouples were placed in the gas cooling stream, one at the inlet and the other at the outlet of the gas cooling coil, and two thermocouples were placed in the inlet and the outlet tube, respectively, to detect any heat leak across the tube walls.

In addition, the face containing the filling port, which is welded into the remainder of the container and is thinner than the opposite face, was instrumented with five strain gages. Heating was provided electrically from the mounting hub, and cooling by dry nitrogen circulating through an external closed loop. The heat input was deduced from the electrical current and voltage through the heater. The cooling rate, on the other hand, was deduced from the cooling gas volume flow rate, pressure, temperature, specific heat and temperature rise of the cooling gas.

The nominal heat input/output rate was 2,5 W. Maintaining this rate during freezing was a difficult task. The inlet gas temperature was varied while keeping constant the fluid mass flow rate. In practice, since the gas density, mass flow rate and specific heat are all functions of temperature, cooling rate was held only approximately constant in the range 2-3 W, with some tests under better control than the others.

The test setup was placed in a vacuum chamber and enclosed by a cryogenic shroud kept at the phase change temperature. The test container itself was enclosed by an MLI blanket. Previous tests indicated that the heat balance was within 10% at a Heating/cooling rate of 5 W.

The tests were made in each of three orientations in the gravity field, namely: mounting hub interface down, gas cooling coils up, and gas cooling coils down. Differences were small, see Figure 8-36a and b. The container temperatures given in these figures are the arithmetic averages of the thermocouple readings at the given instant.

Thermal cycling between the maximum and minimum service temperature. strain gage outputs were recorded. No significant strains were observed during these tests.

NUMERICAL MODELLING

The SINDA lumped capacity network computer programme was used. A phase change subroutine, SUPRCL, to include the effect of supercooling, was developed and incorporated in the programme. The main programme solves the problem assuming no phase change. SUPRCL then calculate the changes to the nodal liquid fraction due to the heat of fusion and net heat flows, and resets the nodal temperatures and admittances. Phase change does not occur during the cooling down until at least one node cools below the melting temperature by the amount corresponding to the supercooling effect, then all temperatures are reset to the melting temperature and all liquid fractions are recalculated to account for the thermal energy released by the PCM crystallization following the supercooled state.

The three dimensional, transient, thermal model used in this particular case consisted of 123 nodes, having fixed locations, and 343 linear conductors. 27 nodes were used to lump the PCM.

Ullage was taken into consideration and the position of the vapor bubble varied according to the orientations of the container in the gravity field. When there is no filler the modeling of the PCM nodes is straightforward. When honeycomb fins are present, some equivalencing of the fin surface areas and masses within the individual PCM node is required to avoid modeling each individual honeycomb cell.

The container is assumed to be thermally isolated. During heating a constant heat input through the container mounting hub was simulated. During cooling the heat transfer process in the cooling coil should be taken into account to write down the boundary conditions at the base.

Surface tension effects, convection in the liquid phase and shrinkage upon phase change were all neglected.

Modeling of the cool down without filler gave defective results. The thermal analysis yielded temperatures corresponding to a device with much higher thermal resistance because of reasons explained in Clause 5.1.3. In a revised thermal model, the entire mass of the PCM was concentrated into the bottom nodes whose conductances to the wall were increased to correspond to an assumed liquid layer thickness of $0{,}8 \times 10^{-3}$ m. The agreement between the modified model and the experimental results was improved, as shown in Figure 8-36.
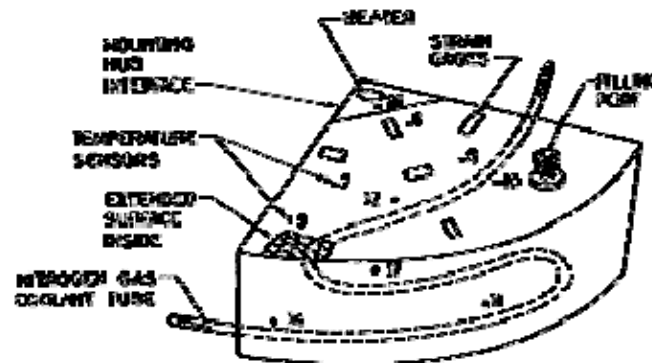
Figure 8-34: Location of the thermocouples and strain gages in the test unit. Thermocouples 12, 17 and 14 are placed on the base; 6, 7 and 8 on the upper face; 9 and 10 on the lateral faces; 11 on the rim, and 26 on the mounting hub interface. Strain gages are placed on his upper face.
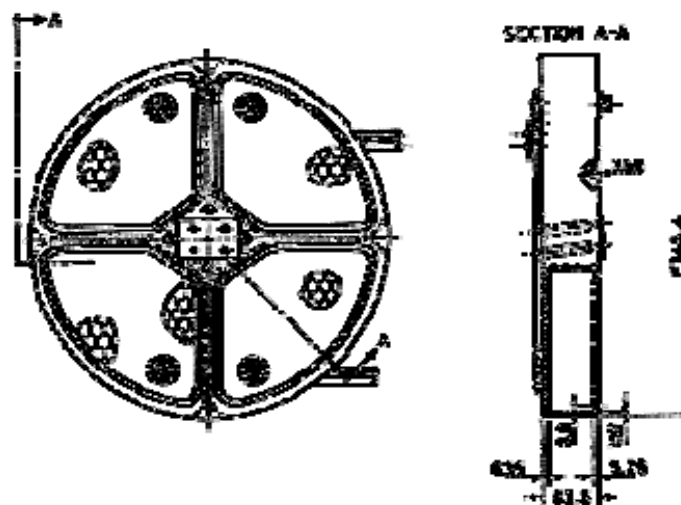
Note: non-si units are used in this figure

Figure 8-35: PCM capacitor developed by Aerojet. All the dimensions are in mm.
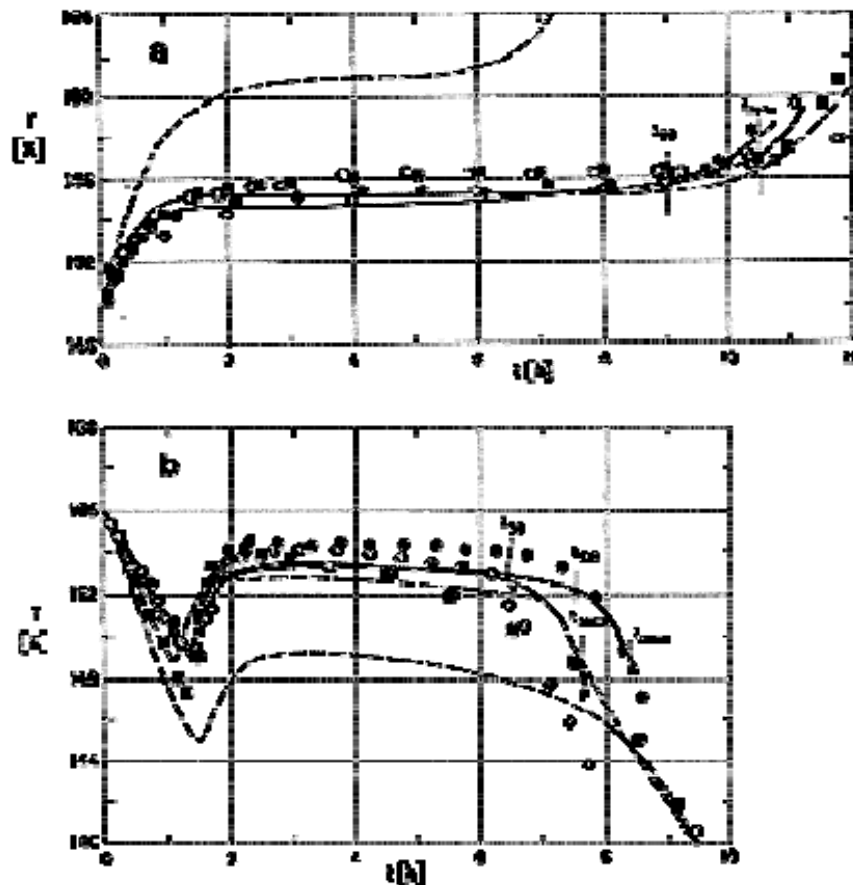
Figure 8-36: Average temperature, *T*, of the container vs. time, *t*, either during heat up or during cool down. a) During heat up with a nominal heat transfer rate *Q* = 2,5 W. b) During cool down with the same nominal heat transfer rate. With honeycomb filler. Mounting hub down. ○ Measured. ‌‌‌‌‌‌ Calculated. Cooling coils down. ● Measured. ‌‌‌‌‌‌ Calculated. Without honeycomb filler. Cooling coils up. □ Measured. ‌‌ ‌‌ Calculated with the original model. ‌‌ ‌‌ Calculated with the modified model. Cooling coils down. ■ Measured. Times for 90% and complete melting (freezing) are shown in the figure by means of vertical traces intersecting the calculated curves. Replotted by the compiler, after Bledjian, Burden & Hanna (1979) [6], by shifting the time scale in order to unify the initial temperatures.

Reference: Bledjian, Burden & Hanna (1979) [6].

8.6 Trans temp

Developer	Royal Industries, Santa Ana, California, USA					
Model	Trans Temp 205 System	Trans Temp 1060 Series				
		1061	1063	1065	1067	1069
Heat Storage [J]						
Heat Storage per Unit Mass [J.kg⁻¹]	Not given. Latent heat of fusion of the PCMs used ranges from 2×10^5 to 3×10^5.					
Thermal Conductance [W.K⁻¹]						
Operational Temperature Range [K]						
Filling Temperature [K]						
Phase Change Temperature [K]	Depends on the PCM used. Available temperatures are: 240, 252, 262, 270, 271, 275, 277, 291, 298, 305, 308, 316, 327, 339.					
Temperature Stability [K]	±2					
Shape	Circular Cylinder	Box-Shaped				
Overall	DiameterxL	LxWxD	LxWxD	LxWxD	LxWxD	LxWxD

Heat Path Sketch

Heating   Cooling

Insulation
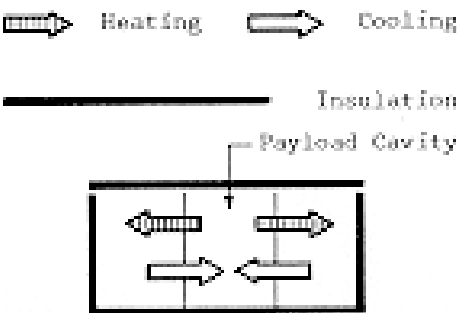
Payload Cavity

Dimensions [m] (Outer Insulation)	0,406x0,457	0,470x0,419x0,305	0,470x0,419x0,381	0,470x0,419x0,343	0,470x0,419x0,267	0,470x0,419x0,457
Payload Cavity Dimensions [m]	DiameterxL 0,152x0,152	LxWxD 0,305x0,152x0,114	LxWxD 0,305x0,152x0,191	LxWxD 0,305x0,152x0,152	LxWxD 0,305x0,152x0,076	LxWxD 0,305x0,152x0,267
Container						
Number of Containers	1	2	4	4	2	2 or 4
Filler						
Inner Volume [m³]						
Ullage [%]						
Mass of Container & Filler [kg]						
Mass of PCM [kg]						
Overall Mass [kg] a	14,51	8,16	11,79	11,79	8,16	15,42
PCM	Salt Hydrate Eutectics. Typical examples are: Trans Temp 12, 27, 65, and 130, where the numbers indicate the phase change temperature in degrees Fahrenheit. Paraffin and non-paraffin organics are also used					
Container Materials						
Filler Materials						
Other Materials	Freon blown rigid polyurethane insulation.					

Thermal Performances	Curves are given representing both ambient and inner temperatures vs. time for systems holding different biological materials. Ambient temperatures can be larger or smaller than phase change temperature.					
Lifetime [h] [b]	up to 240	up to 84	up to 72	up to 60	up to 120	up to 72
Applications	Round or bag-shaped payloads.	Large volume shipments.				

[a]   Payload not included.

[b]   Given values are preserving times (time for complete melting or freezing). The system is reusable.

Developer	Royal Industries, Santa Ana, California, USA					
Model	Trans Temp 1070 System					Trans Temp 509 Series
	1071	1073	1075	1077	1079	
Heat Storage [J]						
Heat Storage per Unit Mass [J.kg⁻¹]	Not given. Latent heat of fusion of the PCMs used ranges from 2×10^5 to 3×10^5.					
Thermal Conductance [W.K⁻¹]						
Operational Temperature Range [K]						
Filling Temperature [K]						
Phase Change Temperature [K]	Depends on the PCM used. Available temperatures are: 240, 252, 262, 270, 271, 275, 277, 291, 298, 305, 308, 316, 327, 339.					
Temperature Stability [K]	±2					
Shape	Box-Shaped					
Overall Dimensions [m] (Outer Insulation)	LxWxD 0,622x0,521x0,470	LxWxD 0,622x0,521x0,622	LxWxD 0,622x0,521x0,546	LxWxD 0,622x0,521x0,394	LxWxD 0,622x0,521x0,775	LxWxD 0,229x0,254x0,279

Heat Path Sketch

Heating   Cooling

Insulation
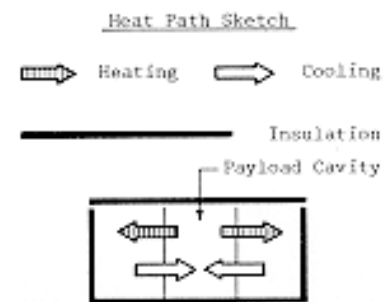
Payload Cavity

Payload Cavity Dimensions [m]	LxWxD 0,305x0,305x0,229	LxWxD 0,305x0,305x0,381	LxWxD 0,305x0,305x0,305	LxWxD 0,305x0,305x0,152	LxWxD 0,305x0,305x0,533	LxWxD 0,152x0,076x0,165
Container						
Number of Containers	4	2 or 8 [a]	8	4	2 or 12 [a]	2
Filler						
Inner Volume [m³]						
Ullage [%]						
Mass of Container & Filler [kg]						
Mass of PCM [kg]						
Overall Mass [kg] [b]	17,24	28,58	25,85	16,78	37,65	4,53
PCM	Salt Hydrate Eutectics. Typical examples are: Trans Temp 12, 27, 65, and 130, where the numbers indicate the phase change temperature in degrees Fahrenheit. Paraffin and non-paraffin organics are also used					
Container Materials						
Filler Materials						
Other Materials	Freon blown rigid polyurethane insulation.					Freon-polyurethane encapsulated in polyethylene set.

Thermal Performances	Curves are given representing both ambient and inner temperatures vs. time for systems holding different biological materials. Ambient temperatures can be larger or smaller than phase change temperature.				
Lifetime [h] c	up to 80	up to 72	up to 100	up to 120	up to 100	up to 120
Applications	Large volume shipments where extended temperature holding times are required.				

ᵃ   Different PCM containers are used in either case.

ᵇ   Payload not included.

ᶜ   The given value is the preserving time (or time for complete melting or freezing). The system is reusable.

Developer [a]	Royal Industries, Santa Ana, California, USA					
Model	Trans Temp 512 System	Trans Temp 301 Series	Trans Temp 309 Series	Trans Temp 310 Series	Trans Temp 312 Series	Trans Temp 313 Series
Heat Storage [J]						
Heat Storage per Unit Mass [J.kg^{-1}]	Not given. Latent heat of fusion of the PCMs used ranges from 2x10^5 to 3x10^5.					
Thermal Conductance [W.K^{-1}]						
Operational Temperature Range [K]						
Filling Temperature [K]						
Phase Change Temperature [K]	Depends on the PCM used. Available temperatures are: 240, 252, 262, 270, 271, 275, 277, 291, 298, 305, 308, 316, 327, 339.					
Temperature Stability [K]	±2					
Shape	Box-Shaped					
Overall Dimensions [m] (Outer Insulation)	LxWxD 0,508x0,229x0,267	LxWxD 0,254x0,254x0,254	LxWxD 0,203x0,229x0,254	LxWxD 0,235x0,178x0,152	LxWxD 0,508x0,229x0,279	LxWxD 0,279x0,171x0,235
Payload Cavity Dimensions [m]	LxWxD 0,330x0,114x0,152	LxWxD 0,127x0,038x0,127	LxWxD 0,127x0,076x0,178	LxWxD 0,038x0,108x0,076	LxWxD 0,330x0,152x0,114	LxWxD 0,076x0,051x0,152

Heat Path Sketch

Heating   Cooling

Insulation

Payload Cavity

Container						
Number of Containers	4	2	2	3	4	1 or 2
Filler						
Inner Volume [m³]						
Ullage [%]						
Mass of Container & Filler [kg]						
Mass of PCM [kg]						
Overall Mass [kg] [b]	10,43	4,54	3,63	1,81	8,16	2,72
PCM	Salt Hydrate Eutectics. Typical examples are: Trans Temp 12, 27, 65, and 130, where the numbers indicate the phase change temperature in degrees Fahrenheit. Paraffin and non-paraffin organics are also used					
Container Materials						
Filler Materials						
Other Materials	Freon-polyurethane encapsulated in polyethylene set.	Freon blown rigid polyurethane insulation. Velcro sealing system in models 301, 309, 312, and 313.				
Thermal Performances	Curves are given representing both ambient and inner temperatures vs. time for systems holding different biological materials. Ambient temperatures can be larger or smaller than phase change temperature.					

Lifetime [h] [c]	up to 110	up to 144	up to 80	up to 24	up to 110	up to $24 \times n$ $n = 1,2$ capacitors.
Applications	Can be sealed to provide CO_2 atmosphere.	Heavy duty, high-performance, 5-15 specimens.	Large payload, light weight, frozen or chilled specimens.	Small quantities of specimens.	Large specimens loads (over 4 kg).	Special payloads, chilled blood bags.

[a]   European representative: Mr. A.C. Thorne, Dynatech AG, Bleichistrasse 3, 6300 Zug, Switzerland.

[b]   Payload not included.

[c]   Given values are preserving times (time for complete melting or freezing). The system is reusable.
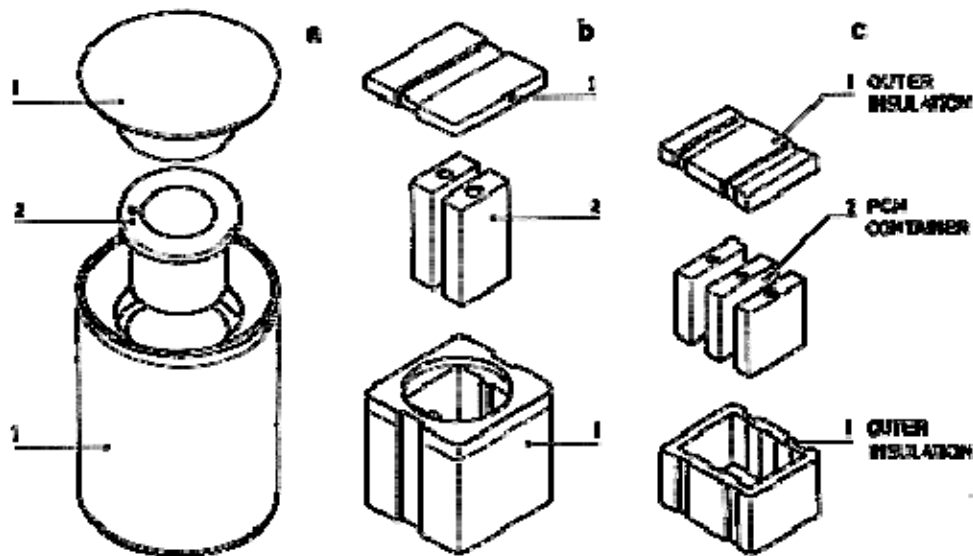
Figure 8-37: Several TRANS TEMP Containers developed by Royal Industries for transportation of temperature- sensitive products. a: 205 System. b: 301 System. c: 310 System. 1: Outer insulation. 2: PCM container.
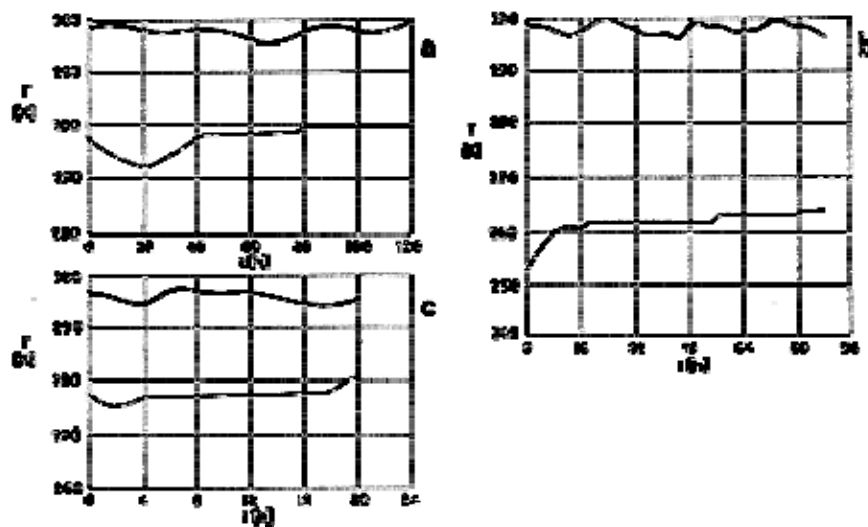

Figure 8-38: Measured ambient and inner temperatures, *T* vs. time, *t*, for several TRANS TEMP Containers holding blood samples. a: 205 System. b: 301 System. c: 310 System. ▬▬▬ Ambient temperature. ▬▬▬ Inner temperature.

Bibliography

[1]   Abhat, A., Groll, M., "Design and Development of a Phase Change Material Thermal
        Control Device for Satellite Temperature Control", ESRO-CR(P)-534, Institut für
        Kernenenergetik Universität Stuttgart, Prepared under Contract No. 1879/73 for ESTEC,
        April 1974.

[2]   Abhat, A., Groll, M., "Investigation of Phase Change Material (PCM) Devices for Thermal
        Control Purposes in Satellites", AIAA Paper No. 74-728, AIAA/ASME 1974
        Thermophysics and Heat Transfer Conference, Boston, Massachusetts, July 15-17, 1974.

[3]   Abhat, A., "Design, Development and Space Qualification of a Prototype Phase Change
        Material Device", Institut für Kernenenergetik Universität Stuttgart, Prepared under
        Contract No. 23331/74 for ESTEC, Oct. 1975.

[4]   Abhat, A., "Experimental Investigation and Analysis of a Honeycomb-Packed Phase
        Change Material Device", AIAA Paper No. 76-437, AIAA 11th Thermophysics Conference,
        San Diego, California, July 14-16, 1976.

[5]   Bentilla, E.W., Sterrett, K.F., Karre, L.E., "Research and Development Study on Thermal
        Control by Use of Fusible Materials", Final Report, NASA CR 75041, Contract No. NAS8-
        11163, Northrop Space Laboratories, Hawthorne, California, April 1966.

[6]   Bledjian, L., Burden, J.R., Hanna, W.H., "Development of a Low-Temperature Phase
        Change Thermal Capacitor", in "Thermophysics and Thermal Control", Progress in
        Astronautics and Aeronautics, Vol. 65, R. Viskanta, Ed., American Institute of
        Aeronautics and Astronautics, New York, 1979, pp. 255-274.

[7]   Brennan, P.J., Suelau, H.J., McIntosh, R., "Development of a Low Temperature Phase
        Change Material Package", AIAA Paper No. 77-762, AIAA 12th Thermophysics
        Conference, Albuquerque, New Mexcio, June 27-29, 1977. Also published under the title
        "Low Temperature Phase Change Material Package, in "Heat Transfer and Thermal
        Control Systems", Progress in Astronautics and Aeronautics, Vol. 60, L.S. Fletcher, Ed.,
        American Institute of Aeronautics and Astronautics, New York, 1978, 371-381.

[8]   Clark, L.G., "LDEF Mission 1 - Experiment Description", Preliminary Copy, Langley
        Research Center, NASA, Sept. 1981, pp. 59-61.

[9]   DORNIER SYSTEM, "Phase Change Materials", Internal Report, Dornier System GmbH,
        Friedrichshafen, Germany, 1971.

[10]   DORNIER SYSTEM, "Heat Storage Devices Using Fusible Materials for Space
        Application", Internal Report, Dornier System GmbH, Friedrichshafen, Germany, 1972.

[11]   FLUKA, "Fluka Catalogue 11-1978", English edition, Fluka AG, Buchs, Switzerland, 1978.

[12]   Grodzka, P.G., "Space Thermal Control by Freezing and Melting", Second Interim Report,
        "Space Thermal Control Study", LMSC/HREC-D148619, Contract NAS8-21123, Lockheed
        Missiles & Space Company, Huntsville, Alabama, May 1969.

[13] Hale, D.V., Hoover, M.J., O'Neill, M.J., "Phase Change Materials Handbook", NASA CR-61363, Lockheed Meissiles and Space Company, Huntsville, Alabama, Sep. 1971.

[14] Hodgman, Ch.D., "Handbook of Chemistry and Physics", 35th ed., Chemical Rubber Publishing Co., Cleveland, Ohio, 1953, pp. 468-2249.

[15] Keville, J.F., "Development of Phase Change Systems and Flight Experience on an Operational Satellite", AIAA Paper No. 76-436, AIAA 11th Thermophysics Conference, San Diego, California, July 14-16, 1976. Also published in "Thermophysics of Spacecraft and Outer Planet Entry Bodies", Progress in Astronautics and Aeronautics, Vol. 56, A.M. Smith, Ed., American Institute of Aeronautics and Astronautics, New York, 1977, pp. 19-36.

[16] Koch, H., Lorschiedter, J., Strittmatter, R., Pawlowski, P.H., "Sounding Rocket Heat Pipe and PCM Thermal Capacitor Experiments", in ESA SP-112, "2nd International HEat Pipe Conference 1976", Papers presented at the 2nd International Heat Papipe Conference Sponsored by CNR, co-sponsored by AIAA, ESA & Euratom, Bologna, Italy, March 31 - April 2, 1976, pp. 607-620.

[17] McIntosh, R., Olledorf, S., Harwell, W., "The International Heat Pipe Experiment", AIAA Paper No. 75-726, AIAA 10th Thermophysics Conference, Denver, Colorado, May 27-29, 1975.

[18] MERCK, "Reactivos - Diagnostica - Productos Químicos", E. Merck, Darmstadt, República Federal de Alemania, 1981.

[19] Napolitano, L.G., "Surface and Buoyancy Driven Free Convection", Paper IAF-81-126, XXXII Congress of the International Astronautical Federation, Rome, Italy, Sept. 6-12, 1981.

[20] Ollendorf, S., "Heat Pipes in Space", Astronautics & Aeronautics, Vol. 14, No. 12, Dec. 1976, pp. 64-65.

[21] Riddick, J.A., Bunger, W.B., "Organic Solvents", Third Edition, Wiley-Interscience, New York-London, 1970, Chap. III, pp. 61-551.

[22] Strittmatter, R., "Development of oa Phase Change Material Thermal Control Device", Dornier System GmbH, Friedrichshafen, Germany, Dec., 1972.

[23] TRANS TEMP, Data Sheets on the following Trans Temp Systems: 205, 301, 309, 310, 312, 313, 509, 512, 1060, 1070, "Temperatures Packaged to Go", Royal Indusries, Energy Products Division, 2040 East Dyer Road, Santa Ana, California 92705.

[24] Vargaftik, N.B., "Tables on the Thermophysical Properties of Liquids and Gases", 2nd ed., Hemisphere Publishing Corporation, Washington-London, 1975.

[25] Weast, R.C., "Handbook of Chemistry and Physics", 57th ed., CRC Press, Inc., Cleveland, Ohio, 1976, pp. C-81 to C-725.

[26] Wilkins, R.A., Jenks, R.H., "Corrosion in Liquid Media, The Atmosphere, and Gases-Copper", in "The Corrosion Handbook", H.H. Uhlig, Ed., John Wiley & Sons, Inc., New York, Chapman & Hall, Ltd., London, 1948, pp. 61-68.

[27] Windholz, M., "The Merck Index", Merck & Co., Inc., Rayway, New Jersey, USA, 1976.